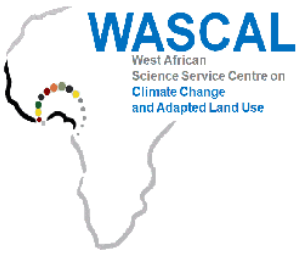

UNIVERSITÉ ABDOU MOUMOUNI

Master Research Program in Climate Change and Energy

Assessing Variability of Potential Variable Renewable Energy in Ghana: Impact on Management of Hydropower Reservoirs (Case of Akosombo Dam)

Submitted by:

Derrick Kwadwo Danso

A thesis submitted in partial fulfilment of the requirements for the degree of Master of Science in Climate Change and Energy

in the:
Faculty of Sciences

Supervisor: Dr. Arona Diedhiou
Co-supervisors: Dr. Benoit Hingray and Dr. Baptiste François

JANUARY, 2018

Thesis Defense Date: 4th January 2018

Venue: WASCAL MRP-CCE Building, Niamey, Niger

Jury Members:

- Chairman: Professor Atanasse Coly

  (Université Cheikh Anta Diop, Dakar-Fann, Senegal)

- Examiner: Professor Adamou Rabani

  (Université Abdou Moumouni, Niamey, Niger)

- Supervisor: Dr. Arona Diedhiou

  (IRD, Université Félix Houphouët Boigny, Abidjan, Ivory Coast)

Abstract

Electricity production in Ghana is shifting towards more fossil-based production in recent periods and amidst the high rates of increasing electricity demand, additional production systems are still needed. However, to achieve the aims of the Paris Agreement, a great deal of decarbonization is required thus a climate-friendly option is to massively develop Variable Renewable Energy (VRE) such as solar and wind power. In this study, the variability of potential solar power production was estimated for selected locations homogeneously distributed over the country while that for potential wind power was assessed for only the coastal offshore region. At sub-daily scale, solar power was observed to have a very high variability with the coefficient of variation (CV) for the average sub-daily cycle computed to be 124% as compared to 14% for wind power. At daily time scale however, wind power was observed to have a higher variability with a seasonal coefficient of variation calculated to be 41% as compared to 13% for solar power. Due to the high variation of solar and wind energy in time, incorporating them in the power system requires the presence of a large flexibility system to cope with the temporal mismatch between production and demand that will be introduced. In this study, the Akosombo hydroelectric dam was used as a flexible power production facility to balance the temporal fluctuations of VRE production. Being used for this purpose, it was expected that higher share of VRE in the power system will lead to a change in the storage and release strategy of the Akosombo dam. Its storage variation was thus simulated with Deterministic Dynamic Programming for a reference case with no VRE production and a number future VRE production cases. It was found that in all scenarios tested, the seasonality of storage in the dam was not significantly affected by VRE production. However, relative to the reference scenario, a higher proportion of wind in VRE production leads to an increase in water level of the dam during its peak months at the end of the rainy season.

Keywords: Variable Renewable Energy, Dynamic Programming, hydropower, storage cycle, residual demand, backup

Acknowledgement

I want to thank God for seeing me through this MSc degree program. I also wish to express a few words of gratitude to some individuals or groups who helped me in various capacities during my study.

First and foremost, I want to express my sincere appreciation to WASCAL and the German Federal Ministry of Education and Research (BMBF) for giving me this scholarship opportunity to study for an MSc degree. The benefits I have obtained from this program cannot be described in few words. I believe that, this high quality training I have received from the program will help me to also contribute to making West Africa better in the near future.

I am very grateful to my MSc. research supervisor, Dr. Arona Diedhiou, you are the best and I know why I say that. You really gave me all the support I needed during the last six months and I appreciate all your kind efforts for me. I know we are going to work together again in future to make West Africa better. Thank you very much.

To Dr. Benoit Hingray and Dr. Baptiste François, the co-supervisors for my MSc. research, I say these words from my heart;
I really appreciate your time, efforts and patience for me during this study. Your dedication and availability to direct me whenever I needed your assistance is second to none and you really pushed me to work hard for this thesis. I could not have done it without you and I will forever remain grateful to you. I also hope to get the opportunity to work again with you in future. Thank you very much.
I wish to acknowledge the effort of Professor Adamou Rabani, Director of WASCAL MRP-CCE to make this program a success and also for his effort in organizing a defense for my Master thesis before the scheduled date in order to allow me to pursue further studies. I also say a huge thank you to the Coordinator of MRP-CCE, Dr. Inusah Maman for his supporting role and kindness during the period of my study in Niamey.

I am very grateful to all my colleagues of MRP-CCE (2nd batch) for all the great times we spent together during the two-year duration of our program. You guys were amazing. I thank the whole community of Université Abdou Moumouni and all WASCAL MRP-CCE staff for hosting us during these last two years with kind reception.

I will also like to thank Mr. Samuel Guug of WASCAL who assisted me to get some data for my work and everybody at the WASCAL Competence Centre in Ouagadougou, Burkina Faso. I thank my brother Wilson Ofori Sarkodie of PAUWES who also assisted me to get information from Energy Commission of Ghana.

Table of Contents

List of Tables

List of Tables

Acronyms

CO_2	Carbon dioxide
CS-GHI	Clear Sky Global Horizontal Irradiance
CV	Coefficient of Variation
DDP	Deterministic Dynamic Programming
DP	Dynamic Programming
GHI	Global Horizontal Irradiance
GSS	Ghana Statistical Service
GWh	Giga Watt Hours
HPP	Hydropower Plant
IEA	International Energy Agency
IPCC	Intergovernmental Panel on Climate Change
IRENA	International Renewable Energy Agency
ITCZ	Inter Tropical Convergence Zone
kW	Kilo Watt
kWh	Kilo Watt Hours
kWp	Kilo Watt Peak
MERRA-2	Modern-Era Retrospective Analysis for Research and Applications
MSD	Mean Specific Discharge
MW	Mega Watt
PV	Photovoltaic
R	Correlation Coefficient
SARAH-2	Surface Solar Radiation - Heliosat
UNFCCC	United Nations Framework Convention on Climate Change
VBA	Volta Basin Authority
VRA	Volta River Authority
VRE	Variable Renewable Energy

1 INTRODUCTION

1.1 Background of Study

Ghana's electricity system has been through various phases from pre-independence to post-independence times. Prior to the construction of the 912 MW (increased to 1020 MW) capacity Akosombo dam, electricity supply was mainly from stand-alone diesel generators across the country. The Akosombo dam was constructed to primarily provide electricity to Volta Aluminium Company (VALCO). In 1982, a 160 MW capacity hydropower plant (HPP) at Kpong was commissioned to meet rising demands. A severe power crisis hit the country during 1982 to 1984 as a result of a serious drought which led to a reduction of inflows to the Akosombo dam (Bekoe and Logah, 2013). Consumption during this period decreased from 4652 GWh to 1151 GWh (Eshun and Amoako-Tuffour 2016). A number of thermal power plants were commissioned as a result to help meet demands. In 2013, the Bui hydroelectric power station with an installed capacity of 400 MW was commissioned to provide support during peak hours in the country (Kumi 2017).

The dependence of hydropower in Ghana is clear to see barring the periodic shortfalls in production primarily due to climate variability. The three major HPPs in Ghana will continue to be vital in the power system and there are possibilities to construct new dams or run-off river plants. However, electricity demand grows between 10 to 15 % annually in Ghana (Energy Commisision, 2015) due to population and economic growth. Total electricity demand in the last decade has increased greatly and keeps on increasing. The study of Eshun and Amoako-Tuffour, (2016) revealed that, growth in total electricity demand between 2003 and 2013 has more than doubled. As no new HPPs have been constructed since Bui, thermal power plants which are relatively easier and takes less time to construct are used to generate electricity to meet the rising demands. In the present (2017) state of Ghana's power system, thermal power plants make up the greatest share of total national installed capacity with 62.5% compared to HPPs with 37%.

The share of thermal power generation in power sector have been increasing steadily since 2008 as shown in Fig 1.1. The main downside of these plants is that they run on fossil fuel and emit CO_2 into the atmosphere and enhance global warming. The concentrations of CO_2 have increased by 40% since pre-industrial times, primarily from fossil fuel emissions (IPCC 2013) with energy

production being a major culprit. With demand for electricity still on the rise, more of these plants may be put up in future leading an even more emissions. The Paris Agreement which was signed at the COP21 aims to keep the global temperature rise below 2°C above pre-industrial levels (UNFCCC 2014) and thus clean energy options are needed. Another downside for thermal power production in Ghana is that, the supply of fuel for thermal plants (gas) have not always been reliable due to several technical and administrative hitches. This sometimes leads to arbitrary blackouts in different parts of the country.

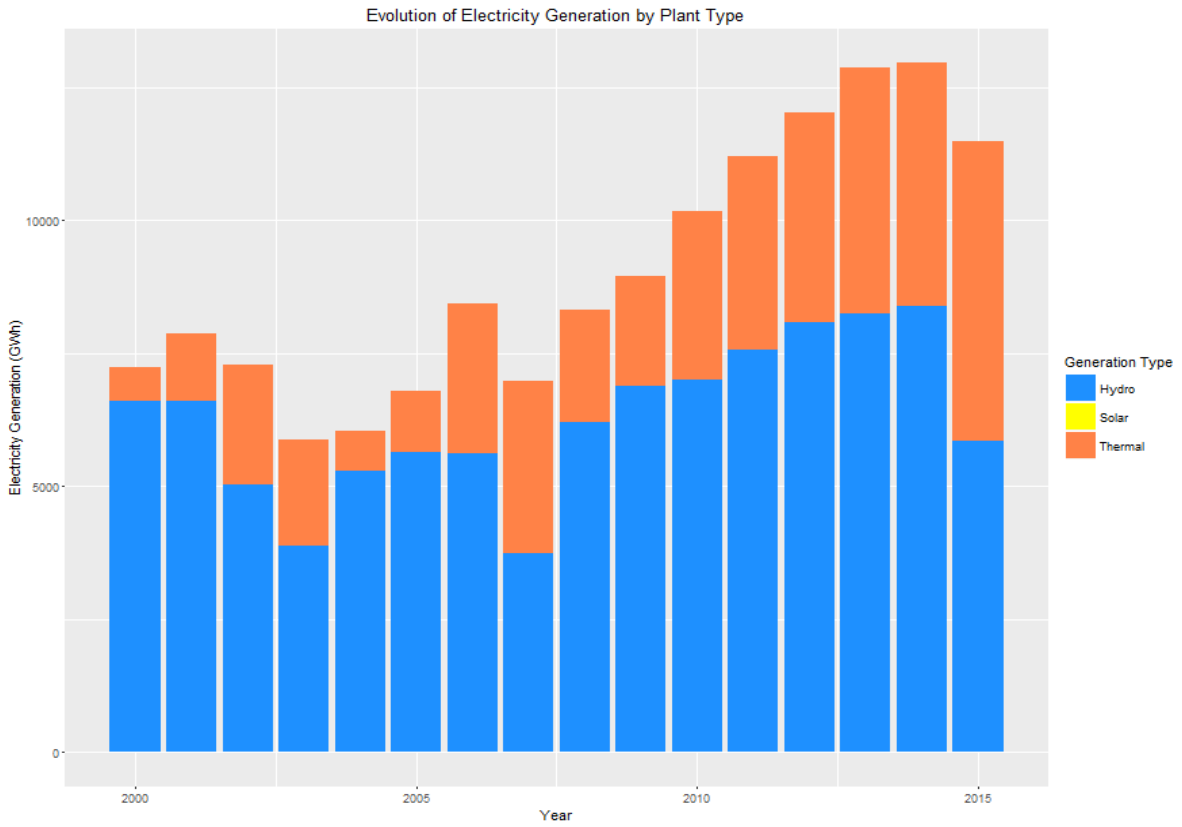

Fig 1.1: Trend of electricity generation (GWh) by source (Data source: Energy Commission of Ghana)

One climate – friendly option is to massively develop renewable energies such as wind and solar energies. Unlike thermal power production, electricity generated from wind and solar sources have relatively insignificant levels of greenhouse gas emission and are considered as clean energies. Renewable energy alone has the possibility to contribute to 21% of reductions in energy-related CO_2 emissions by 2050 (International Energy Agency 2008). Renewable energy resources such as wind and solar are also freely available in nature but their exploitation in Ghana is rather minimal

currently. So far, only a 2.5 MW solar photovoltaic plant owned by the Volta River Authority (VRA) in Navrongo and a 20 MW solar plant owned by BXC Ghana have recently been added to the national grid to increase renewable energy production in the country (see Table 1.1). This represents only about 0.5 % of the national total installed capacity.

Table 1.1: Electricity generating units in Ghana and their installed capacities (Source: VRA)

Plant Name	**Installed Capacity (MW)**	**Fuel Type**
HYDRO		
Akosombo Hydro Plant	1,020	Water
Kpong Hydro Plant	160	Water
Bui Hydro Plant	400	Water
Sub-Total	**1,580**	
THERMAL		
TAPCO - T1	330	LCO/Gas
TICO - T2	330	LCO/Gas
Mines Reserve plant (MRP)	80	Gas
Tema Thermal 1 Plant (TT1P)	110	Gas/LCO
Tema Thermal 2 Plant (TT2P)	49.5	Gas
Tema Thermal 2 Plant Expansion (TT2PP-X)	38	Gas
Kpone Thermal Power Plant (KTPP)	220	Gas/DFO
Kar Power Barge 1	235	HFO
Sunon Asogli Phase 1	200	Gas
Sunon Asogli Phase 2 Stage 1	180	LCO/Gas
Sunon Asogli Phase 2 Stage 2	180	Gas/LCO
CENIT Power Plant	110	LCO
Ameri Power Plant	250	Gas
AKSA	360	HFO
Sub-Total	**2672.5**	
RENEWABLES		
VRA Navrongo Solar Plant	2.5	Sunlight
BXC Solar	20	Sunlight
Sub-Total	**22.5**	
TOTAL INSTALLED CAPACITY	**4,275**	

Monthly average solar irradiation in Ghana ranges between 4.4 and 5.6 kWh/m^2/day (IRENA, 2015) and considering that many parts of the country receive 5-8 hours of sunshine per day at 1 kW/m^2, the potential for using solar for electricity generation is very high (Gyamfi et al., 2015). As there is a huge potential for solar energy in the country, several international and local organizations have expressed interest in developing utility-scale solar PV plants. One of such

organizations is Blue Energy which has announced plans to build a 155 MW solar PV plant in the Western Region of Ghana (IRENA, 2015).

Countries located further from the equator generally have relatively high wind energy potential than countries near the equator. In Ghana, average daily wind speeds range between 4 – 6 m/s and are rather low for large scale wind power investments (German Federal Ministry for Economic Affairs and Energy 2015). However, IRENA (2015) indicates that the theoretical wind power potential in Ghana is more than 5000 MW. This huge potential is mainly found on the eastern coastal region of the country (WWEA Technical Committee 2014) where average daily wind speeds for some locations ranges between 6.4 – 7.5 m/s (IRENA, 2015) as shown in Fig 1.2.

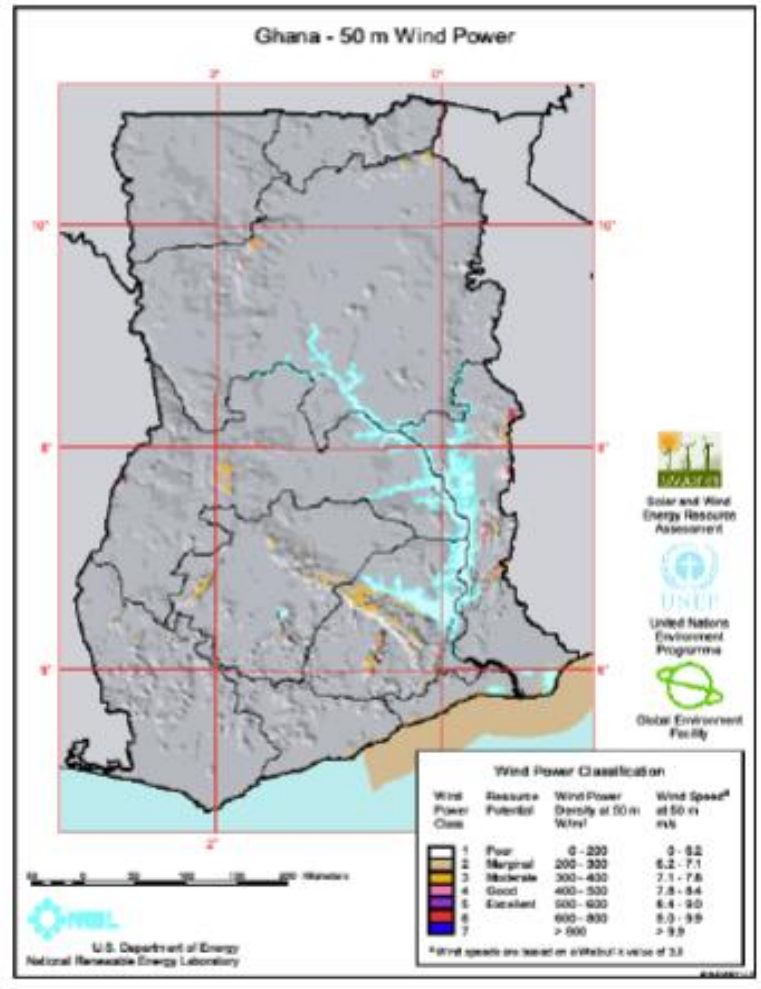

Fig 1.2: Wind resource map for Ghana. (Source: World Wind Energy Association)

With such potential as shown in the studies described above, solar and wind power are thus capable of helping the country to meet its rising electricity needs whiles ensuring the sustainability of the environment. What most of these studies has failed to elaborate is the temporal variability of solar and wind resources. The lack of temporal variability assessment in resource potential studies in Ghana may be the reason why wind and solar power is absent or very minimal in the electricity generation mix. For any long term planning on renewable energy implementation, important questions investors will look to get answers to, includes especially the temporal variability of the resources. Understanding the sub-daily, day-to-day, seasonal and inter-annual variability of these renewable energy resources in Ghana, is thus very crucial for not only utility scale systems which are fed directly into the national grid but also to off-grid or mini scale systems that will be directly affected by the variability of these resources. Characterizing the temporal variability of wind and solar resource is therefore very necessary.

The major global energy challenges are threefold; securing energy supply to meet growing demand, providing everybody with access to energy services and curbing energy's contribution to climate change (Asumadu-Sarkodie and Owusu 2016). Development of a massive solar and wind energy systems can help address these challenges to a large extent. However, due to the intermittent nature of solar and wind energy, their integration in the power system creates some challenges. Solar and wind resources are both significantly variable in space and time (Engeland et al., 2017; François et al., 2016) and are referred to as Variable Renewable Energy (VRE). The uncertainty and high variability of wind and solar energy generation can pose challenges for the power system and especially for grid operators (Bird et al., 2013). A massive implementation of VRE will thus require increased flexibility from the power system to cope with the variability and uncertainty of the generation (Cochran et al. 2012).

Both hydro and thermal generation systems may be used as flexibility facilities to balance the temporal mismatch between demand and production. Thermal systems possess two major challenges when being used as large flexibility facilities. Firstly, the problem of CO_2 emissions as already stated. A greater amount of decarbonization is needed to be able to achieve the aims of the Paris Agreement and thus the percentage of thermal production in the power system should be minimized as possible. Secondly, conventional power plants are associated with high costs of maintenance and serious infrastructural degradation due to corrosion, thermal fatigue etc. when

the variability of their cycling operations are high (Niamh 2011). Cycling operations of power plants include. the processes of starting up, shutting down, ramping up and ramping down of the plants (Meibom et al. 2007; Holttinen and Pedersen 2003). Gas turbines in thermal power plants are more sensitive to degradation due to high cycling variability than hydro turbines. A low variability in the cycling processes of thermal power plants will prolong the life time of such plants and lead to lower costs associated with their maintenance and operations. Due to the less sensitive nature of hydro turbines to degradation caused high variability of cycling, hydropower systems will be better options to provide flexibility required to ease a large share of VRE into the power system.

As energy is stored in reservoirs for hydropower generation in the form of water, the storage-release operations of these water reservoirs can provide the flexibility needed to cope with the variability and uncertainty of the VRE production. In Ghana, the Akosombo HPP can be used to provide such flexibility. The operations of hydropower dams can for instance be optimized to ensure that the residual demand after VRE and hydro production, to be met with a backup production (such as thermal production) becomes less variable as possible. The operational rules have actually to account for multiple objectives. They can for instance also be optimized to ensure that maximum benefits are derived from the power system. They may also account for other usages of the water resources such as: irrigation water, environmental flows downstream the water reservoirs (de Condappa et al., 2008; McCartney et al. 2012). The optimal operations required for the optimal management of the reservoirs are expected to depend on the temporal variability of input/output variables given the management constraints applying to the system. In this work, we explore how these optimal operations would change when introducing VRE in the energy production mix.

The optimal operation is usually identified via some optimization algorithm. We here consider the Dynamic Programming (DP) method (Bellman 1957) to optimize the operations of the reservoir (François et al., 2014; Labadie, 2004; Yakowitz, 1983). The optimization requires to define some objective function to be maximized (or minimized).

In the present work, we consider a very rough representation of the Akosombo dam. For instance, it remains unknown to the author whether the management strategy currently used for the operational management of the dam is obtained with some optimization process and if especially

it is optimized to achieve maximum economic benefits or not. We will assume that the operational management aims to minimize the variability of the production from backup plants available within the energy mix. With a higher introduction of VRE in the power system, a same objective function will likely lead the present storage-release strategy of Akosombo reservoir to be modified.

1.2 Research Objectives

The main objective of the study is to estimate how the massive development wind and solar power in Ghana could influence the storage and release operation of the Akosombo dam.

The specific objectives of this study are:

1. to characterize the temporal variability of the different resources that could be used for renewable electricity production (wind, solar, hydro).
2. to simulate the best management strategy of the Akosombo hydropower plant reservoir for the present and future in a number of very simplified scenarios.

1.3 Problem Statement

The current electricity generation mix of Ghana is composed mainly on thermal and hydro power productions. Due to increasing population and economic growth, electricity demand has also risen a lot since the last decade and this is even expected to increase more in coming years. To meet increasing demands, a lot of thermal power plants have been commissioned and used to produce electricity leading to a lot of CO_2 emissions. Also due to periodic climate variability effects, hydropower production has experienced shortfalls leading to decreased production in some years and the need for more thermal production. To meet the expected future increase in electricity demand, VRE can be developed in large scale to be used instead of thermal electricity production. VRE resources are intermittent in nature and thus will create challenges during their integration into national the power system. However, with the presence of a large flexibility facility in the power system, those challenges can be coped with. In Ghana, the Akosombo HPP is a suitable flexibility facility which can be used to allow integration of VRE. With the high variability of VRE

resources, their integration into the power system may require a change in the management operations of the Akosombo dam. In this study we will attempt to find the answers to the following questions:

1. What is the temporal variability of VRE production in Ghana?
2. How will the development of VRE in Ghana influence the management operations of the Akosombo HPP?

The rest of this report is structured as follows. Chapter 2 presents the study area and the data used. Chapter 3 presents the methodology used for the study while Chapter 4 presents and discusses the results obtained in the study. Chapter 5, concludes the study and give some recommendations for stakeholders and future studies.

2 STUDY AREA AND DATA DESCRIPTION

2.1 Overview of Study Area

Ghana is a West African country that lies between latitude 4˚N and 11˚N and longitude 4˚W and 2˚E. It is bounded by Togo to the east, Burkina Faso to the north, Ivory Coast to the west and the Atlantic Ocean to the south, and covers an area of 238,538 square kilometers (Rademacher-Schulz and Mahama 2012). There are currently ten administrative regional divisions in Ghana with a total population of about 28,000,000 in 2016 (GSS 2016) and an average annual growth rate of 2.4%. Ghana's economy is driven mainly by agriculture which accounts for 75% of foreign exchange earnings and contributes 37% to the nation's GDP (Armah et al. 2011). Farming is a major occupation for majority of people in the country with cocoa one of the much cultivated crops. Ghana also has mineral resources like gold, bauxite, diamond and recently have started exploration and production of oil.

The climate of Ghana is tropical, influenced strongly by the West African Monsoon and characterized by a dry and rainy season marked by severe floods and droughts (Nkrumah et al. 2014). The principal feature of rainfall in Ghana is its seasonal and year to year variability (Ghana Meteorological Agency 2017). The southern part of Ghana has a relatively longer rainy season than the northern part, thus creating two cropping seasons in most places in the south and one cropping season in the north. These seasons correspond to the northern and southern passages of the ITCZ across Ghana.

For regions south of the ITCZ, the prevailing wind direction is southwesterly, blowing moist air from the Atlantic Ocean onto the continent while the prevailing hot and dry winds to the north of the ITCZ is known as the Harmattan. The Harmattan originates from the northeast, bringing in hot and dusty air from the Sahara Desert between December and March (Nkrumah et al. 2014). Four types of rainfall are recognized, although adjacent types shade into one another. No very definite lines of demarcation exist, as they are a consequence of the north and south movement of the ITCZ and its associated weather zones(Ghana Meteorological Agency 2017). Annual rainfall is highly variable on inter-annual and inter-decadal timescales (McSweeney et al. 2010) which means that there are difficulties in identifying long term trends (Nkrumah et al. 2014).

The average annual mean temperature is about 27 °C (Srivastava et al. 2017) and the annual range of mean temperatures increases from in the south to in the north. It is mainly warm and dry in the southeast, hot and humid in the southwest and hot and dry in the north. Average temperatures range between 21° and 32°C, with relative humidity between 50% and 80%. The highest temperature so far recorded in Ghana is 43.9°C at Navrongo in the north of the country (Ghana Meteorological Agency 2017).

Ghana's topography is undulating consisting mainly of low plains but its south-central area does have a small plateau and highlands (Ministry of Food and Agricuture, 2011) of mean elevations above 800m. A large part of the Volta basin lies in Ghana covering about 45% of the country's total area as shown in Fig 2.1. The Volta Basin is home to the Volta Lake on which is situated the Akosombo HPP.

2.1.1 The Akosombo Hydropower Plant

The Akosombo plant is a vital electricity generation unit in the power system of Ghana. It is the largest HPP in Ghana by capacity and size. Its construction began in 1961 when a lower section of the Volta River was dammed and was opened in 1965 for commercial purposes. The construction of the dam led to the formation of the world's largest man-made lake by surface area called the Volta Lake with a surface area of 8500 km^2. The Volta Lake primarily serves as a water reservoir for the Akosombo power plant. It also provides water for irrigation, fish farming and transportation.

The reservoir is fed by water inflows from three upstream catchments: Oti, the Black and White Volta. It has a total storage capacity of 148 km^3. By design, the minimum operating level of the Akosombo dam is 240 ft. above the downstream tail water whiles the maximum level is 278 ft. With a maximum head of 226 ft. from the level of the penstocks to the tail water level, six Francis turbines with a total capacity of 1020 MW are used to convert falling water into electricity. Just downstream of the Akosombo dam is the Kpong power plant which has a relatively low dam elevation. It is considered as a run-of-river hydro system and it is used to optimize water use from the Volta Lake (VRA, 2017). Electricity production from the Kpong plant is used to supplement the national power supply.

Different environmental and social challenges were faced in Ghana as a result of creation of the Volta Lake. It led to flooding of a vast area of land consequently leading to the dislocation and resettlement of about 80,000 people from about 740 villages (Kalitsi 2003). Positive impacts that arose from the lake's creation included the wiping out of the vector of river blindness normally found near fast flowing rivers. The creation of the dam also enhanced commercial activities such as fishing and wide-ranging navigation on the lake.

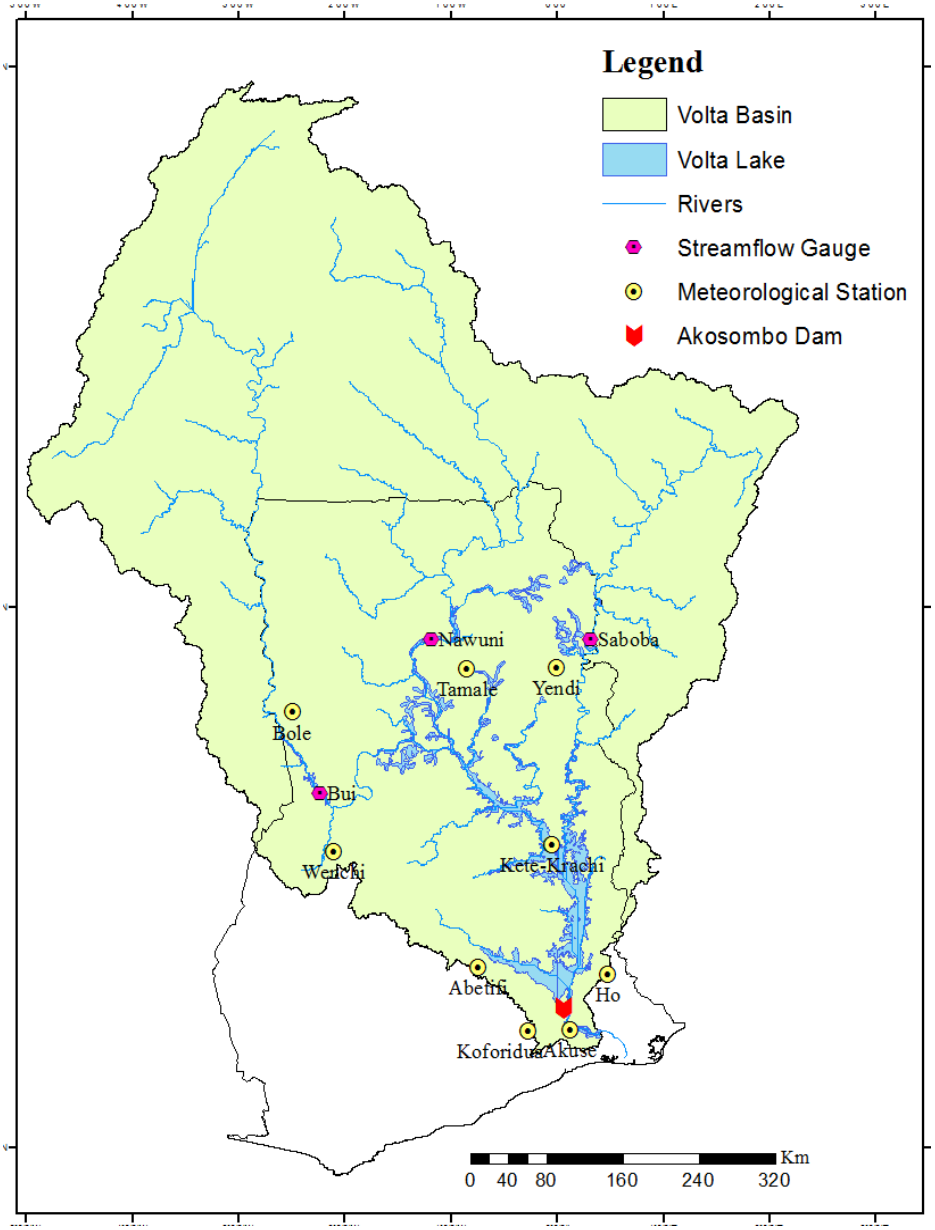

Fig 2.1: Map of Ghana and Volta Basin, also showing selected meteorological stations and discharge gauge points used for this study

2.2 Datasets Description

Availability of high quality and continuous data is a big issue in West Africa. This sometimes limits and reduces the quality of research work in the region. The major sets of data used for this study are hydrological and meteorological data, wind and solar resource data and GIS data. These datasets and their sources are presented in the next sub-sections.

2.2.1 Hydro-meteorological Data

Data for inflow discharge into the Volta Lake from the Saboba, Nawuni and Bui gauging sites (see Fig 2.1 for gauging stations) was obtained from VBA and VRA. Daily reservoir elevations in the Akosombo reservoir have also been collected from the VRA and used. Some gauging stations present several missing data. They can be sometimes reconstructed with data from other gauging stations.

Rainfall and temperature data has been obtained from the Ghana Meteorological Agency for stations shown on Fig 2.1. The rainfall data was used to estimate the average areal precipitation on Lake Volta. The temperature data have been used together with gridded temperature dataset from MERRA-2 reanalysis in the estimation of solar power production over Ghana.

2.2.2 Wind and Solar Resource Data

The ground measurements required to assess wind and solar energy potential are scarce and in West Africa. In the present work, we estimate wind and solar energy potential from pseudo-observations of solar and wind selected at various locations in Ghana as shown in Fig 2.2.

Pseudo-observation of wind speed at a resolution of $0.625° \times 0.5°$ are extracted from the second Modern-Era Retrospective Analysis for Research and Applications (MERRA-2) dataset (Bosilovich et al. 2016). According to McPherson et al., 2017, several studies have validated the MERRA wind data against other datasets, including the National Renewable Energy Laboratory (Gunturu and Schlosser 2012).

To determine solar power production potential and variability in Ghana, we use the Solar Radiation Data Set - Heliosat (SARAH-2). This product is available as monthly and daily means as well as an instantaneous 30-minute data on a regular latitude/longitude grid with a very high spatial resolution of $0.05° \times 0.05°$ (Pfeifroth et al. 2017).

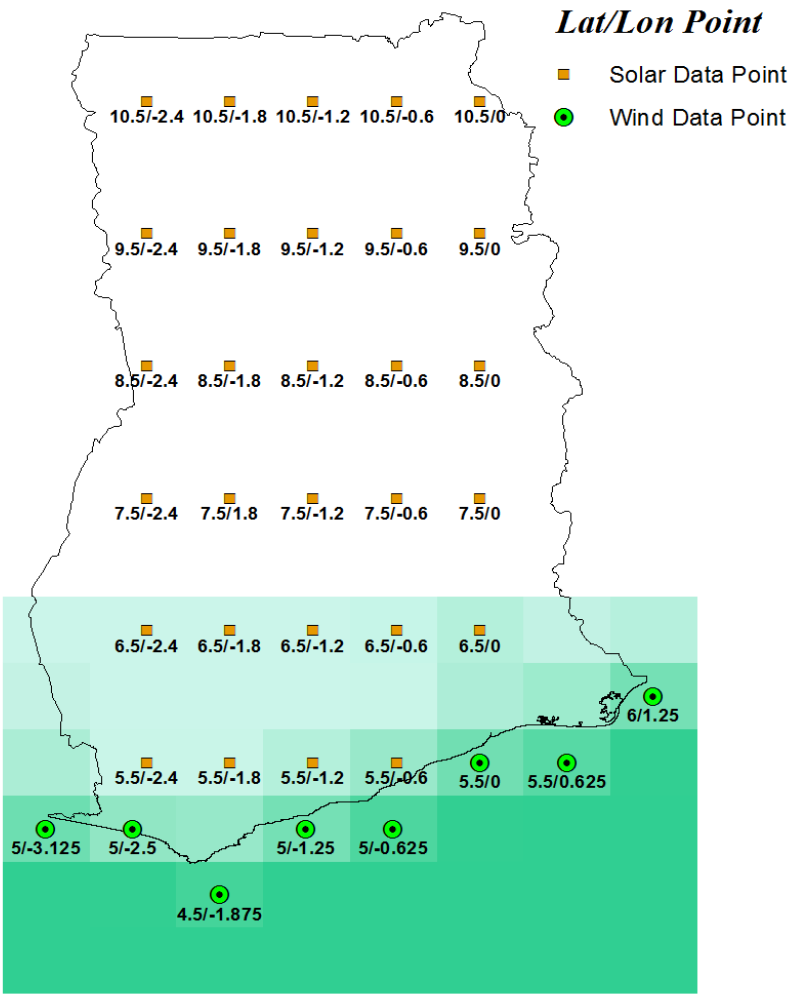

Fig 2.2: Wind and Solar data extraction locations

3 METHODOLOGY

3.1 Water Inflow into Volta Lake

Discharge time series from 1992 to 2015 for three gauging stations mentioned in Section 2.2 were used to estimate the inflows into the reservoir. Part of the discharge time series were missing within the period and were thus reconstructed using the parent-child technique. In this technique, a missing measurement at one point in a catchment can be reconstructed when there are measurements available from gauging stations upstream or downstream of that point. For a given time step, it can be expressed as

$$Q_{parent} = Q_{child} \times \frac{A_{parent}}{A_{child}} \tag{3.1}$$

where, Q_{parent} is the discharge from the point where measurement is to be reconstructed, Q_{child} is the discharge from the point where measurement is available, A_{parent} is the area of the catchment from the point where reconstruction is needed and A_{child} is the area of the catchment from the point where measurement is available.

Table 3.1: Locations of selected discharge gauging stations. For these estimations the surface areas of each catchment was determined first with ArcGIS 10.1. Mean interannual discharge were estimated for the period 1992 to 2011.

Gauging Station	Longitude	Latitude	Sub-basin	Area of Catchment (km^2)	Mean Interannual Discharge (m^3s^{-1})	Average Interannual Mean Specific Discharge ($m^3s^{-1}m^{-2}$)
Bui	8.2783	−2.236	Black Volta	129606	9.4×10^4	5.23×10^{-7}
Saboba	9.7046	0.3137	Oti	54275	1.28×10^5	1.95×10^{-6}
Nawuni	9.7	−1.18	White Volta	96130	1.02×10^5	8.77×10^{-7}

The discharge into the Volta Lake from the three gauging stations selected for this study is presented in Table 3.1. These stations were selected because they had less missing gaps within the period of consideration.

Each of the time series of discharge covers the period 1992 to 2015. However, stream flows for Bui shows a rather unusual and contrary to expected trend in the latter part of the time series from 2012 to 2015 (see Fig 3.1). This situation is due to the existence of the Bui hydroelectric dam which became operational in 2012 and therefore affected the flows into downstream Volta basin. This period of perturbed behavior was thus excluded from all further analysis. To ensure temporal homogeneity in the assessment of all resources the period 1992 to 2011 was used in the study.

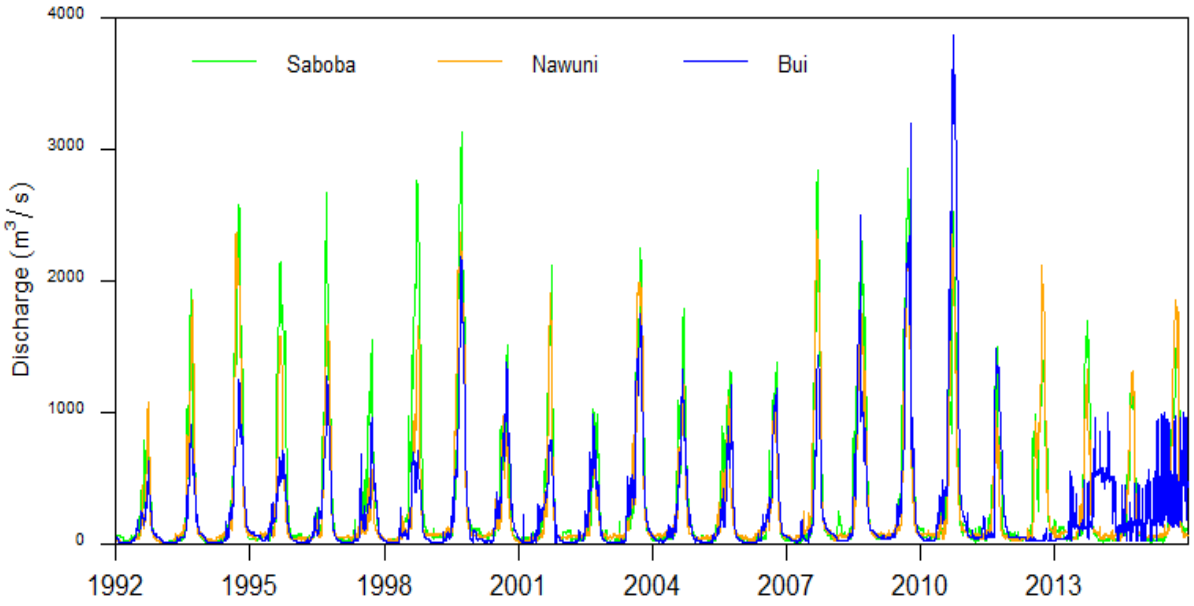

Fig 3.1: Daily discharge into the Volta Lake measured from three gauging stations in the three main upstream catchments (1992-2015)

3.1.1 Mean Specific Discharge into the Akosombo Reservoir

The discharge gauging stations are located upstream from the lake. As a result, the discharge observations at the upstream stations will underestimate the inflow to the lake/ reservoir. Therefore, an estimate of inflow discharge into the Volta is obtained with a classical scaling methodology based on the hypothesis that *"the mean specific discharge of the full upstream Volta lake is equal to the mean of the specific discharges obtained from the three upstream catchments"*.

$$Q_s = \sum_{i=1}^{n} \frac{q_{s_i}}{n} \tag{3.2}$$

where, Q_s is mean Volta full upstream specific discharge and q_{s_i} is specific discharge for a catchment.

The water inflow to the lake was estimated from the specific discharge and the actual surface of the upstream catchment drained by the lake.

The reservoir is partly fed by water inflow from riparian areas. Estimate of this contribution different from upstream contribution can be obtained from a similar scaling methodology. This was however ignored in the present study as there is not sufficient data on riparian areas and also the contribution from these riparian areas to the total inflow to the lake is minimal. The temporal structure of the inflow to the lake is the mean temporal structure obtained from the three upstream catchments.

3.2 Determination of Solar PV Power Production Potential

3.2.1 Solar Radiation Resource

SARAH2 hourly Global Horizontal Irradiance (GHI), was selected for 29 grid points as shown in Fig 2.2. A PV panel can be fixed at angle or it can be installed to track the position of the sun. Fixed systems are more common in the West African region because tracking systems are more expensive due to the additional costs of incorporating a tracking system in a PV system's set-up. For fixed PV system applications, panels must be tilted at certain inclination angle depending on the latitude in order to maximize the amount of irradiation received by the panel surface at a given point in time (Li and Lam 2007; Kehinde et al. 2016).

Therefore, SARAH2 GHI radiation data was converted to radiation falling on an inclined surface. The R package *solaR* developed for Radiation and Photovoltaic systems applications (Perpiñán 2012, 2016) was used to convert GHI to solar irradiance falling on a tilted surface. In so doing, we tested a number of different inclination angles from 0 to 90° in steps of 5 to determine the optimum inclination angle for PV panels at each latitude. At each latitude, the tilt angle which receives the maximum irradiation was selected as the optimum.

The optimal inclination obtained with *solaR* for SARAH2 data was compared with the optimal tilt angle given by PVGIS. The optimal angles obtained for both methods tend to agree with each other. They were used in the following to calculate power production by a PV panel. In all, 29 grid points on 6 different latitudes and different longitudinal points covering the whole Ghana territory were selected and used for the calculations.

The clear sky horizontal irradiance (CS-GHI) was also computed. Different models can be used to estimate CS-GHI, depending on available data (Reno et al. 2012). One of the simplest models is Haurwitz model (Haurwitz 1945). Haurwitz model computes the CS-GHI as a function of the solar zenith angle, z only, and is expressed as

$$GHI_{CS} = 1098 \cdot \cos(z) \cdot exp\left(\frac{-0.057}{\cos(z)}\right) \tag{3.3}$$

As with many CS-GHI models, the Haurwitz model has some uncertainties. It is essentially based on empirical correlations and calibration of measurements for a location and astronomical parameters (Reno et al. 2012). The use of the Haurwitz model (and all other simple CS-GHI models) in other locations will therefore introduce some uncertainties.

3.2.2 Power Production Estimated with a Generic Panel

We assume here that in each of the selected grid points (Fig 2.2), there is a generic PV module of 1 kWp capacity. The solar power generation at a given hour *t* and from a particular grid cell *i* depends on the air temperature, T_a (˚C) and the effective irradiance on a tilted plane, I_{eff} (W/m^2), and is given by the following expression (Perpiñan et al. 2007; François et al. 2016)

$$P_{PV}(t) = \sum_{i} B\, I_{eff}(t,i)\big(1 - \mu\big(T_a(t,i) - T_{c,STC}\big) - \mu\, C\, I_{eff}(t,i)\big) \tag{3.4}$$

with B a constant production parameter, defined as the product of the surface area of the PV array (m^2) by the generator and invertor efficiencies (%), and with μ and C respectively the temperature and the radiation dependent efficiency reduction factors (%). $T_{c,STC}$ (˚C) is the photovoltaic cell temperature corresponding to standard test conditions.

3.3 Determination of Wind Power Production Potential

3.3.1 Wind Speed Resource

MERRA-2 wind speed data at 50m elevation (Lawrence et al. 2015; Rienecker et al. 2011) was selected for 8 grid points denoted by an index *i*, over the coastal offshore region of Ghana (see Fig 2.2). The 50m wind speed was scaled to 80m using the Hellman exponential law. Hellman exponential law relates the wind speeds measured at two different heights (Bauelos-Ruedas et al. 2011). It is given by

$$v_1 = v_2 \left(\frac{h_1}{h_2}\right)^a \tag{3.5}$$

where, v_1 and v_2 are the wind speeds at altitudes h_1 and h_2. a is a dimensionless friction coefficient which is a function of topography at a specific site and frequently assumed to be $1/7$.

3.3.2 Power Production with a Generic Wind Turbine

The wind power production was estimated with the power curve of a generic wind turbine. This wind turbine has a rated power of 1000 kW (1 MW). We assume that there is one of such wind turbines in each of the selected grid points. The power curve of this wind turbine is shown in Fig 3.2. A cut-in wind speed value of 2.5 m/s starts to turn the wind turbine and begins power production. The maximum power production is reached after wind speeds reaches 11 m/s. The wind turbine has a cut-off wind speed of 25 m/s and stops working when the wind speeds reaches this values.

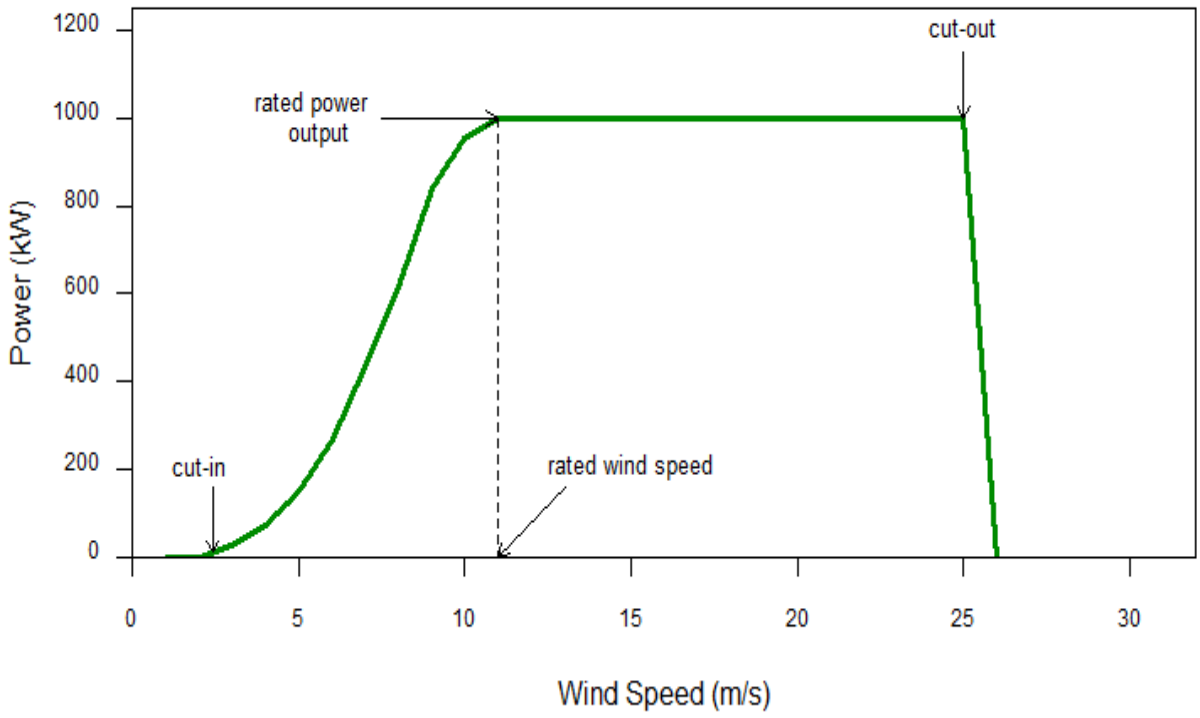

Fig 3.2: Power curve of Leitwind LTW77-1000 wind turbine

The total daily wind power generation for all grid cells for a particular day's average wind speed $P_w(V_m)$ is given by the expression (François et al. 2016),

$$P_w(V_m) = \sum_i \int_0^\infty p_{Vm}(v, i) W(v)\, dv \tag{3.6}$$

where, $W(v)$ is the instantaneous power production in Watts when the wind speed is v and p_{Vm} is the probability density function of the intra-daily wind speed for a grid cell.

The hourly power production for wind speed *v*, at a particular time and for a particular grid cell *i*, were calculated with the power curve of the generic wind turbine. This was done by a linear interpolation of the wind power that correspond to a given wind speed based on the wind power given for the two integers situated up and down of that wind speed.

$$P(v) = p(v_1) + \left(\frac{v - v_1}{v_2 - v_1}\right)(p(v_2) - p(v_1)) \quad (3.7)$$

where, *v* is the wind speed, v_1 is the truncated wind speed to an integer value (*trunc*(v)) and v_2 is $v_1 + 1$.

For a particular day, the daily total production was then determined by summing productions for all the hours in the day. Finally, the total wind power production obtained from the coastal offshore Ghana is computed by summing the daily values for all grid cells.

3.4 Variability and Correlation Between Resources

The variability for each resource has been calculated for different time scales using the coefficient of variation (CV). The coefficient of variation (CV) has been used in several studies (François, et al., 2016) to analyze the relative variability between measured variables.

For wind and solar resources, data is available in hourly time resolutions and therefore the coefficient of variation has been computed for the average daily cycle (intra-daily variation) and also for the seasonal cycle (seasonal variation). The CV for the seasonal cycle of discharge has also been computed and compared with wind and solar resources.

The correlation coefficient (R) between resources has also been computed.

3.5 Simulation of Management Strategy of the Akosombo Reservoir

The operations of the Akosombo power plant needs to be optimized in order to minimized the variability of the residual demand (to be met by some backup production such as thermal) when highly variable renewable energy production is introduced in the power system. For the present study, a deterministic type of Dynamic Programming was used to simulate and optimize the operations of the Akosombo HPP's reservoir. Description of the Dynamic Programming model used to simulate the operations of the Akosombo reservoir is detailed in Appendix A.

3.5.1 Optimal Management Strategy of Akosombo Reservoir

A simplified representation of the Akosombo HPP reservoir system is considered in this study. For simplicity sake, the system considered is assumed to be mainly used for the production of hydroelectricity but the reservoir must at all times maintain a minimum buffer zone (minimum level for ecological sustainability). Also, in the conversion of stored water into energy, we assume that storage level (i.e. elevation) does not influence the efficiency of hydropower generation. This means that one cubic meter of water will produce the same amount of energy whatever the storage level.

Water storage at any given time of the Akosombo dam can be expressed as

$$W_{t+1} = W_t + [q_{in} + P_t - Evap_t - q_{out}] \cdot \Delta t \tag{3.8}$$

where, W (in m^3) is the water storage in the Akosombo dam, q_{in} and q_{out} (in m^3/s) is the water discharge flowing into the Akosombo dam and the water release from the dam respectively, P and $Evap$ (in m^3/s) are the volume of water from precipitation and evaporation over the lake (see Appendix A for the estimation of P and Evap), Δt is the time step from the present day (t) to the next day (t+1).

To conventionally represent the Akosombo dam as a water storage system will require a detailed description of all technical and geometrical characteristics of the dam such was water depth to storage relationship, water depth dependency on efficiency of the different turbines etc. This information is however, not easy to obtain. When water is stored in the reservoir, energy is actually stored (in a different form) since this water can be readily released from the reservoir at any point in time to generate electricity.

Therefore, for this study, the Akosombo reservoir is considered as an "energy storage system", i.e. in this system, we have a storage of energy and not of water. This reservoir is fed by energy inflows from upstream water discharge in a simplified configuration where water from upstream rivers is instantaneously converted to energy and stored. In this analysis, a balance of energy productions and energy demand will be considered. It is therefore easier at this stage to convert all hydrometeorological variables (i.e. discharge, rainfall and evapotranspiration) to energy variables.

The management model can then be applied directly to these energy variables to simulate the optimal management operations of the reservoir. For the present study a very simplified representation of the characteristics of the Akosombo dam will be used to simulate its management strategy. A more detailed and precise representation of the dam would be worth looking at for any future studies.

The conservation equation for this energy storage system is given as

$$S(t+1) = S(t) + [E_{in}(t) - E_{out}(t)] \cdot \Delta t \quad (3.9)$$

where, S is energy storage of the reservoir for a given day in kWh, $E_{in}(t) \cdot \Delta t$ is the daily energy input to the reservoir in kWh, $E_{out}(t) \cdot \Delta t$ is the daily energy output from the reservoir in kWh i.e. the amount of energy released from the dam. Δt stands for the daily time step used for all variables.

The maximum amount of energy that can be released from the reservoir (turbine release capacity) in a given day is derived simply by determining the total amount of water $Q_{max}(t)$, that can be released through the turbines assuming the Akosombo power plant runs at full capacity for 24 hours in a given day (i.e. when $E_{max}(t) = 1020\ MW \times 24\ hours\ [MWh]$)

$$E_{max}(t) = \rho g h Q_{max}(t) \quad (3.10)$$

where, ρ is the density of water (in $kg\ m^{-3}$), g is the acceleration due to gravity ($9.8\ m\ s^{-2}$), h is the head of water in the reservoir (in m).

In most reservoir systems, an environmental flow regulation ensures the minimum amount water (energy) that can be released at a given time to ensure ecological sustainability. However, this value has not been found from literature on the Volta Lake and thus the minimum amount of energy that can be released from the Akosombo reservoir was set to the 95th percentile of the energy inflows into the reservoir i.e. the flow value that is below that natural flow 95% of the time.

The release capacity and minimum releases through the turbines will be used as constraints in the management model.

In Equation 3.9, energy input to the reservoir $E_{in}(t) \cdot \Delta t$, is simply derived from the amount of water $Q_{in}(t) \cdot \Delta t$, that flows into the reservoir from the upstream rivers during the time step $[t, t + \Delta t]$.

$$E_{in}(t) = \rho g h \, Q_{in}(t) \tag{3.11}$$

where, $Q_{in}(t)$ is obtained via the following mass conservation equation applied to the reservoir

$$Q_{in}(t) = Q(t) + P(t) - ET(t) \tag{3.12}$$

where, $Q(t)$, is the inflow discharge from the upstream rivers, P(t) is the mean areal precipitation intensity that falls directly on the reservoir, $ET(t)$ is the mean areal evaporation loss from the reservoir.

As solar and wind energy are not stored, in an instance where there is very high generation from them, DDP will use this generation and conserve the water in the hydropower reservoir for later use. The conserved water will be released when there is minimal production from VRE. In a situation when generation from VRE is greater than the demand, the surplus energy will have to be wasted as there is no storage facility considered in this study.

In the entire power system, hydro, solar and wind productions will supply a portion of the demand in a given day. The remaining demand is referred to as the residual to be met by a backup capacity (this will practically be obtained from thermal production in Ghana). Eventually, for a given time t (one day), backup needs are given by the equation

$$BackUp(t) = L(t) - \{P_H(t) + P_{PV}(t) + P_W(t)\} \tag{3.13}$$

where $P_H(t)$and $L(t)$ are the energy produced from the Akosombo HPP, the energy demand at a given time t. $P_{PV}(t)$ and $P_W(t)$ are the energy generation from solar and wind respectively.

The objective function for DDP was thus chosen accordingly to the aforementioned objective. It aims to minimize the squared deviation between the demand and the generation from hydro, PV and wind. Minimization applies to the sum of instantaneous backup power over the whole

simulation period (1992-2011). The objective function g, depending on energy release from the reservoir u_{t_i}, the electricity demand L_{t_i} and the VRE production E_{t_i} is expressed as

$$g\left(u_{t_i}, L_{t_i}, E_{t_i}\right) = \sum_{i=1}^{n} \{\min(P_H(t) + P_{PV}(t) + P_W(t) - L(t), 0)\}^2 \quad (3.14)$$

3.5.1.1 Present Demand-Production Scenario

We consider the different simplifications and hypotheses below:

1. The mean annual energy production is equal to the mean annual demand L_o for a given time (t) during the whole simulation period.

The present (reference) configuration of the electricity system in Ghana for the considered period (i.e. 1992-2011) does not include any production from VRE sources. Therefore,

$$P_H(t) + BackUp(t) = L_o(t) \quad (3.15)$$

Based on available annual generation data published by the Energy Commission of Ghana (2017) for a 16-year period as shown in Fig 3.3, we find that electricity generation from the Akosombo plant accounted for an average of 57 % to the nation's total generation for this 16-year period. For this reason, the proportion of hydroelectricity production in the energy mix was set in the reference configuration to 0.57 (57%).

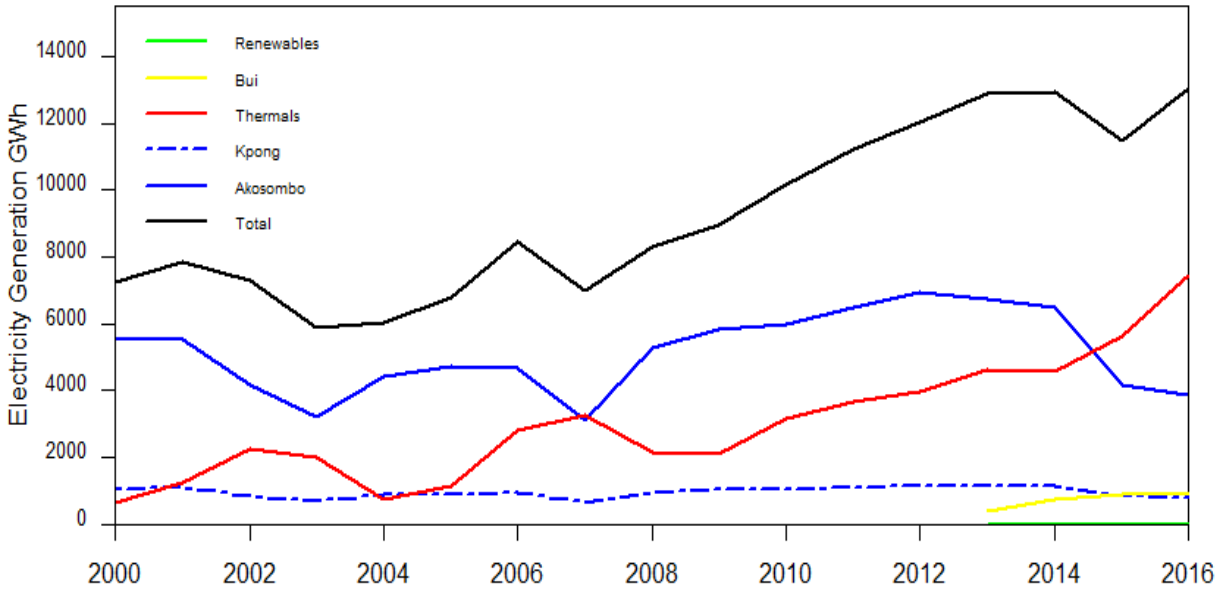

Fig 3.3: Electricity generation in Ghana by plant (2000-2016)

2. The temporal pattern of the demand is the normalized average seasonal demand cycle estimated from the time series of electricity demand for different mega poles of Guinean region (Kondi et al. 2016).

It has a significant seasonality with lower demand in the summer period due to lower cooling requirements of buildings as shown in Fig 3.4. The annual demand cycle for 2016 in Ghana has been published by the Energy Commission of Ghana and was compared with the average seasonal demand cycle in the study cited above as shown in Fig 3.4. It can be seen that the seasonality of the demand is represented well by estimation of Kondi et al., (2016) and has therefore been adapted for the present study. We disregard the trend in the annual demand that would have resulted (for the simulation period) from population growth over the simulation period.

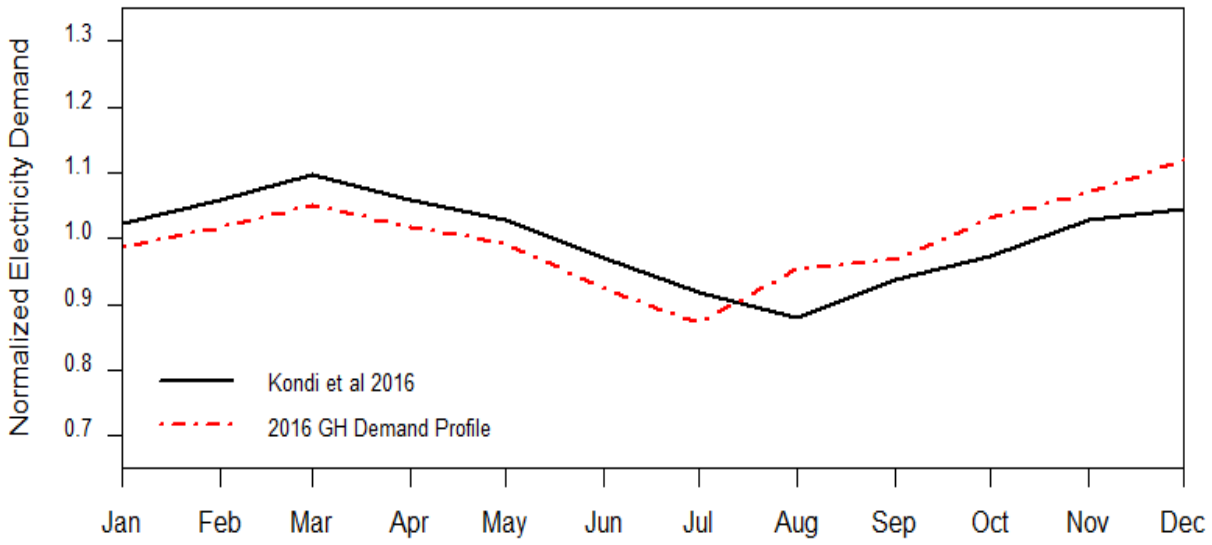

Fig 3.4: Electricity demand cycles (comparison between the 2016 actual demand cycle of Ghana and the average seasonal demand cycle by Kondi et al. 2016)

3.5.1.2 Future Demand-Production Scenarios

We consider a number of different scenarios for the future power system in Ghana. For future scenarios, we assume,

1. No change in water inflows to the lake.

2. The mean annual demand L_0 is increased by n%. The new demand L_{new} will thus be the sum of the initial demand and the extra demand L_{extra}

$$L_{new} = L_o + L_{extra} \tag{3.16}$$

where, $L_{extra} = n(L_o)$

3. The extra demand is covered with a mix solar and wind power production (VRE) in Ghana. Mean VRE production over the whole simulation period is such that, VRE production is equal to L_{extra} with α% from wind and (1-α)% from solar i.e.

$$VRE = WindProd + SolProd \tag{3.17}$$

where, $WindProd = \alpha(\ L_{extra})$ and $SolProd = (1 - \alpha)\ L_{extra}$ are the mean production from wind and solar for the entire simulation period.

The production from wind for a given time t, is defined as

$$P_W(t) = \ P_{W_i} \cdot (t) \times [WindProd/mean(P_W \cdot (t))] \tag{3.18}$$

where, $P_W \cdot (t)$ is the wind production time series obtained from wind turbine described in Section 3.3 for the selected region of Ghana. We thus assume here that, the temporal fluctuation of wind production within each future scenario is that obtained from the computations presented in Section 3.3.

Similarly, the production from solar for a given time t, is defined as

$$P_{PV}(t) = \ P_{PV_i} \cdot (t) \times [SolProd/mean(P_{PV} \cdot (t))] \tag{3.19}$$

where, $P_{PV} \cdot (t)$ is the solar power production time series obtained from the PV module described in Section 3.2. We here also assume that, the temporal fluctuation of solar production within each future scenario is that obtained from the computations presented in Section 3.2.

Different configurations of the power system including VRE production with different mixes of solar and wind were considered and simulated as future scenarios. The management of the reservoir was adapted and optimized with DDP with a main aim to minimize the variability of production from the backup power system. Table 3.2 summarizes the different future scenarios considered and the reference scenario.

Table 3.2: Description of Reference and future scenarios to be simulated with DDP

	Scenario	Demand Increase (n)	α	Share of Solar in L_{extra} (%)	Share of Wind in L_{extra} (%)
Reference	Present	0	0	0	0
Near-Future	FConfg 1	0.5	0.25	75	25
	FConfg 2	0.5	0.5	50	50
	FConfg 3	0.5	0.75	25	75
Intermediate-Future	FConfg 4	1	0.25	75	25
	FConfg 5	1	0.5	50	50
	FConfg 6	1	0.75	25	75
Far-Future	FConfg 7	2	0.25	75	25
	FConfg 8	2	0.5	50	50
	FConfg 9	2	0.75	25	75

4 RESULTS AND DISCUSSIONS

4.1 Water Input and Losses from the Akosombo Reservoir

We present in this section water inputs and losses from the Akosombo reservoir which are important inputs to the management model. Inputs include discharge (water inflow) and precipitation whiles losses include evaporation, and water extraction for irrigation and domestic purpose. Since these variables are just inputs for the management model, in-depth analysis on them have not been made. We just here give a rough description of their temporal variability.

4.1.1 Water Inflows into the Reservoir

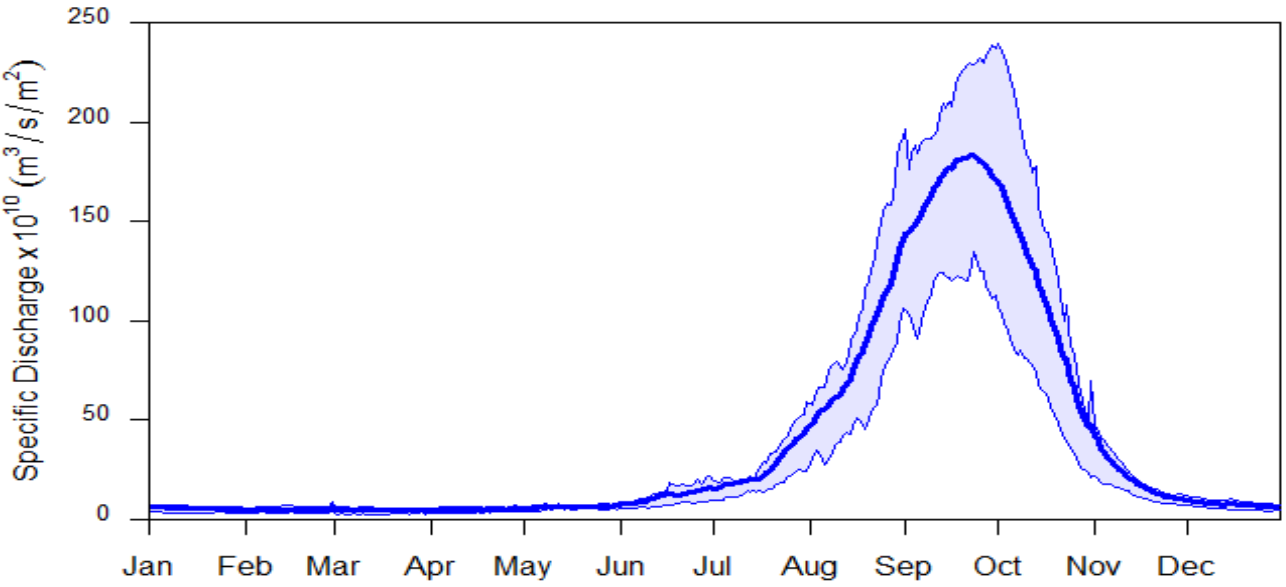

Fig 4.1: Average annual mean specific discharge into the Volta Lake with 75th and 25th percentiles (1992 – 2011). Estimates from the discharges observations available for the 3 upstream basins

The average annual cycle of estimated inflows into the Volta Lake is shown in Fig 4.1. They are low from January to July. They increase gradually from July after the start of the rainy season and reaches a maximum during the September and October months. They then drop gradually again reaching a low in December.

Some years have lower inflows into the lake (Kabo-Bah et al. 2016). This was due to reduced rainfall levels during those years and effects of land cover and land use changes (Akpoti et al. 2016; Obahoundje et al. 2016).

4.1.2 Precipitation on the Reservoir Surface

The average daily cycle (1992 – 2011) of precipitation recorded at the different stations around the lake is shown in Fig 4.2.

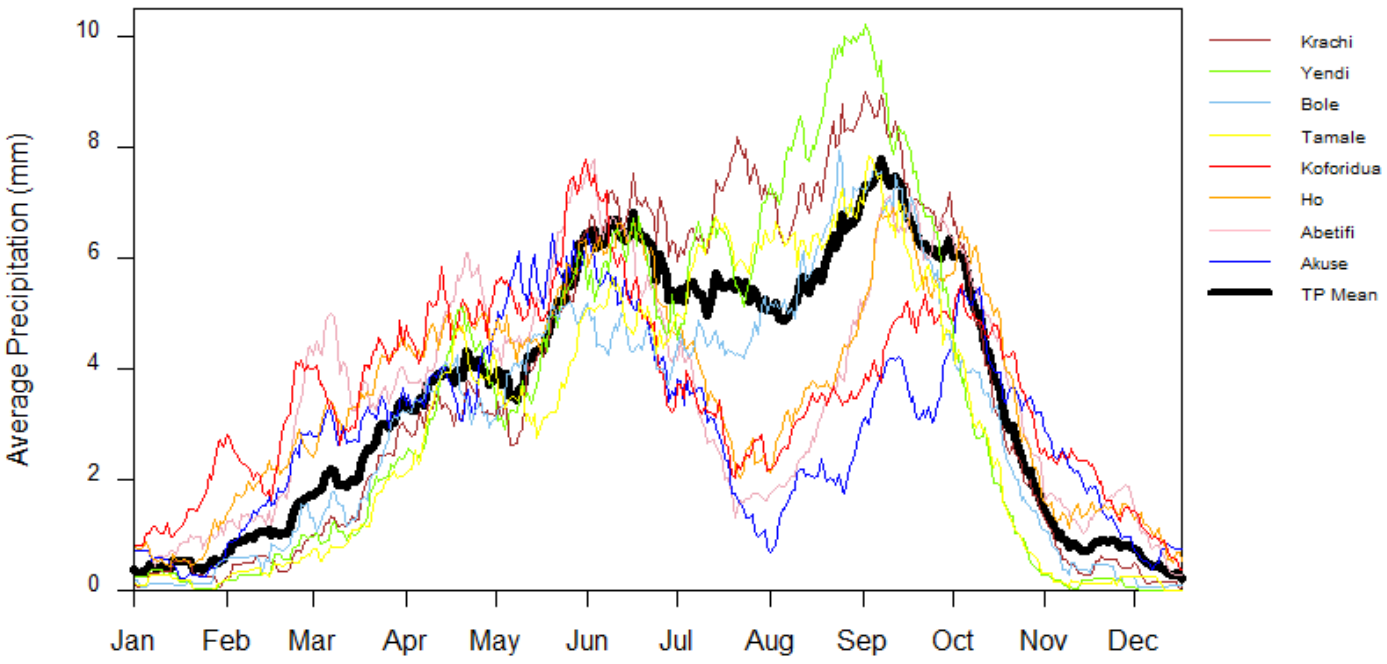

Fig 4.2: Comparison of daily average precipitation (1992-2011) Black : weighted mean of the stations (Thiessen weights).

Four stations in the southernmost part of the country show a strongly marked bimodal profile unlike the stations north of the country. The Krachi station which is relatively the closest to the lake surface and Yendi station show slightly higher average values than the areal average precipitation especially during the rainy season. Table 4.1 shows the total annual average precipitation values of all stations and the total annual average precipitation.

Table 4.1: Total annual average precipitation (1992-2011)

Station	**Annual Precipitation (mm)**
Kete-Krachi	1326
Abetifi	1259
Akuse	1037
Ho	1267
Koforidua	1274
Yendi	1240
Bole	1096
Tamale	1072
TP areal average	**1270**

4.1.3 Evaporation from the Reservoir Surface

The average annual cycle of the evaporation is shown in Fig 4.3. Evaporation is maximum during February and March, minimum during the rainy season during July and August. the annual profile of evaporation follows the annual cycle of temperature (Fig 4.8), with periods of high average temperature also having high evaporation from the reservoir surface and vice versa.

Losses from irrigation and domestic water extraction have not been included in the management model due to lack of data on them.

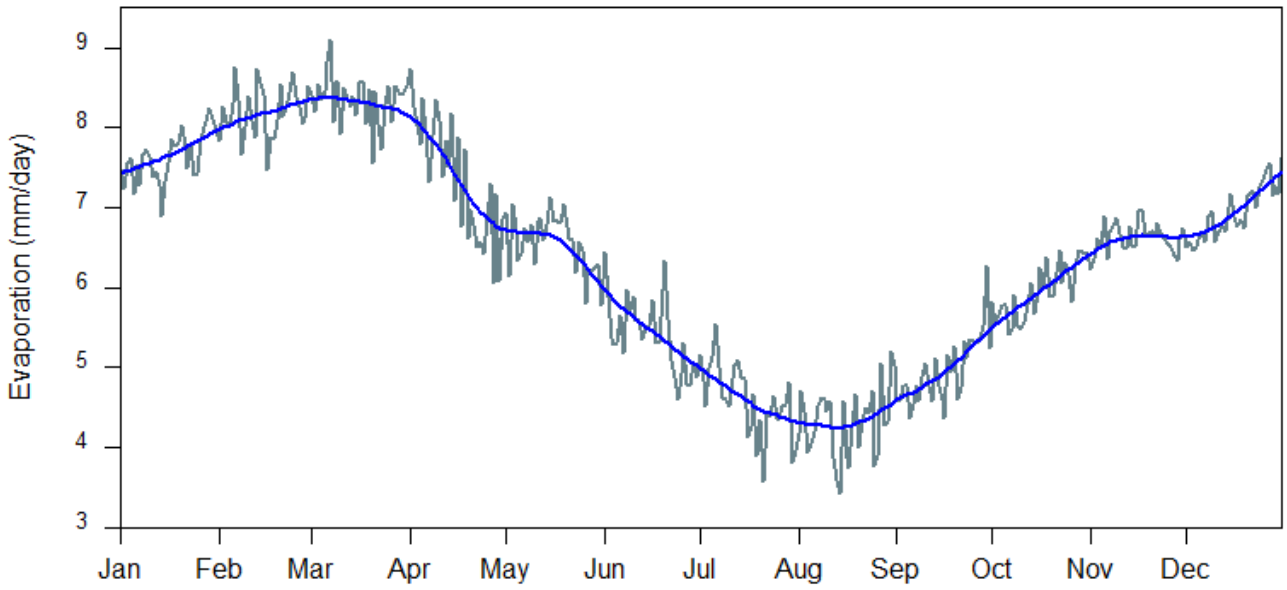

Fig 4.3: Annual cycle of evaporation from the surface of Lake Volta

4.2 Solar Radiation and Power Production

4.2.1 Optimum Inclination Angles for PV Modules

For each latitude, the irradiation falling on a tilted plane has been calculated for several PV module inclination angles. The yearly average of daily sum of irradiation as a function of inclination angle at different latitudinal positions is shown in Fig 4.4 (see Appendix B1 for detailed results). A small difference between two inclination angles does not significantly change the mean annual irradiation. However, significant differences are obtained between the optimal inclination (around 20°) and large ones (more than 100% of decrease/increase).

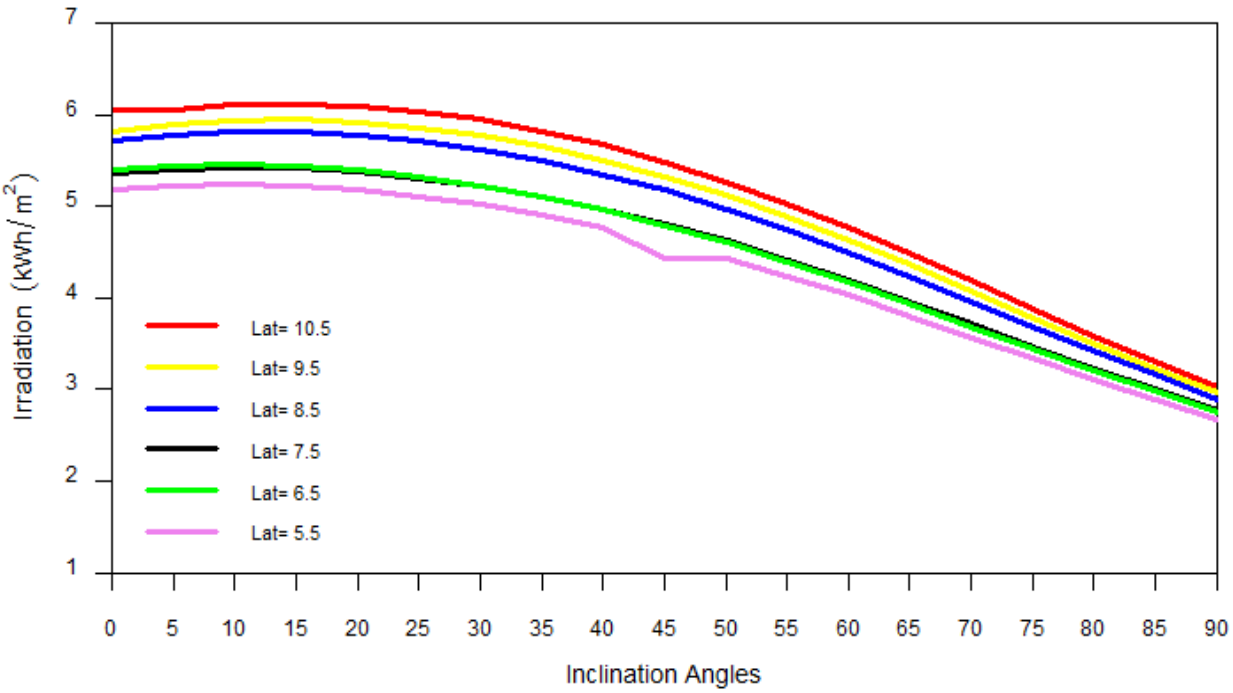

Fig 4.4: Dependence of annual average total daily irradiation on inclination angle

The optimum tilt angle determined with *solaR* calculations thus tend to agree with the optimum angles given by the PVGIS web application (see Table 4.2 for PVGIS optimum angles)

Table 4.2: Optimum inclination angles for different latitudes provided by PVGIS

Lat/Lon	PVGIS Optimum Inclination (°)
10.5°/-2.4°	14
9.5°/-2.4°	13
8.5°/-2.4°	13
7.5°/-2.4°	11
6.5°/-2.4°	10
5.5°/-2.4°	9

4.2.2 Spatial and Temporal Variability of Solar Radiation

The average daily sum of irradiation per square meter (kWh/m^2) was compared for each selected longitudinal point on a latitude. At most latitudes, longitude has very little influence on the daily total irradiation received on a plane (see Appendix B2 for Figures). At shorter timescales however, longitude is expected to have much more influence on irradiation received.

The daily average total irradiation received at a given latitude was then computed from the individual longitudinal irradiation values at that latitude. In all six different irradiation time series were obtained for the six latitudes. These were compared as shown in Fig 4.5. The lower latitudes have lower irradiation values compared to the higher latitude (solid curves), but these differences are not very much. This is in line with the study of IRENA (2015) on the potential of solar energy in Ghana. These difference are likely due to meteorological and physical factors.

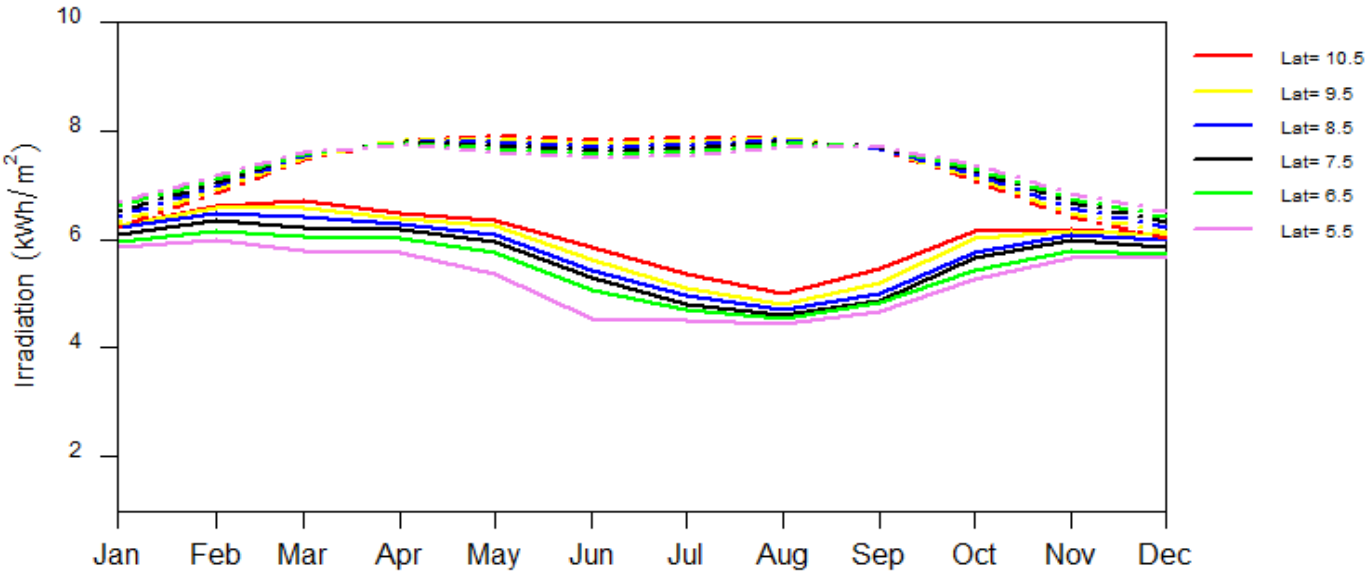

Fig 4.5: Dependence of average total daily irradiation on latitude and comparison with clear sky radiation. The clear sky horizontal radiation is computed with the Haurwitz CS-model (see Section 3.2.1 for Haurwitz model estimation)

In the northern hemisphere, the length of daylight period is longer during the summer and therefore in a clear sky atmosphere configuration where radiation only depends on astronomical effects, radiation received will be higher during the summer (see dashed curves on Fig 4.5). However, minimum radiation is observed for all latitudes during the summer months (see solid curves on Fig 4.5). This is due to the high nebulosity due to the monsoon arrival and the high convective activity in this region.

The average irradiation for the whole region show a similar temporal variation as the individual latitudinal irradiation variation. The maximum values were recorded in the dry months of November to March whiles the minimum irradiation values were recorded in the rainy season as shown in Fig 4.6 (red curve). For the whole region, the mean annual irradiation is 5.7 kWh/m^2 and the standard deviation is 0.9 kWh/m^2. The coefficient of variation for the considered period is 16 %.

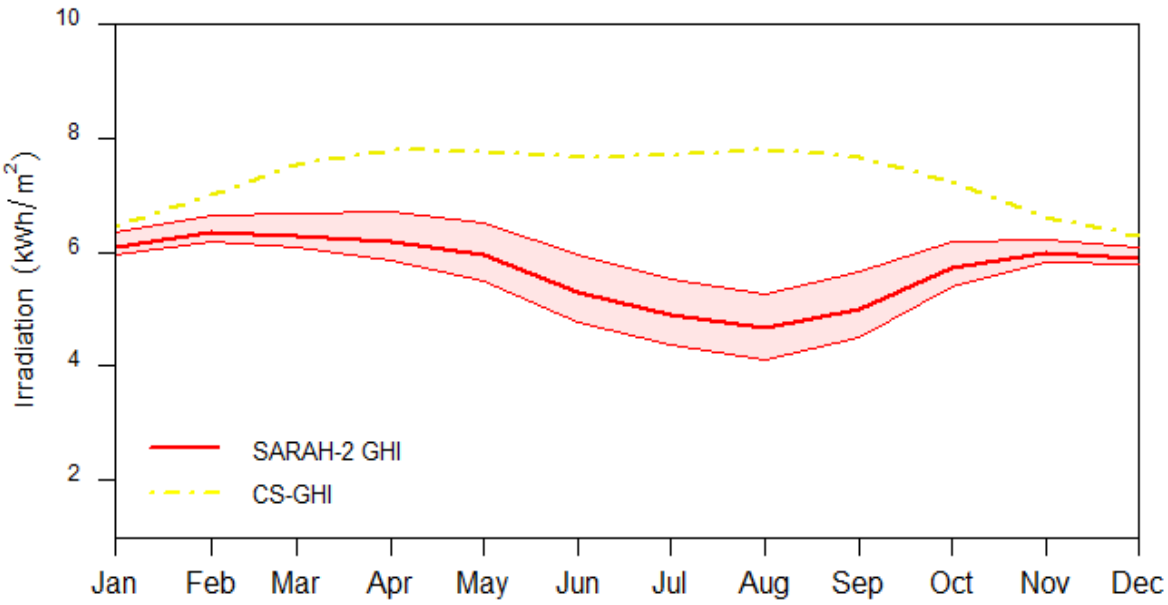

Fig 4.6: Annual cycle of average daily sum of irradiation per square meter (kWh/m2) for Ghana (1991-2011)

The average sub-daily cycle of irradiance for the whole period considered is shown in Fig 4.7 (see Appendix B2 for detailed description of on sub-daily variations in all months)

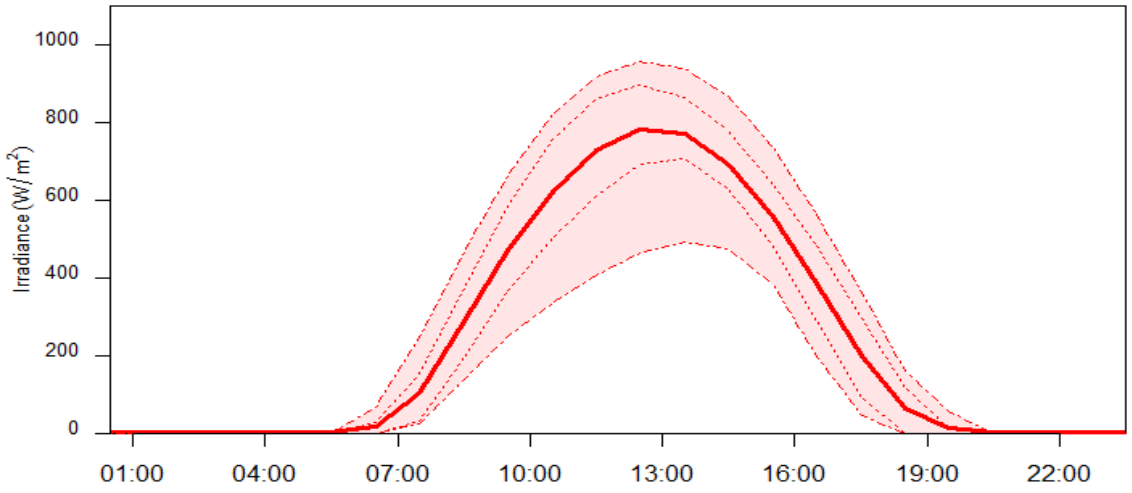

Fig 4.7: Average sub-daily variation of solar radiation (from bottom to top: 5th, 25th, 50th [mean], 75th, and 95th percentiles)

4.2.3 Solar Power Production

The average yearly cycle of solar power production (kWh) over Ghana is shown in Fig 4.8. Lower power production values were observed during the rainy season months while the dry season months have higher power productions. This pattern was expected however, as from Equation 3.4, solar power production depends on the available solar radiation which shows similar variation pattern (see Fig 4.6). Hence, average sub-daily cycle of solar power production is also expected to follow a similar shape as shown in Fig 4.7 with higher power production during the mid-day when solar radiation reaching the panels is greatest and no production at night as there is no incoming solar radiation. For the annual cycle, the mean power production was calculated to be 4 kWh with a standard deviation of 0.7 kWh. Further details on the variability of the annual cycle of solar power production will be discussed in Section 4.4.

The average annual cycle of the air temperature over Ghana is shown also on Fig 4.8. The average air temperature in the annual cycle ranges from 24°C to 31°C is highest during the months of March, April and May and lowest during July and August. Very high temperatures reduce the efficiency of PV modules, reducing power production. However, air temperatures shown here are mean daily values, and therefore do not clearly show the effect of high temperatures on PV modules' performance. Air temperature values at smaller time scales are likely to show the effects of very high temperatures on PV modules' efficiency.

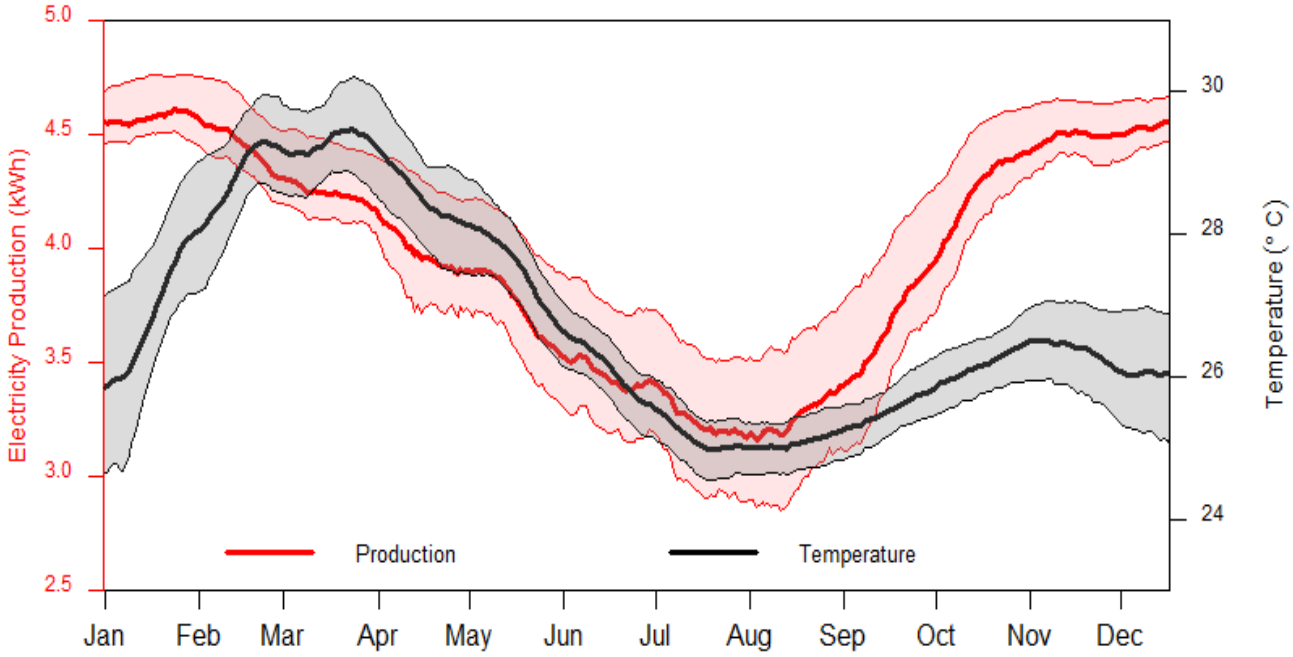

Fig 4.8: Average annual cycles of solar power production (with 25th and 75th percentiles – thin red curves) and air temperature (with 25th and 75th percentiles – thin black curves, Temperature Data Source: MERRA Reanalysis) (1992-2011)

Average annual solar power production was calculated for each year of the 1992 to 2011 period. It presents a rather negligible inter-annual variability (Fig 4.9). Inter-annual average solar production deviated between -1.5 % and 1.2 % of the mean of the period considered indicating no significant inter-annual variation.

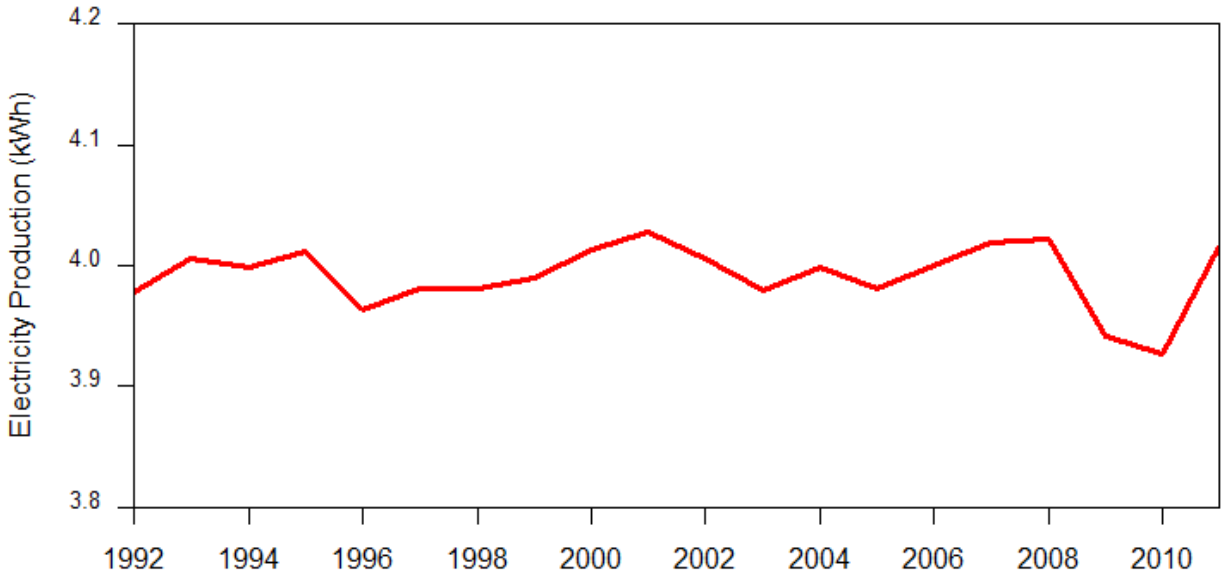

Fig 4.9: Mean Inter-annual solar power production

4.3 Wind Speed Resource and Power Production

4.3.1 Spatial and Temporal Variability of Wind Speed

For each of the selected grid points for siting wind farms, the average annual cycle of daily mean wind speed is shown in Fig 4.10. All grid points exhibit similar annual cycle of mean wind speed with higher intensities during the rainy season while the dry months (Nov, Dec and Jan) have lower wind speeds. This result also indicate that average wind speeds are relatively higher on the eastern coast of the country. This result is in line with various studies (WWEA Technical Committee, 2014; German Federal Ministry for Economic Affairs and Energy, 2015) The eastern coast of the country is therefore relatively favorable for siting wind farms.

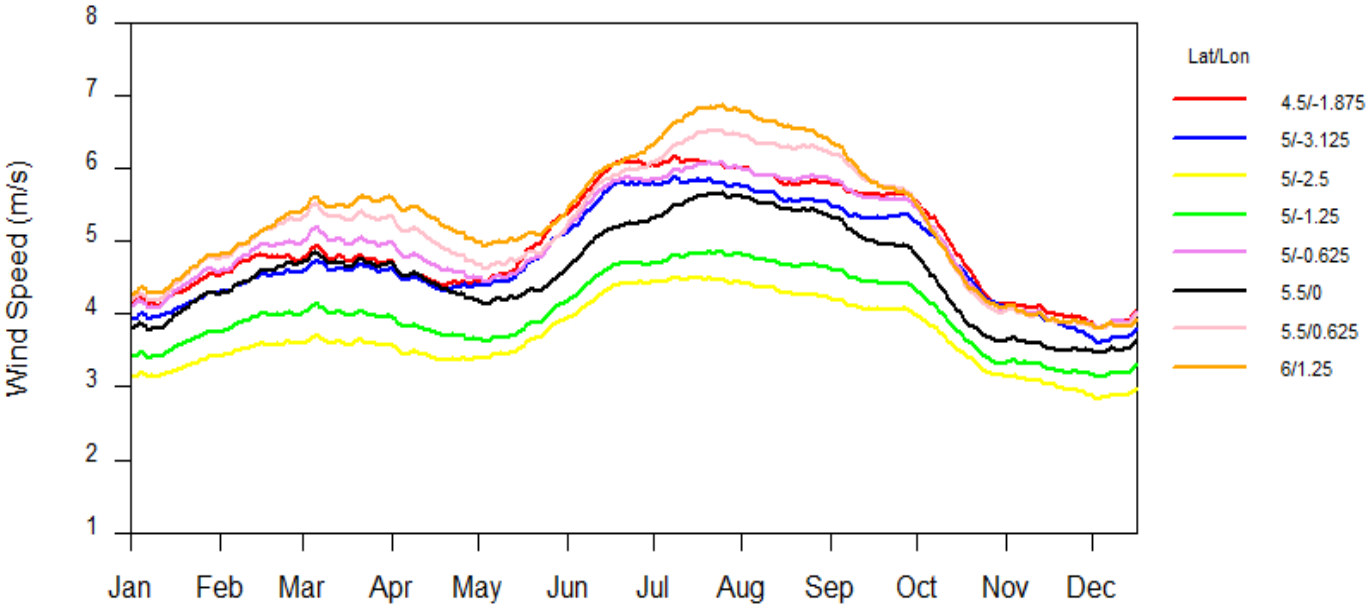

Fig 4.10: Average annual cycle of daily mean wind speed at selected lat/lon locations (1992-2011)

The average annual cycle daily mean wind speed over the whole coastal offshore region is presented in Fig 4.11. The mean wind speed is 4.7 m/s and the standard deviation value of 0.7 m/s over the average cycle.

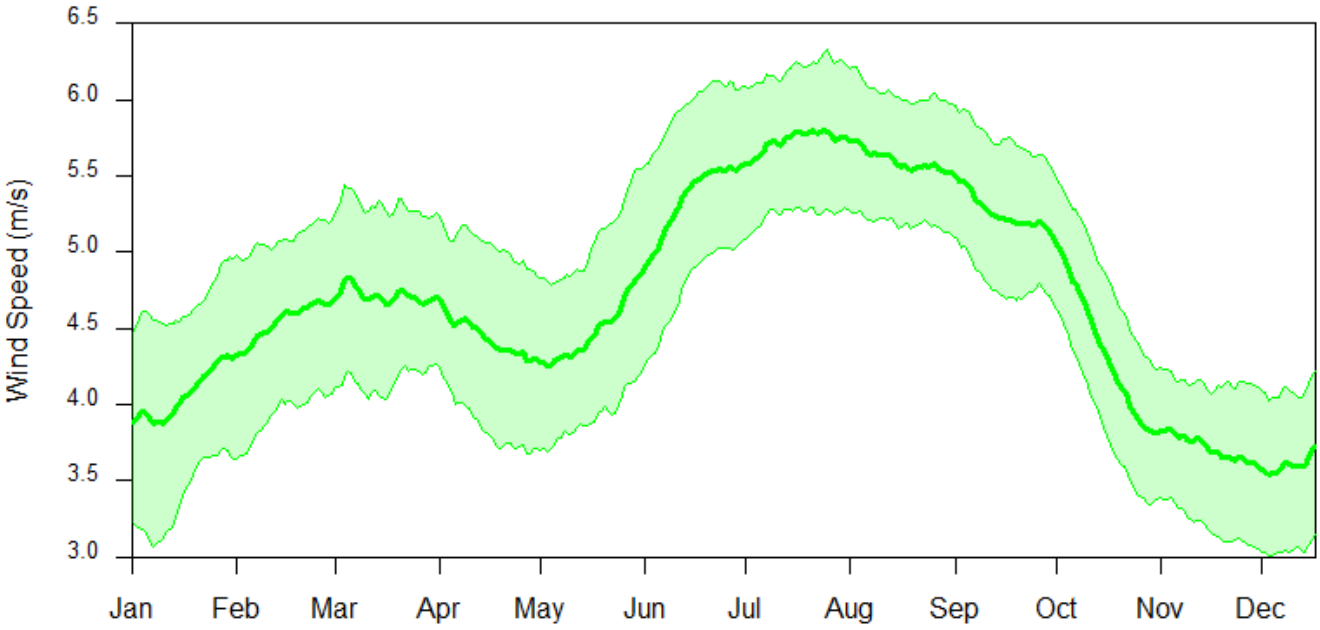

Fig 4.11: Average annual cycle of daily mean wind speed at 80m with the 25th and 75th percentiles (1992-2011)

The average sub-daily variation of wind speed over the entire region is presented in Fig 4.12. Lower wind speeds are observed in the late morning to midday while the intensities rise steadily from the late afternoon into the evening and night. Maximum power production from the wind turbines are thus expected to be attained during the evening and nighttime.

It is important to note that, the average sub-daily pattern of wind speed in most months of the calendar year exhibits similar cycle with the exception of April, May and June. In these months, there is no clear sub-daily pattern of wind speeds with some days having high wind speeds in the evening while other days exhibit the opposite situation. This will therefore lead to a high variation of production within a day for those months. Detailed figures for average sub-daily wind speed pattern in all months and also the sub-daily pattern for some days in April, May and June are presented in Appendix C.

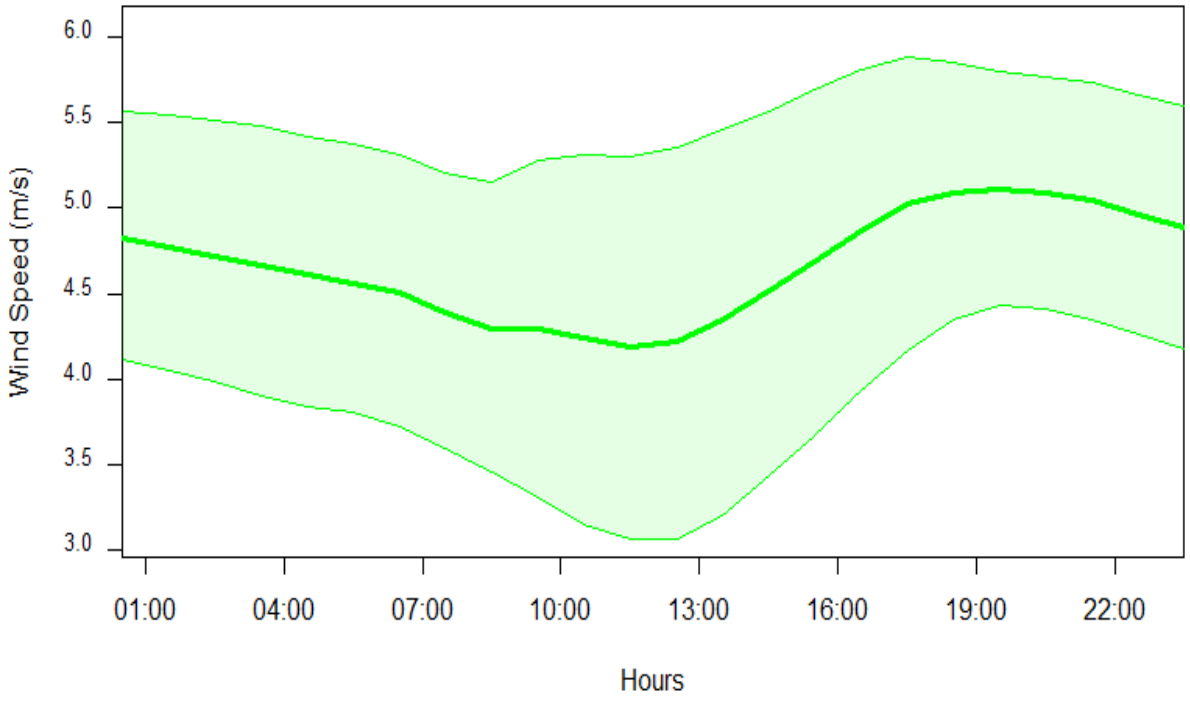

Fig 4.12: Average sub-daily variation of wind speed over the whole region

4.3.2 Wind Power Production

The average annual cycle of daily power production (kWh) at 80m for the whole coastal offshore region of Ghana is shown in Fig 4.13. Generally, lower power production values were recorded for days in the dry season (November, December and January) similar to Fig 4.11. Conversely, power productions are much higher on the average for days in the rainy season in the months of July to September. With one turbine in each of the 8 selected regions, the mean of total daily productions for the period of consideration is 31100 kWh with a standard deviation of 19900 kWh signifying a high variation of power production. A high variation characterizes the average annual cycle of power productions with a relative percentage difference of 145 % between the maximum and minimum production values taking their mean as a reference. The CV of annual wind power production is discussed in Section 4.4. The average sub-daily pattern of wind power production is

expected to follow the sub-daily pattern of wind speed (see Fig 4.12) as production directly depends on wind speeds.

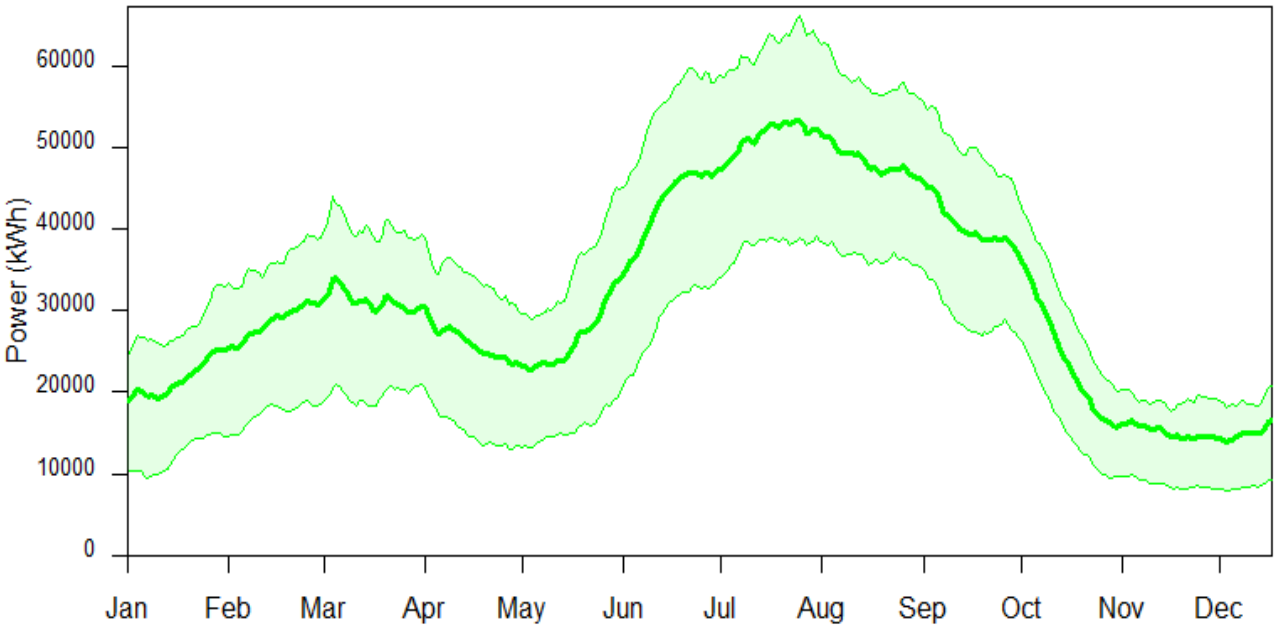

Fig 4.13: Average annual cycle of wind power generation at 80m elevation with 25th and 75th percentiles (1992-2011)

There is little variability in the average annual power production from one year to the other as shown in Fig 4.14. Changes from one year to the other are not so high as compared to the seasonal and intra-daily cycles which are very significant. With a mean of 31100 kWh, the average inter-annual productions vary between minimum and maximum values of 26600 kWh and 36100 kWh. In terms of percentage deviations, inter-annual power productions deviated between -15 % and 15 % of the mean of the period of consideration.

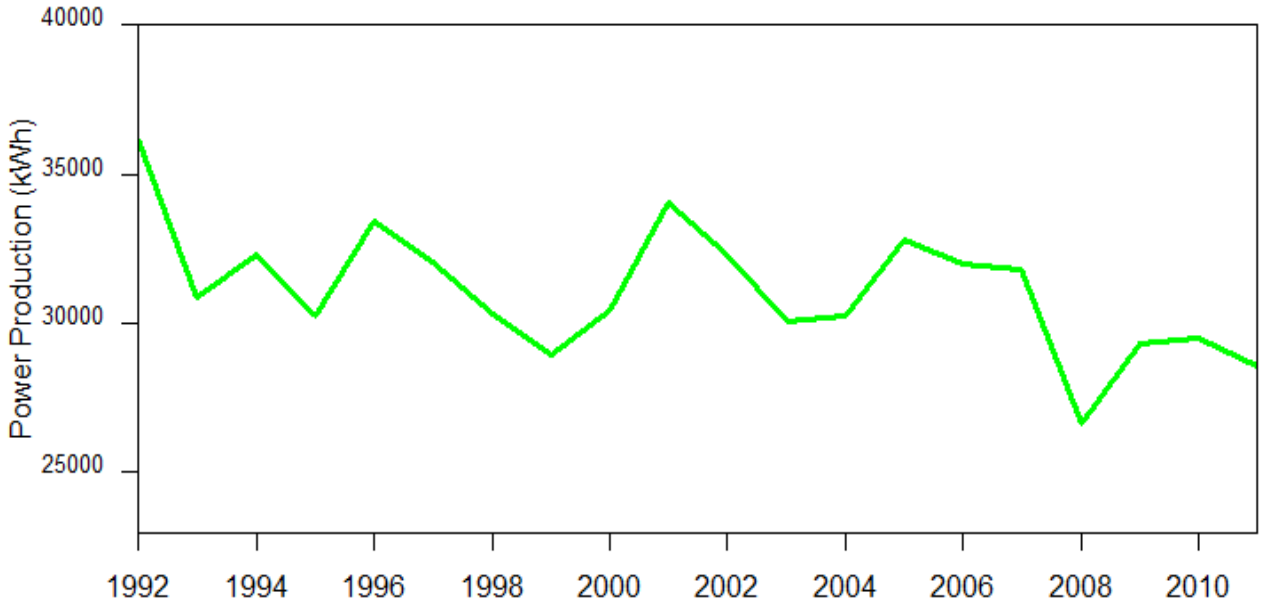

Fig 4.14: Inter-annual average wind power production

4.4 Correlation Between VRE Production and Discharge into Lake Volta

In Fig 4.15, we present a synthesized comparison of normalized average annual cycles of VRE productions (wind and solar) and the inflows to the Akosombo hydropower reservoir for the period 1992-2011. The red and green curves show mean and percentiles (25^{th} and 75^{th}) of solar and wind power production cycles respectively and the blue curve shows the mean cycle of inflows into the Akosombo HPP reservoir (Lake Volta).

On the average, solar power production remains almost the same during the whole year with just slight reduction in production during the rainy season. During this same period (i.e. the rainy season), the production from wind is very high. We show on Fig 4.15 the average annual cycle

and thus it is important to highlight the anti-correlation (or correlation) between wind and solar production but also inflows into the reservoir on different aggregation temporal scales. We use the correlation coefficient R, to identify the temporal opposition (or correlation) between wind and solar production and inflows to the reservoir. VRE production and inflows have been aggregated into hourly (for wind and solar only), daily, weekly, monthly and annual time scales (see Table 4.3)

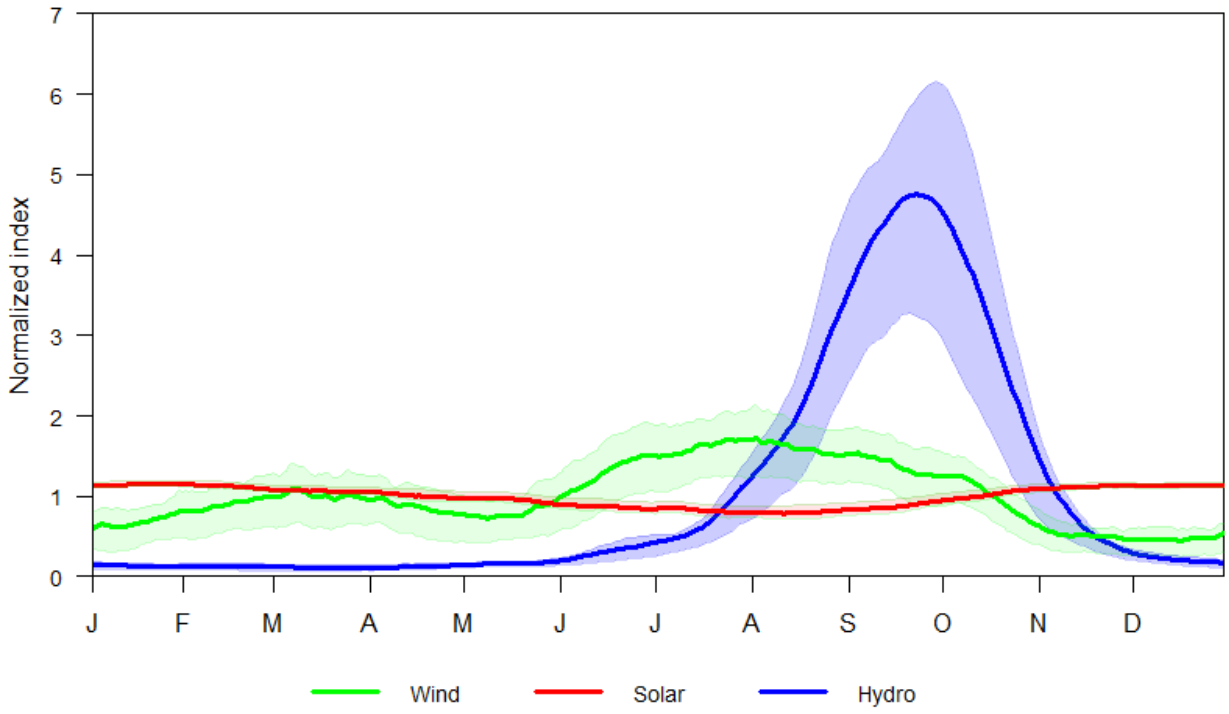

Fig 4.15: Comparison of normalized average annual cycles of VRE production and inflows into Volta Lake (MSD)

Solar and wind productions are anti-correlated for all aggregated timescales considered except for the yearly aggregations which shows a very weak correlation (0.05) between them. This shows that wind and solar productions are somehow complementary at the smaller time scales i.e. wind production can be used when solar production is minimal. Especially, it has been shown that, wind production is mostly high at night (in Fig 4.12) when there is no solar production. Therefore, wind will be used in place of solar at night. On hourly time scale, solar production has very high variability compared to wind production (no discharge data at hourly timescale hence this is not compared).

Table 4.3: Calculated correlation coefficients for different timescale aggregations between wind, solar and MSD

	R (in aggregated Temporal Scales)				
	Hourly	**Daily**	**Weekly**	**Monthly**	**Yearly**
Solar vs Wind	-0.162	-0.54	-0.73	-0.84	0.05
Solar vs MSD	-	-0.31	-0.38	-0.41	-0.43
Wind vs MSD	-	0.24	0.32	0.37	-0.61

Seasonally, solar production has a much lower variability than wind and MSD (Mean Specific Discharge). This is shown by the coefficient of variation (CV) in Table 4.3. MSD shows a strong distinctive seasonal variation and has the highest variability (CV = 141.7%) of all resources in the average annual cycle due to its distinctly marked seasonal variability (Seasonal variability of MSD is 11 times higher than solar power production and about 3 times higher than wind power production).

Annual average solar and wind power productions have a relatively small year to year variability compared to MSD (see Fig 4.16) which has a high inter-annual variability (Table 4.4). For instance, the inter-annual variability of MSD is 8 times higher than wind.

Table 4.4: Coefficients of variation for solar and wind production and MSD

	CV (%)	
	Seasonal	**Inter-Annual**
Solar	12.6	0.7
Wind	40.6	6.9
MSD	141.7	57.4

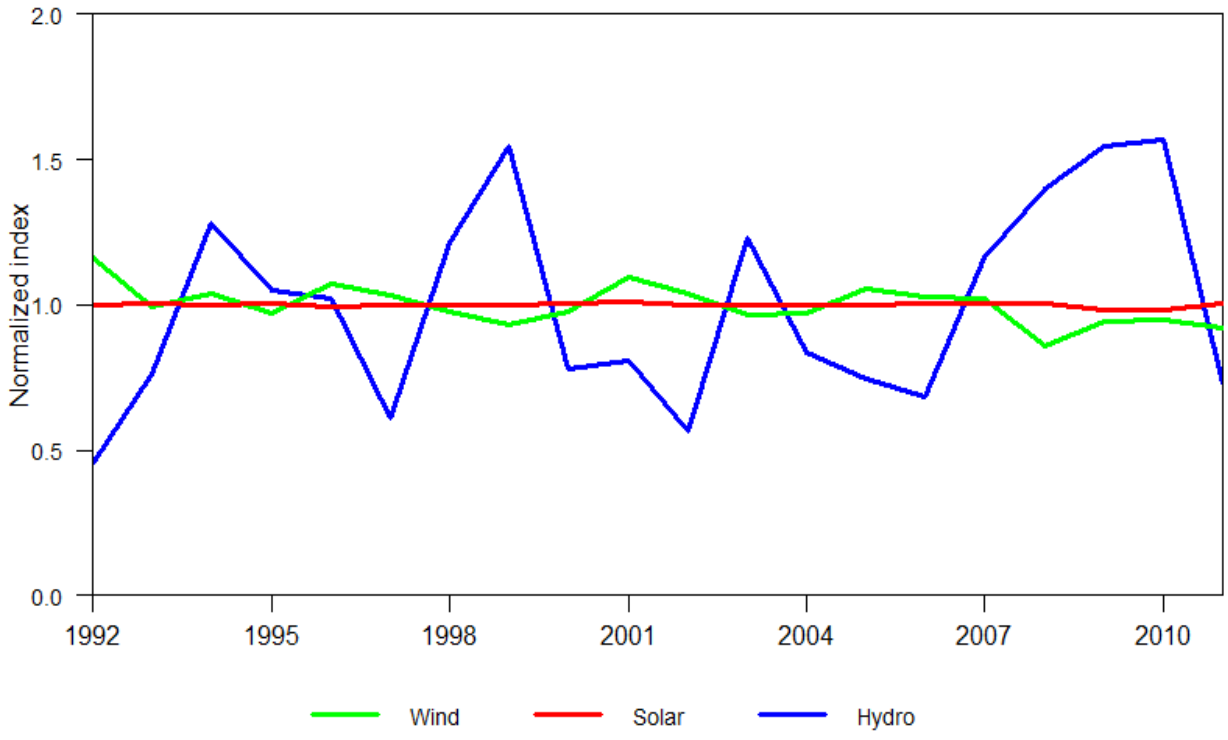

Fig 4.16: Normalized inter-annual variability of solar, wind and MSD (hydro)

4.5 Management Strategy of Akosombo Hydropower Reservoir

4.5.1 Optimizing Reservoir Operations to Minimize Residual Demand Variability

The impacts of VRE production on the storage scheme of the Akosombo reservoir is presented in this section. First we look at optimizing the management of the reservoir to achieve the objective of minimizing the variability of residual demand. Secondly we look at the impacts of different VRE production configurations on the storage scheme of the Akosombo dam.

4.5.1.1 Present Day Configuration (Reference Case)

Fig 4.17 shows the electricity production and its variability in the present (reference) scenario. Here, the pattern of hydropower production is the same from one year to the other. This is because

a constant pattern of average seasonal demand (Kondi et al., 2016) was used for all years in the simulation period, so that the influence of increasing trend due to population growth was ignored. The management strategy of the reservoir was optimized such that, the variability of residual demand to be met by the backup production (for example gas production) is minimized. The variability of backup production [1] obtained after DDP optimization in the reference scenario is relatively smaller then hydro (Fig 4.17). Within the simulation, the CV for the backup and hydro productions is about 2 % and 13 % respectively.

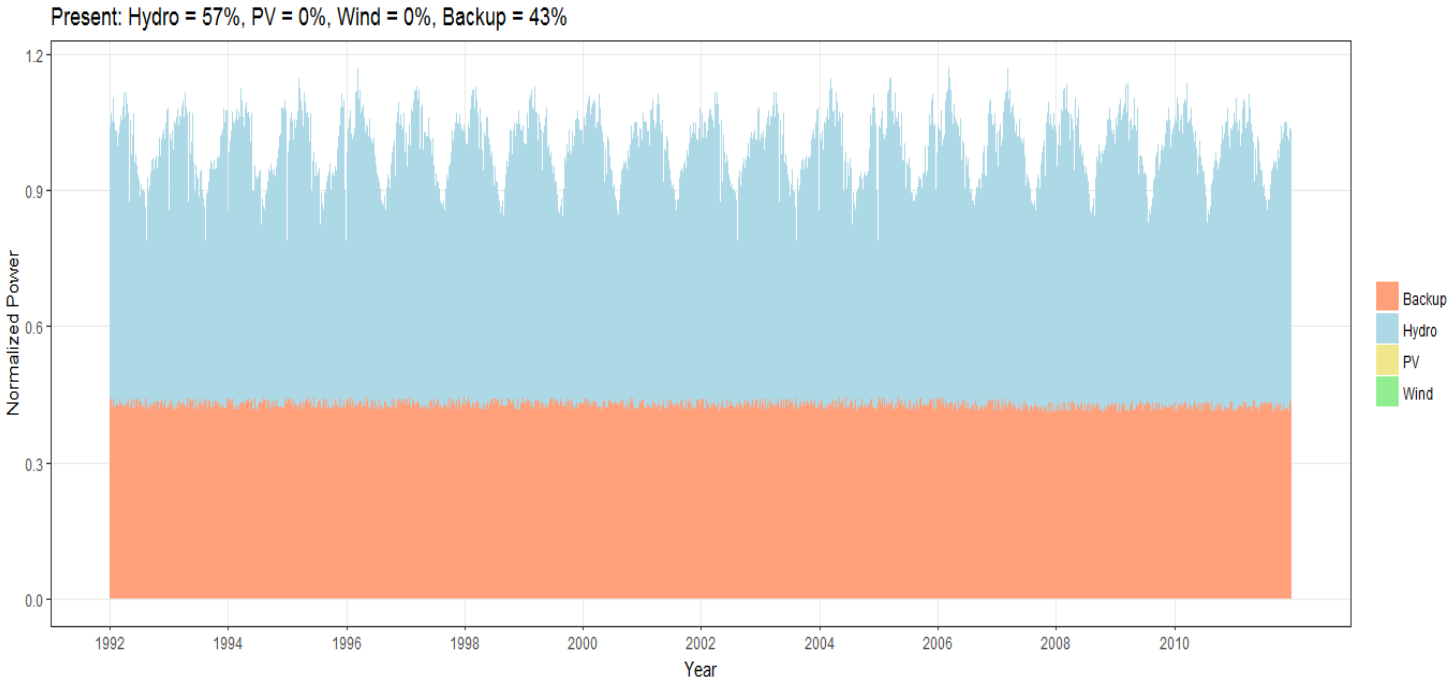

Production Source	Coefficient of Variation (%)
Backup	2.12
Hydro	13.047
PV	0
Wind	0

Fig 4.17: Present scenario of electricity configuration

[1] The remaining variations are actually due to numerical constraints in the DP model, and especially the level of discretization chosen for the release decision (hydropower production) variable. A higher resolution for discretization for the release decisions lead to fairly constant gas production. However, a higher resolution increases the computation time of DDP and might have memory problems depending on the system used for the simulations. We therefore used here a rather rough resolution for the discretization of release decision.

The simulation of storage variation with optimization for the present period was compared to the actual storage variation of the Akosombo reservoir as shown in Fig 4.18. Here the pattern of the actual storage cycle measured is represented very well by the DDP simulation. The deviation between actual and simulated storage curves follow the fact that, contrary to DDP, the Akosombo reservoir's operators did not know future river flow in advance. Also, some other uses and constraints of the reservoir (such as water extraction from the reservoir for irrigation, domestic purposes, etc.) were not included in the simulation of the management model and could have contributed to the deviation between actual and simulated storage curves. With optimization, it can be seen that, the reservoir does not reach its full capacity (i.e. 278 ft) during the period of simulation but also does not go lower than the minimum operating level (i.e. 240 ft). The average annual storage cycle simulated with DDP for the reference scenario will be compared with the average storage variations of different VRE configurations in the next section.

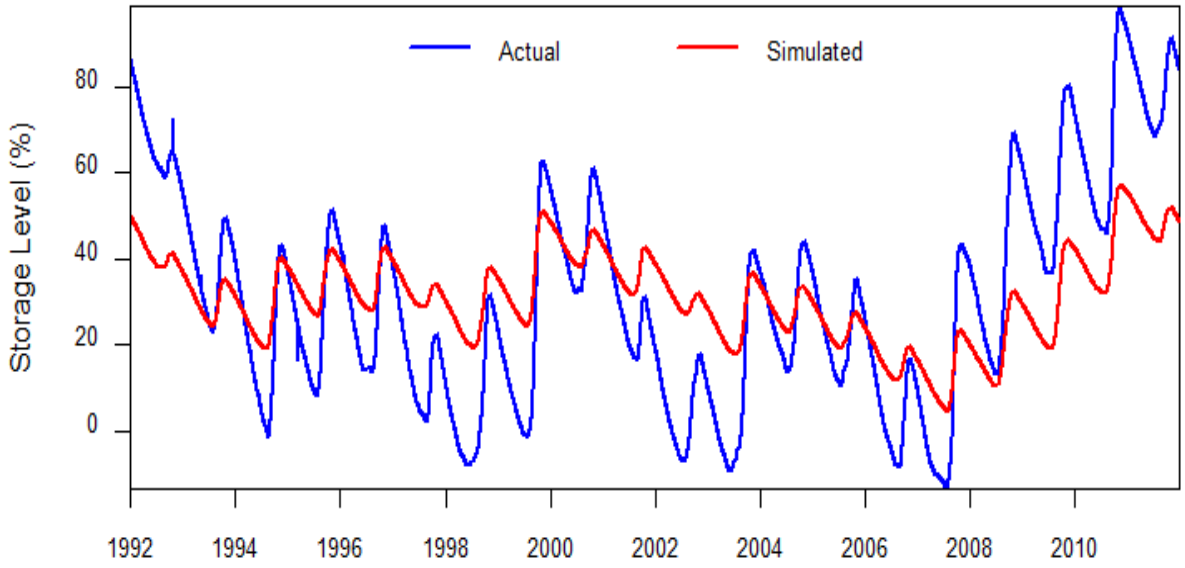

Fig 4.18: Comparison of present storage variation for 1992 to 2011 (actual water levels recorded at the Akosombo dam vs simulated water levels with DDP optimization)

4.5.1.2 Future VRE Development Configurations

For future scenarios of electricity demand and productions, we consider three main future periods; the near-future, intermediate future and the far future scenarios. In each of these scenarios, we analyze the variability of three different configurations of VRE production (see Table 3.2 for detailed description on these configurations).

A combination of wind and solar production (VRE) is used to supply the increase in demand during the simulation period. Production from VRE actually leads to increased variability in backup production. This is especially true when there is a greater share of wind in the VRE production (see Table 4.5 for CV calculated for all scenarios). The variability of backup production even increases more when the proportion of VRE in the electricity system is larger (and with a greater share from wind production). Similarly, the variability of our flexibility power facility (hydro production) also increases with a greater share of wind production in the VRE production. It is important to note that wind production has a higher day to day variability than solar production. Since simulations were done at daily time steps, this result obtained shows the impact of high variability of wind production. For simulations at hourly time step, a similar result is expected but with a high share of solar production due its high sub-daily variability.

Fig 4.19, Fig 4.20, and Fig 4.21 shows the variability of different production configurations in the near-future scenario. (see Appendix D for remaining figures for variabilities in the other future scenarios). Between hydro and gas productions, hydro presents the highest variation in all scenarios due to the high variability of storage-release operations of the reservoir. Among all scenarios, the lowest variability for hydro production is seen in the present scenario with no production for VRE. This is because there is no additional temporal mismatch (due to VRE production) to balance in the system and thus, hydro operations are optimized independently to minimize variability of the residual demand (or the backup).

With DDP optimization, it is ensured that demand is always satisfied for any given day during the simulation period due to the use of hydro as a flexibility power source. However, in some cases there are days where production actually exceeds the demand. In the same scenario, a greater share of wind production leads to a higher percentage of days with over production in the simulation period as shown in Table 4.5.

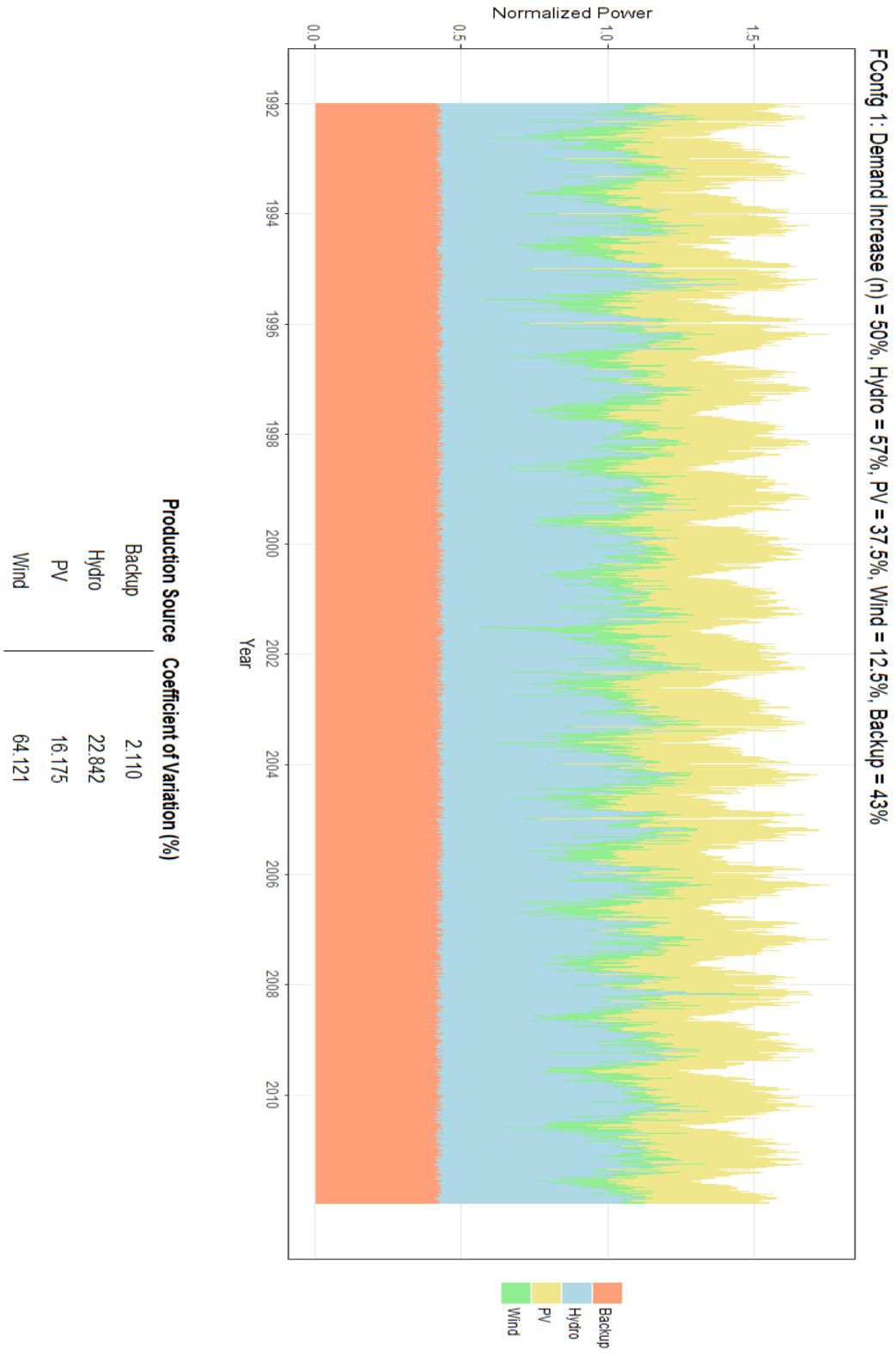

Fig 4.19: Near Future VRE Scenario- Configuration 1

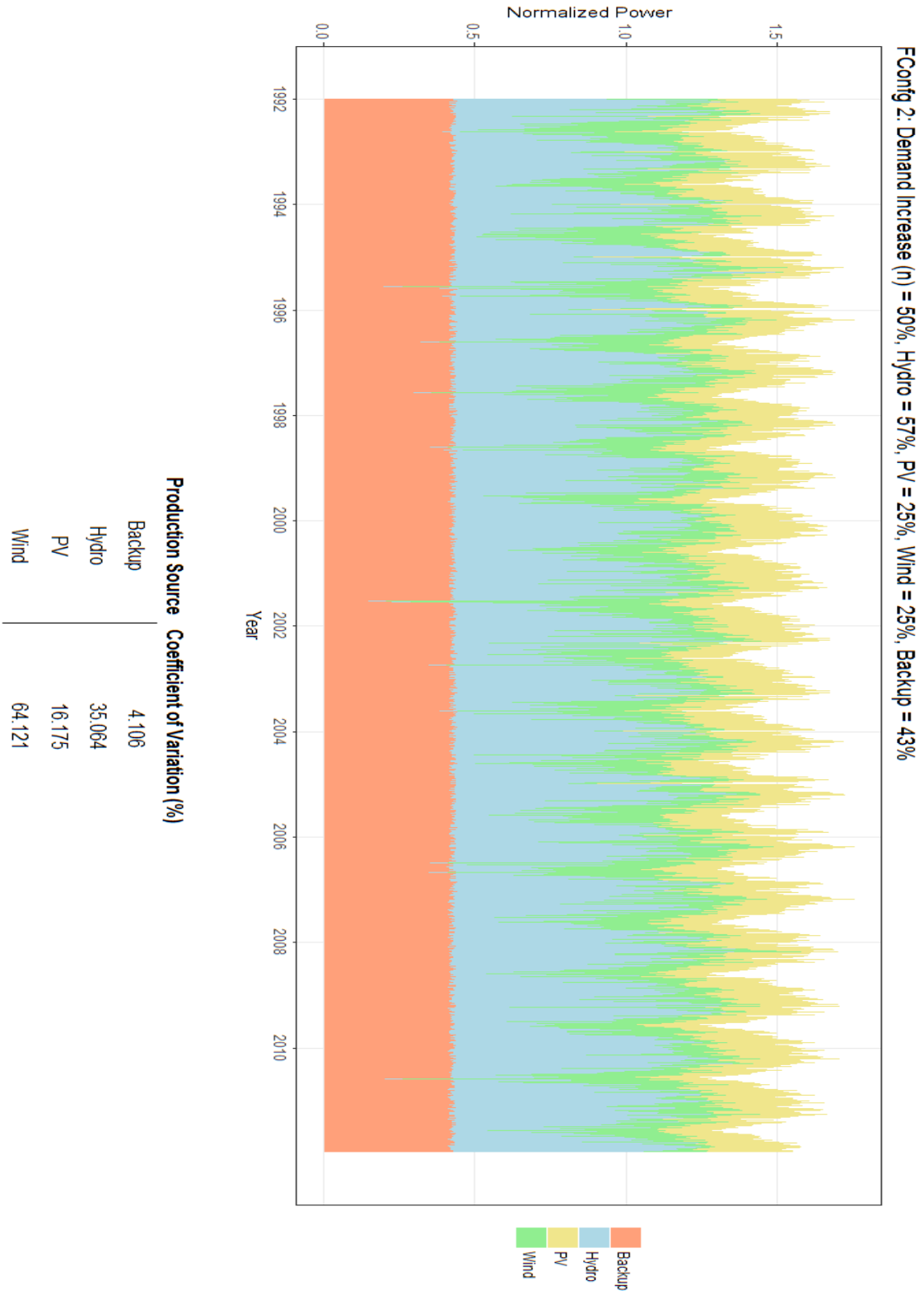

Fig 4.20: : Near Future VRE Scenario- Configuration 2

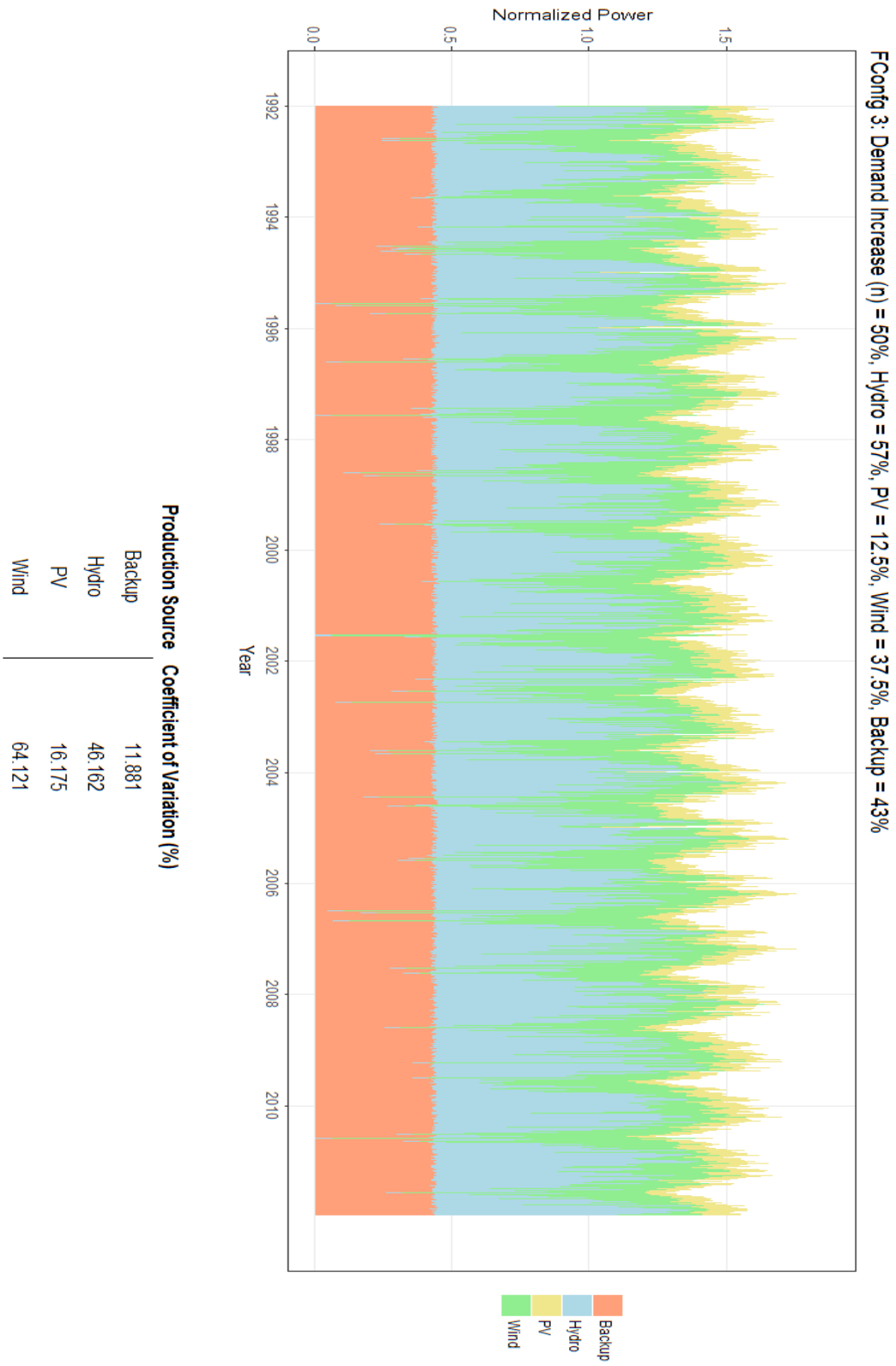

Fig 4.21: Near Future VRE Scenario- Configuration 3

Table 4.5: Calculated statistics for demand-production scenarios

Scenario	CV for Backup (%)	CV for Hydro (%)	Days with Unmet Demand (%)	Days with Over Production (%)
Present	2.12	13.047	0	0
FConfg 1	2.110	22.842	0	0
FConfg 2	4.106	35.064	0	0.027
FConfg 3	11.881	46.162	0	0.479
FConfg 4	3.404	34.890	0	0.014
FConfg 5	18.281	53.595	0	1.342
FConfg 6	33.015	67.018	0	6.146
FConfg 7	15.608	55.196	0	0.808
FConfg 8	41.066	76.133	0	9.829
FConfg 9	55.670	90.624	0	18.056

4.5.2 Impact of VRE Production on Storage Variation of the Reservoir

To determine the impacts of VRE production on the storage variation of the reservoir, the average annual storage variations for all configurations in each scenario were compared with the storage variation for the reference scenario. Fig 4.22, Fig 4.23 and Fig 4.24 compares the annual average storage cycles of the near (50 % increase), intermediate (100 % increase) and far (200 % increase) futures respectively with the present state.

Generally, the seasonality of storage is not significantly affected with VRE production in all scenarios. The annual cycle of the storage cycle is rather fully determined by the seasonality of hydrological inflows. However, the far (extreme) future scenario with a 200 % increase in demand (configurations with higher wind share), shows just slightly shifting seasonal storage variation.

This suggests that an even bigger VRE generation (for example 400 % with a higher share from wind production) may significantly change the storage cycle.

In all cases, with a higher share of wind production, the peak of the annual storage cycle (occurring at the end of the rainy season) is increased compared to the reference scenario. This is because during the rainy season which is also the inflow season for the reservoir, there is a higher production from wind power (see Fig 4.15) and thus less water is released from the dam to produce electricity leading to the slightly higher levels after the inflow season (relative to the present-no-VRE scenario). The level of increase in the peak is higher with a higher VRE generation (i.e. increase in peak of storage cycle in near future scenario < intermediate future scenario < far future scenario). A theoretical implication for this is that, the higher reservoir level during the peak months may potentially lead to an increase risk of flooding.

The impact of having a greater percentage of solar production in the VRE mix on the storage cycle is however not significantly pronounced. In all cases, the seasonality of storage would be roughly conserved, whatever the share of wind + solar in the mix.

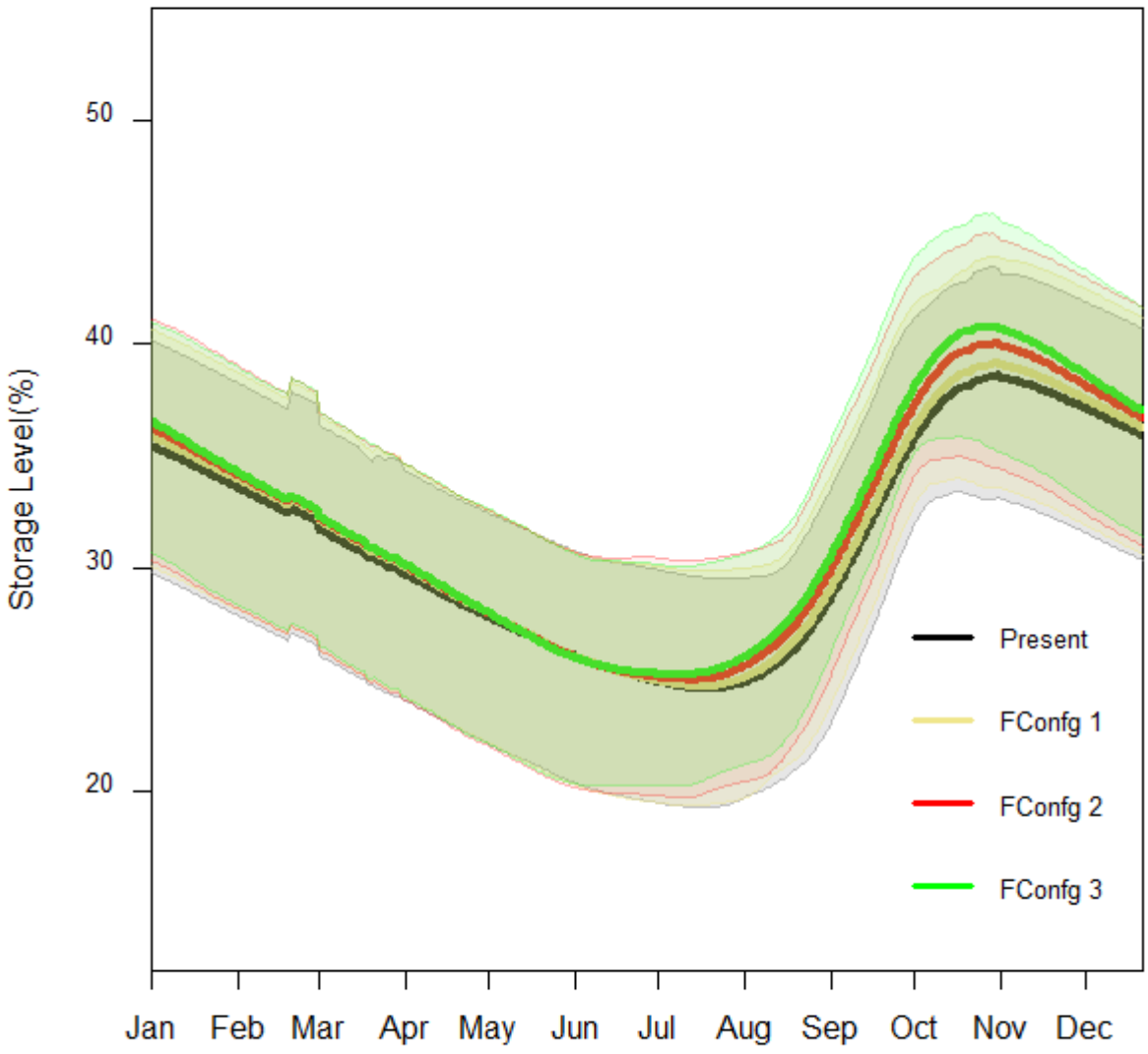

Fig 4.22: Impact of VRE production on storage cycle- Near future scenario: extra demand = 50%; FConfg 1: wind = 12.5%; FConfg 2: wind = 25%; FConfg 3: wind = 37.5%

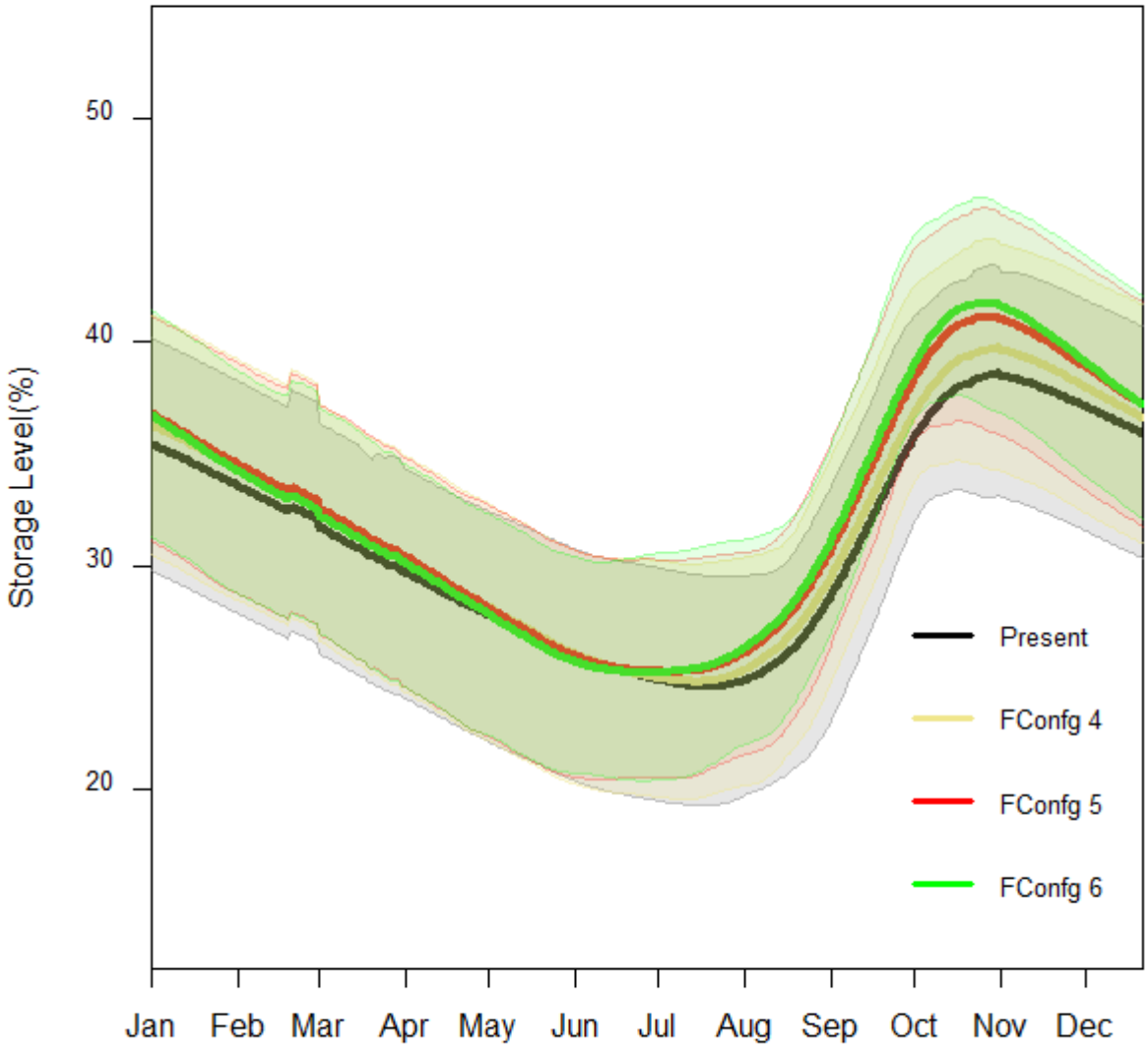

Fig 4.23: Impact of VRE production on storage cycle- Intermediate future scenario: extra demand = 100%; FConfg 1: wind = 25%; FConfg 2: wind = 50%; FConfg 3: wind = 75%

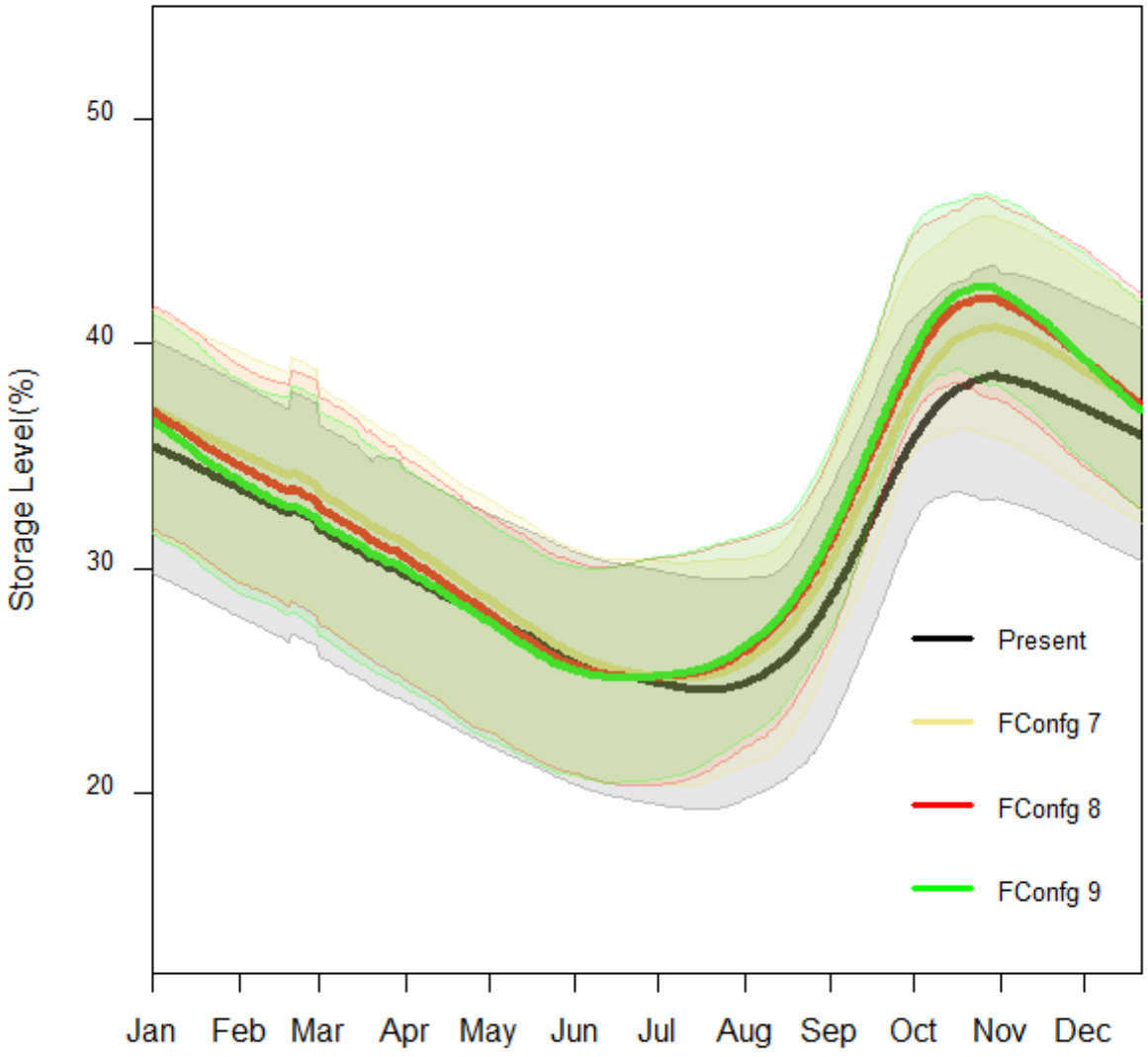

Fig 4.24: Impact of VRE production on storage cycle- Far future scenario: extra demand = 200%; FConfg 1: wind = 50%; FConfg 2: wind = 100%; FConfg 3: wind = 150%

5 CONCLUSION AND RECOMMENDATIONS

Various studies on Variable Renewable Energy (VRE) potential assessment in Ghana normally analyze the availability of the resource in a location. The present study however goes a step further to estimate the actual power that can be produced from the available resource and its temporal variability. Integration of VRE in any power system will create major temporal mismatch between demand and production hence the need for another power system that is flexible enough to balance the mismatch. In Ghana the Akosombo hydropower system can be used for such a purpose. The main contribution of this study is to determine the impacts of VRE integration on management strategy of the Akosombo HPP.

Regional VRE production was estimated from the mean production of a number of generic solar/wind farms. For solar, those farms were distributed homogeneously over the whole Ghanaian territory. For wind, 8 different grid locations in the coastal offshore region were selected. For each farm, solar power production was obtained from solar radiation data of the SARAH2 for a generic PV module and wind power production, from MERRA-2 reanalysis wind dataset for a generic wind turbine. Power production for both solar and wind was found to be very variable at different time scales but for all further analysis in this study, daily time steps were considered. Relative to solar power, wind power production was found to have the highest variability at daily time scale with a CV of 41% for its average annual cycle against 13% for solar.

The high day-to-day variability of VRE production in Ghana means that, their integration into the power system requires a major flexible system to balance the temporal fluctuations that will be introduced in supply. The Akosombo HPP will be a suitable system to ease the integration of VRE into Ghana's electricity. Integration of VRE while using the Akosombo dam as adapt to the temporal mismatch between demand and supply that will be created, is thus expected to have an impact of the storage cycle of the dam. It was seen that, a greater share of wind power in the total VRE mix will have a much more pronounced impact on the storage cycle due to more variability in wind power production than solar. This impact on the storage cycle is rather minimal when the total share of VRE supplying the total load is small. However, with a higher percentage of VRE supplying the national demand, the impact will be much more pronounced. A risk of flooding

during the peak months of reservoir water level is thus increased in such an instance. There is a need for future studies to investigate potential for flooding during VRE integration.

In a nutshell, the studied revealed that, VRE can be developed on a large scale in Ghana. Their integration into the power system can be done with flexible operations of production facilities such as the Akosombo hydropower plant. In the case of the Akosombo plant, its operations can be optimized with an optimization scheme such as Dynamic Programming to ensure that some objective function is achieved (for this study, variability of residual demand was minimized with DDP).

After the findings of this study, the following recommendations are given:

For policy makers and stakeholders

i. There is potential for VRE in Ghana and thus stakeholders must invest in developing more solar and wind power generators in the country.
ii. Managers and operators of the HPP's in Ghana should consider using predictions of water inflows into plants' reservoirs to optimize the long term power production from these plants in order to achieve maximum benefits from the power system.

For further research

i. The present study did not consider how climate change will influence future inflows into the dam, VRE production and electricity demand (for future scenarios). Future studies should thus consider how climate change could modify the availability of resources and their variabilities and how electricity will also change in future.
ii. A simple representation and configuration of the Akosombo dam system was used in the present study. A more precise and detailed representation of the system and its constraints should thus be considered in future studies (especially need to account for the upstream dams which also produce hydroelectricity). The objective function was to minimize the variability of the backup production which are practically obtained from thermal power productions and other HPPs. These plants also can provide some flexibility has also some flexibility. They should be considered in future studies.

6 References

Akpoti, K, E. Antwi, and A. Kabo-bah. 2016. “Impacts of Rainfall Variability, Land Use and Land Cover Change on Stream Flow of the Black Volta Basin, West Africa.” *Hydrology* 3 (3): 26. doi:10.3390/hydrology3030026.

Armah, Frederick A., Justice O. Odoi, Genesis T. Yengoh, Samuel Obiri, David O. Yawson, and Ernest K.A. Afrifa. 2011. “Food Security and Climate Change in Drought-Sensitive Savanna Zones of Ghana.” *Mitigation and Adaptation Strategies for Global Change* 16 (3): 291–306. doi:10.1007/s11027-010-9263-9.

Asumadu-Sarkodie, S. & Owusu, P.A. 2016. “The Potential and Economic Viability of Solar Photovoltaic Power in Ghana.” *Energy Sources, Part A* 38 (0): 1–8.

Bauelos-Ruedas, F., C. Angeles-Camacho, and S. Rios-Marcuello. 2011. “Methodologies Used in the Extrapolation of Wind Speed Data at Different Heights and Its Impact in the Wind Energy Resource Assessment in a Region, Wind Farm - Technical Regulations, Potential Estimation and Siting Assessment.” *InTech*. doi:10.5772/20669.

Bekoe, Emmanuel Obeng, and Fredrick Yaw Logah. 2013. “The Impact of Droughts and Climate Change on Electricity Generation in Ghana.” *Environmental Sciences* 1 (1): 13–24.

Bellman, R. 1957. *Dynamic Programming*. New Jersey: Princeton University Press., Defense Technical Information Center.

Bird, L, M Milligan, and D Lew. 2013. “Integrating Variable Renewable Energy: Challenges and Solutions.” doi:NREL/TP-6A20-60451.

Bosilovich, M. G., R. Lucchesi, and M. Suarez. 2016. *MERRA-2: File Specification*. GMAO Office Note No. 9 (Version 1.1). http://gmao.gsfc.nasa.gov/pubs/office_notes.

Cochran, Jaquelin, Lori Bird, Jenny Heeter, and D.J. Arent. 2012. “Integrating Variable Renewable Energy in Electric Power Markets: Best Practices from International Experience, Summary for Policymakers.” *NRELTP-6A20-60451*, no. April: 16. http://www.nrel.gov/docs/fy12osti/53730.pdf.

Condappa, Devaraj de, Anne Chaponniière, and Jacques Lemoalle. 2008. “Decision-Suppor Tool for Water Allocation in the Volta Basin.” *Volta Basin Focal Project Report*. Vol. 1. Montpellier, France, Colombo, Sri Lanka.

Energy Commisision. 2015. “2015 ENERGY (SUPPLY AND DEMAND) OUTLOOK FOR GHANA.”

Eshun, Maame Esi, and Joe Amoako-Tuffour. 2016. “A Review of the Trends in Ghana’s Power Sector.” *Energy, Sustainability and Society* 6 (1). Energy, Sustainability and Society: 9. doi:10.1186/s13705-016-0075-y.

François, B., B. Hingray, F. Hendrickx, and J. D. Creutin. 2014. “Seasonal Patterns of Water Storage as Signatures of the Climatological Equilibrium between Resource and Demand.” *Hydrology and Earth System Sciences* 18 (9): 3787–3800. doi:10.5194/hess-18-3787-2014.

François, B, M Borga, J D Creutin, B Hingray, D Raynaud, and J F Sauterleute. 2016. “Complementarity between Solar and Hydro Power: Sensitivity Study to Climate Characteristics in Northern-Italy.” *Renewable Energy* 86. Elsevier Ltd: 543–53. doi:10.1016/j.renene.2015.08.044.

François, B, B Hingray, and J D Creutin. 2015. “Estimating Water System Performance Under Climate Change : Influence of the Management Strategy Modeling,” 4903–18. doi:10.1007/s11269-015-1097-5.

François, B, B Hingray, D Raynaud, M Borga, and J D Creutin. 2016. “Increasing Climate-Related-Energy Penetration by Integrating Run-of-the River Hydropower to Wind/solar Mix.” *Renewable Energy* 87. Elsevier Ltd: 686–96. doi:10.1016/j.renene.2015.10.064.

German Federal Ministry for Economic Affairs and Energy. 2015. “Wind Energy in Ghana: Potential, Opportunities and Challenges.” *Renweables Made in Germany*. www.renewables-made-in-germany.com.

Ghana Meteorological Agency. 2017. “Climatology.” *Climatology*. http://www.meteo.gov.gh/website/index.php?option=com_content&view=article&id=62:climatology&catid=40:features&Itemid=67.

GSS. 2016. “Projected Population Growth by Sex 2010-2016.” *Ghana Statistical Service (GSS),*

2.

Gunturu, U. B., and C. A. Schlosser. 2012. “Characterization of Wind Power Resource in the United States.” *Atmospheric Chemistry and Physics* 12 (20): 9687–9702. doi:10.5194/acp-12-9687-2012.

Gyamfi, Samuel, Mawufemo Modjinou, and Sinisa Djordjevic. 2015. “Improving Electricity Supply Security in Ghana - The Potential of Renewable Energy.” *Renewable and Sustainable Energy Reviews* 43: 1035–45. doi:10.1016/j.rser.2014.11.102.

Haurwitz, B. 1945. “Insolation in Relation To Cloudines and Cloud Density.” *Journal of Meteorology* 2: 154–66. doi:10.1175/1520-0493(1954)082<0317:IIRTCA>2.0.CO;2.

Holttinen, Hannele, and Jens Pedersen. 2003. “The Effect of Large Scale Wind Power on a Thermal System Operation.” *Proceedings of the 4th International Workshop on Large-Scale Integration of Wind Power and Transmission Networks for Offshore Wind Farms*, 1–7. lib.tkk.fi/Diss/2004/isbn9513864278/article5.pdf.

International Energy Agency. 2008. “Empowering Variable Renewables - Options for Flexible Electricity Systems.” doi:10.1787/9789264111394-en.

International Renewable Energy Agency (IRENA). 2015. “Ghana: Renewables Readiness Assessment.”

IPCC. 2013. *Climate Change 2013: The Physical Science Basis. Contribution of Working Group I to the Fifth Assessment Report of the Intergovernmental Panel on Climate Change*. Edited by V. Bex & P.M. Midgley Stocker, T.F., D. Qin, G.-K. Plattner, M. Tignor, S.K. Allen, J. Boschung, A. Nauels, Y. Xia and (eds.). Cambridge University Press, Cambridge, United Kingdom and New York, NY, USA.

Kabo-Bah, Amos, Chuks. Diji, Kaku Nokoe, Yacob Mulugetta, Daniel Obeng-Ofori, and Komlavi Akpoti. 2016. “Multiyear Rainfall and Temperature Trends in the Volta River Basin and Their Potential Impact on Hydropower Generation in Ghana.” *Climate* 4 (4): 49. doi:10.3390/cli4040049.

Kalitsi, E.A.K. 2003. “Problems and Prospects for Hydropower Development.” *The Workshop for African Energy Experts on Operationalizing the NGPAD Energy Initiative*.

Kondi, A.G., A. Diedhiou, and B. Hingray. 2016. “Weather Sensitivity of Electricity Consumption in Cotonou, and Abidjan, Two Coastal Megacities in Western Africa.” In *International Workshop on Evolving Energy Models in Emerging Economies. Post COP21, Ahmadabad, Gujarat, India,* 16.

Kumi, Ebenezer Nyarko. 2017. “The Electricity Situation in Ghana: Challenges and Opportunities.” *CGD Policy Paper. Washington, DC: Center for Global Development*, no. September. https://www.cgdev.org/ publication/electricity-situation-ghana-challenges-and-opportunities.

Labadie, John W. 2004. “Optimal Operation of Multireservoir Systems: State-of-the-Art Review.” *Journal of Water Resources Planning and Management* 130 (2): 93–111. doi:10.1061/(ASCE)0733-9496(2004)130:2(93).

Lawrence, Z D, G L Manney, K Minschwaner, M L Santee, and A Lambert. 2015. “Comparisons of Polar Processing Diagnostics from 34 Years of the ERA-Interim and MERRA Reanalyses.” *Atmospheric Chemistry and Physics* 15 (7): 3873–92. doi:10.5194/acp-15-3873-2015.

Li, Danny H W, and Tony N T Lam. 2007. “Determining the Optimum Tilt Angle and Orientation for Solar Energy Collection Based on Measured Solar Radiance Data.” *International Journal of Photoenergy* 2007. doi:10.1155/2007/85402.

Linacre, E. 1999. “Estimating the Dewpoint.” http://www.das.uwyo.edu/~geerts/cwx/notes/chap06/dewpoint.html.

Linacre, Edward T. 1993. “Data-Sparse Estimation of Lake Evaporation, Using a Simplified Penman Equation.” *Agricultural and Forest Meteorology* 64 (3–4): 237–56. doi:10.1016/0168-1923(93)90031-C.

Ly, S., and A. Degre. 2011. “Geostatistical Interpolation of Daily Rainfall at Catchment Scale: The Use of Several Variogram Models in the Ourthe and Ambleve Catchments, Belgium.” *Hydrology and Earth System Sciences* 15 (7): 2259–2274. doi:10.5194/hess-15-2259-2011.

McCartney, Matthew, Gerald Forkuor, Aditya Sood, Barnabas Amisigo, Fred Hattermann, and Lal Muthuwatta. 2012. “The Water Resource Implications of Changing Climate in the Volta

River Basin." In *IWMI Research Report*. Colombo, Sri Lanka.

McPherson, M., Theofilos Sotiropoulos-Michalakakos, D L D Harvey, and Bryan Karney. 2017. "An Open-Access Web-Based Tool to Access Global, Hourly Wind and Solar PV Generation Time-Series Derived from the MERRA Reanalysis Dataset." *Energies* 10 (7). doi:10.3390/en10071007.

McSweeney, C., M. New, G. Lizcano, and X. Lu. 2010. "The UNDP Climate Change Country Profiles." *Bulletin of the American Meteorological Society* 91 (2): 157–66. doi:10.1175/2009BAMS2826.1.

Meibom, P, C Weber, R Barth, and H Brand. 2007. "Operational Costs Induced by Fluctuating Wind Power Production in Germany and Scandinavia." *IET, Renewable Power Generation* 3 (1): 75–83. doi:10.1049/iet-rpg:20070075.

Ministry of Food and Agriculture. 2011. "Facts and Figures (2010)."

Niamh, T. 2011. "Generator Cycling due to High Penetrations of Wind Power." University College Dublin, Ireland. http://erc.ucd.ie/files/theses/Niamh PhD - Generator Cycling due to High Penetrations of Wind Power.pdf.

Nkrumah, Francis, Nana Ama Browne Klutse, David Cudjoe Adukpo, Kwadwo Owusu, Kwesi Akumenyi Quagraine, Alfred Owusu, and William Gutowski. 2014. "Rainfall Variability over Ghana: Model versus Rain Gauge Observation." *International Journal of Geosciences* 5 (7): 673–83. doi:10.4236/ijg.2014.57060.

Obahoundje, S., E. A. Ofosu, K. Akpoti, and A.T. Kabo-bah. 2016. "Land Use and Land Cover Changes under Climate Uncertainty : Modelling the Impacts on Hydropower Production in Western Africa." *Hydrology* 4 (2). Colombo, Sri Lanka. doi:10.3390/hydrology4010002.

Olawoyin, R., and P.K. Acheampong. 2017. "Objective Assessment of the Thiessen Polygon Method for Estimating Areal Rainfall Depths in the River Volta Catchment in Ghana." *Ghana Journal of Geography* 9 (2): 151–74.

Olusola Kehinde, Olufemi, Frederick Ojiemhende Ehiagwina, Lateef Oroseniwo Afolabi, and Olajide Abdulmutolib Olaoye. 2016. "Photovoltaic Cell Output Voltage Variations with Time and Inclination Angle." *IOSR Journal of Electrical and Electronics Engineering Ver. II* 11

(4): 2278–1676. doi:10.9790/1676-1104024047.

Perpiñan, O., E. Lorenzo, and M. A. Castro. 2007. “On the Calculation of Energy Produced by a PV Grid-Connected System.” *Prog. Photovolt: Res. Appl.* 15: 265–74. doi:10.1002/pip.

Perpiñán, Oscar Lamigueiro. 2012. “solaR : Solar Radiation and Photovoltaic Systems.” *Journal of Statistical Software* 50 (9). http://www.jstatsoft.org/.

Pfeifroth, Uwe, Steffen Kothe, Richard Müller, Jörg Trentmann, Rainer Hollmann, Petra Fuchs, and Martin Werscheck. 2017. “Surface Radiation Data Set - Heliosat (SARAH) - Edition 2, Satellite Application Facility on Climate Monitoring.” doi:10.5676/EUM_SAF_CM/SARAH/V002.

Pimenta, Felipe M, and Arcilan T Assireu. 2015. “Simulating Reservoir Storage for a Wind-Hydro Hydrid System.” *Renewable Energy* 76. Elsevier Ltd: 757–67. doi:10.1016/j.renene.2014.11.047.

Rademacher-Schulz, Christina, and Edward Salifu Mahama. 2012. “″Where the Rain Falls″ Project - Case Study: Ghana. Resuts from Nadowli District Upper West Region. Report No. 3.” Bonn: United Nations University Institute for Environment and Human Security (UNU-EHS).

Reno, Matthew J, Clifford W Hansen, and Joshua S Stein. 2012. “Global Horizontal Irradiance Clear Sky Models: Implementation and Analysis.” *SANDIA REPORT*, no. March: 1–66. doi:10.2172/1039404.

Rienecker, Michele M., Max J. Suarez, Ronald Gelaro, Ricardo Todling, Julio Bacmeister, Emily Liu, Michael G. Bosilovich, et al. 2011. “MERRA: NASA’s Modern-Era Retrospective Analysis for Research and Applications.” *Journal of Climate* 24 (14): 3624–48. doi:10.1175/JCLI-D-11-00015.1.

Srivastava, Amit Kumar, Cho Miltin Mboh, Thomas Gaiser, and Frank Ewert. 2017. “Impact of Climatic Variables on the Spatial and Temporal Variability of Crop Yield and Biomass Gap in Sub-Saharan Africa- a Case Study in Central Ghana.” *Field Crops Research* 203. Elsevier B.V.: 33–46. doi:10.1016/j.fcr.2016.11.010.

UNFCCC. 2014. “The Paris Agreement.” http://unfccc.int/paris_agreement/items/9485.php.

WWEA Technical Committee. 2014. “World Wind Resource Assessment Report.” *World Wind Resource Assessment Report*.

Yakowitz, S. 1983. “Dynamic Programming Applications in Water Resources.” *Water Resources Research* 18 (4): 673–96.

7 Appendices

7.1 Appendix A

Description of Dynamic Programming

Dynamic programming (DP) is an optimization method developed by Bellman (1957). For a given planning horizon (t_i, t_N), DP aims either to maximize or to minimize an objective function according a set of constraints. Since the first developments by Bellman (1957), DP has been applied for a large variety of applications whose water resource management is one of the main (Yakowitz 1992; Labadie 2004). In water resource management, common objective functions are income from hydropower generation and / or from agriculture crops; and / or any indicator of the satisfaction of water needs downstream the dam or the recreational activities on the lake. DP holds on the principle of optimality (Bellman, 1957): whatever the initial state is, remaining decisions must be optimal with regard the state following from the first decision. In other, principle of optimality implies that a combination of optimal decisions leads to the optimal system trajectory. In DP, optimal decisions are defined as the ones that maximize (or minimize) the immediate income (related to the immediate use of water) with the income that would be obtained from the state following the immediate decision.

DDP is composed by two stages: an optimization stage and a simulation stage. The optimization stage consists at computing the so-called Bellman Values (hereafter denoted as F). For a given storage state and a given time, Bellman Values represents the expected future incomes up to the planning horizon (for Stochastic Dynamic Programing) or the best future income that could be obtained (for Deterministic Dynamic Programming). They are obtained from a backward recursive calculation from the future benefits (Equation 7.1).

$$F_{t_i}(S_{t_i}) = [g(u_{t_i}, S_{t_i}, t_i) + F_{t_{i+1}}(S_{t_{i+1}})] \quad (7.1)$$

where u_{t_i} is release discharge from the reservoir (operational decision variable) at a given time step, S_t is the storage level at time t, $F_t(S_t)$ is the Bellman Value for the storage level S_t at time t.

The function g represents the immediate income linked with the immediate use of water. In this work, we consider Deterministic Dynamic Programming;

Depending on the considered system and considered objective function, g may depend on u, S and time t. The state and decision variables are the major constraints for this DDP algorithm and they are such that

$$S_{min} \leq S_{ti} \leq S_{max} \tag{7.2}$$

and,

$$u_{min} \leq u_{ti} \leq u_{max} \tag{7.3}$$

where, S_{min} and S_{max} are the minimum and maximum operating levels for the reservoir while u_{min} and u_{max} are the minimum and maximum bounds for release discharges respectively. u_{max} is the total volume of energy that can be generated if the plant runs at full capacity during 24 hours i.e. Q (in energy units) in Equation 7.4.

$$H_p = \rho \cdot h \cdot Q \cdot g \tag{7.4}$$

where H_p is hydropower generation, ρ is the density of water and h is the head of water in the reservoir. Following Francois et al, 2017, u_{min} is set to the second percentile of the inflow volume into the reservoir. This value is then converted to energy using the hydroelectricity generation equation.

The future storage at time t_{i+1} is given as:

$$S_{t_{i+1}} = S_{t_i} + q_{t_i} - u_{t_i} - o_{t_i} \tag{7.5}$$

Where, q_{t_i} is the inflow to the reservoir between the present and future period [t_t and t_{t+1}], o_{t_i} is the losses from the reservoir in the form of evaporation, water extraction etc.

Bellman Values at the end of the planning horizon t_N are required to solve the backward recurrence in equation 1. We estimate $F_{t_N}(S)$ following François et al., 2014 and François et al., 2015, i.e. by first initializing the values as 0, whatever the reservoir level so that the Bellman values at t_N are not influenced by the boundary conditions. The backward recurrence is solved for the entire planning horizon (i.e. 20 years). The optimization stage is then repeated a second time with new initial Bellman Value at t_N as equal to the climatological average as obtained at this calendar date during the first backward recurrence. In the case of this study, Bellman values have been estimated at 50 storage states uniformly distributed between the maximum and minimum bounds of the

Akosombo reservoir. For a storage level between the initialized storage states, the Bellman value is determined using a cubic spline interpolation technique.

Once the Bellman Values are known for the entire planning horizon, it is possible, from a given initial storage level, to simulate the release operations that maximize (or minimize, depending on the considered objective function g) the objective function. This is done by solving the forward recursive calculation also expressed in Equation 4.9. This stage is the so-called simulation stage.

Estimation of precipitation and evaporation from the reservoir surface

The Thiessen Polygon (TP) technique (Ly and Degre 2011; Olawoyin and Acheampong 2017) was used to find the areal average precipitation on the Volta Lake surface. The average depth of rainfall (P_{ave}) over the entire water body is estimated as:

$$P_{ave} = \frac{\sum A_i P_i}{\sum A_i} \tag{7.6}$$

Where A_i is the area of influence for a given gauge and P_i the precipitation from a given gauge station. The area of influence for each station has been determined with ArcGIS. For this study, the average areal rainfall over the Volta Lake was computed from eight rain gauge stations as shown in Figure 4.1 using the Thiessen Polygon technique. The surface area of the lake was determined to be 7864km^2 from the shapefile of the Volta Lake obtained from Ghana hydro database. The area of influence by each of these stations was determined with ARCGIS 10.1.

The different stations with their lat/lon locations, areas of influence on the Volta Lake and weights for TP interpolation are given in Table 7.1.

Table 7.1: Thiessen weights of rain gauge stations around the Volta Lake

Rain Gauge Station	Latitude (°)	Longitude (°)	Area of Influence (km^2)	Weight
Abetifi	6.0903	0.1235	597	0.08
Ho	6.6101	0.4785	1812	0.23
Yendi	9.4450	-0.0093	40	0.01
Tamale	9.4329	-0.8485	631	0.08
Koforidua	6.0784	-0.2714	205	0.03
Kete-Krachi	7.8014	-0.0513	4144	0.53
Akuse	6.0903	0.1235	377	0.05
Bole	9.0322	-2.4851	57	0.01

Evaporation from the lake surface was estimated using a method proposed by Linacre (1993). As used by Pimenta and Assireu (2015), this method requires inputs of air temperature (T), dew point temperature (T_d), solar irradiance (I_s), wind speed (u) and elevation (z). It is given as:

$$E_i = (0.015 + 0.00042T_i + 10^{-6}z)[0.8I_{s_i} - 40 + 2.5Fu_i(T_i - T_{d_i})] \quad (7.7)$$

Where, E_i is the evaporation from the lake surface in a given day ($mm\ day^{-1}$), F is a correction factor for the local attitude and is given by

$$F = 1 - 8.7 \times 10^{-5}z \quad (7.8)$$

Linacre, (1999) proposed an empirical method to calculate the dew point temperature using the daily extreme temperatures (i.e. maximum and minimum temperatures of the day). This relationship has been tested and validated in a wide range of places around the world and has been observed to on the average, give values which are very close to actual values. It is given as

$$T_{d_i} = 0.38\,T_{x_i} - 0.018\,{T_{x_i}}^2 + 1.4\,T_{n_i} - 5 \quad (7.9)$$

where T_{x_i} and T_{n_i} are the maximum and minimum temperatures respectively for a given day. For the computation of evaporation from the lake, data measured and extracted from the location of the Kete-Krachi station shown in Fig 2.1 has been used. This station has been chosen because among all stations for which data has been obtained for, it is the closest to the lake surface.

7.2 Appendix B1

Tables for yearly average irradiance as a function different tilt angles i.e. determining optimal tilt angles.

Table 7.2: Irradiance as a function of inclination at Lat 5.5

Tilts	Jan	Feb	Mar	Apr	May	Jun	Jul	Aug	Sep	Oct	Nov	Dec	Yearly Average
0	5.81	5.92	5.69	5.65	5.23	4.46	4.42	4.37	4.48	5.08	5.62	5.6	5.19
5	6.04	6.06	5.72	5.59	5.11	4.35	4.33	4.31	4.47	5.15	5.8	5.85	5.23
10	6.24	6.16	5.71	5.5	4.97	4.23	4.21	4.23	4.44	5.19	5.95	6.06	5.24
15	6.4	6.24	5.68	5.38	4.81	4.08	4.07	4.14	4.39	5.21	6.06	6.23	5.22
20	6.52	6.27	5.62	5.24	4.63	3.92	3.92	4.03	4.33	5.2	6.14	6.37	5.18
25	6.6	6.27	5.54	5.07	4.42	3.74	3.75	3.9	4.24	5.16	6.18	6.47	5.11
30	6.65	6.24	5.42	4.88	4.2	3.56	3.58	3.75	4.14	5.1	6.19	6.53	5.02
35	6.66	6.18	5.28	4.66	3.97	3.37	3.4	3.6	4.03	5.02	6.17	6.56	4.91
40	6.62	6.08	5.11	4.43	3.72	3.16	3.22	3.44	3.89	4.91	6.11	6.55	4.77
45	6.45	5.78	4.7	3.91	3.19	2.74	2.82	3.1	3.59	4.63	5.9	6.42	4.43
50	6.45	5.78	4.7	3.91	3.19	2.74	2.82	3.1	3.59	4.63	5.9	6.42	4.43
55	6.3	5.58	4.47	3.63	2.91	2.53	2.62	2.92	3.42	4.46	5.74	6.29	4.24
60	6.12	5.36	4.21	3.33	2.63	2.31	2.42	2.73	3.24	4.26	5.55	6.14	4.03
65	5.9	5.1	3.94	3.03	2.36	2.12	2.23	2.55	3.05	4.05	5.33	5.94	3.8
70	5.65	4.82	3.65	2.72	2.1	1.95	2.06	2.36	2.85	3.82	5.08	5.71	3.57
75	5.37	4.52	3.35	2.42	1.9	1.88	1.95	2.18	2.64	3.57	4.81	5.45	3.34
80	5.05	4.18	3.03	2.12	1.82	1.84	1.9	2.04	2.43	3.3	4.5	5.16	3.11
85	4.71	3.83	2.7	1.91	1.79	1.79	1.85	1.95	2.21	3.03	4.18	4.83	2.9
90	4.34	3.46	2.36	1.8	1.75	1.74	1.8	1.88	2.02	2.74	3.83	4.48	2.68

Table 7.3: Irradiance as a function of inclination at Lat 6.5

Tilts	Jan	Feb	Mar	Apr	May	Jun	Jul	Aug	Sep	Oct	Nov	Dec	Yearly Average
0	5.91	6.09	5.97	5.95	5.72	4.98	4.60	4.35	4.60	5.30	5.73	5.58	5.40
5	6.16	6.25	6.01	5.89	5.59	4.85	4.50	4.29	4.59	5.38	5.93	5.83	5.44
10	6.38	6.38	6.01	5.80	5.42	4.69	4.37	4.22	4.57	5.44	6.10	6.05	5.45
15	6.57	6.47	5.99	5.68	5.23	4.52	4.23	4.13	4.52	5.47	6.23	6.24	5.44
20	6.71	6.52	5.93	5.53	5.02	4.32	4.07	4.01	4.45	5.47	6.33	6.39	5.39
25	6.81	6.53	5.84	5.35	4.77	4.11	3.89	3.89	4.37	5.44	6.38	6.50	5.32
30	6.87	6.51	5.72	5.14	4.52	3.89	3.70	3.75	4.26	5.38	6.41	6.58	5.23
35	6.90	6.45	5.58	4.91	4.26	3.66	3.52	3.60	4.14	5.30	6.39	6.61	5.11
40	6.88	6.35	5.40	4.66	3.97	3.42	3.32	3.44	4.00	5.19	6.35	6.61	4.97
45	6.82	6.22	5.20	4.39	3.67	3.16	3.11	3.28	3.84	5.06	6.26	6.57	4.80
50	6.72	6.05	4.97	4.11	3.36	2.91	2.89	3.10	3.67	4.90	6.14	6.49	4.61
55	6.57	5.85	4.72	3.81	3.04	2.66	2.68	2.92	3.49	4.72	5.98	6.38	4.40
60	6.39	5.62	4.45	3.49	2.73	2.41	2.47	2.74	3.29	4.51	5.80	6.22	4.18
65	6.18	5.36	4.16	3.17	2.42	2.18	2.27	2.55	3.09	4.28	5.57	6.03	3.94
70	5.92	5.06	3.85	2.84	2.14	1.98	2.09	2.36	2.87	4.04	5.32	5.81	3.69
75	5.63	4.74	3.52	2.51	1.90	1.88	1.97	2.18	2.65	3.77	5.04	5.55	3.45
80	5.30	4.40	3.18	2.20	1.80	1.84	1.91	2.03	2.42	3.49	4.73	5.25	3.21
85	4.95	4.03	2.82	1.94	1.77	1.81	1.87	1.93	2.19	3.19	4.39	4.93	2.98
90	4.56	3.63	2.46	1.82	1.75	1.77	1.81	1.87	1.97	2.88	4.02	4.58	2.76

Table 7.4: Irradiance as a function of inclination at Lat 7.5

Tilts	Jan	Feb	Mar	Apr	May	Jun	Jul	Aug	Sep	Oct	Nov	Dec	Yearly Average
0	6	6.18	6.01	5.97	5.72	5.04	4.51	4.23	4.44	5.11	5.51	5.54	5.36
5	6.28	6.36	6.06	5.92	5.59	4.91	4.41	4.18	4.44	5.2	5.71	5.8	5.41
10	6.52	6.5	6.08	5.83	5.43	4.75	4.3	4.11	4.42	5.26	5.88	6.03	5.43
15	6.73	6.61	6.06	5.71	5.24	4.57	4.16	4.02	4.38	5.29	6.01	6.22	5.42
20	6.89	6.67	6.01	5.57	5.03	4.37	4.01	3.92	4.32	5.29	6.11	6.38	5.38
25	7.01	6.7	5.92	5.39	4.79	4.16	3.84	3.8	4.24	5.27	6.17	6.5	5.31
30	7.09	6.68	5.81	5.19	4.54	3.94	3.66	3.67	4.14	5.22	6.2	6.58	5.23
35	7.12	6.63	5.66	4.96	4.28	3.71	3.49	3.53	4.02	5.14	6.19	6.62	5.11
40	7.11	6.54	5.49	4.71	4	3.46	3.3	3.38	3.89	5.04	6.15	6.62	4.97
45	7.06	6.41	5.28	4.44	3.7	3.21	3.1	3.22	3.75	4.92	6.07	6.58	4.81
50	6.97	6.24	5.06	4.16	3.39	2.94	2.9	3.06	3.58	4.77	5.96	6.5	4.63
55	6.83	6.04	4.8	3.86	3.07	2.7	2.69	2.89	3.41	4.6	5.81	6.39	4.42
60	6.65	5.8	4.52	3.54	2.76	2.44	2.5	2.71	3.23	4.4	5.64	6.23	4.2
65	6.42	5.53	4.23	3.21	2.45	2.21	2.3	2.53	3.04	4.18	5.43	6.04	3.96
70	6.16	5.23	3.91	2.88	2.16	2	2.13	2.35	2.83	3.95	5.19	5.82	3.72
75	5.86	4.9	3.57	2.54	1.9	1.87	2	2.18	2.62	3.69	4.92	5.56	3.47
80	5.53	4.54	3.22	2.22	1.77	1.84	1.94	2.02	2.4	3.42	4.62	5.26	3.23
85	5.16	4.16	2.85	1.94	1.74	1.81	1.89	1.91	2.18	3.14	4.3	4.93	3
90	4.76	3.75	2.48	1.78	1.72	1.77	1.83	1.84	1.96	2.84	3.95	4.58	2.77

Table 7.5: Irradiance as a function of inclination at Lat 8.5

Tilts	Jan	Feb	Mar	Apr	May	Jun	Jul	Aug	Sep	Oct	Nov	Dec	Yearly Average
0	6.18	6.45	6.3	6.19	6.01	5.38	4.84	4.57	4.95	5.74	6	5.91	5.71
5	6.5	6.66	6.36	6.14	5.88	5.24	4.73	4.51	4.95	5.86	6.25	6.22	5.78
10	6.77	6.83	6.38	6.05	5.71	5.07	4.61	4.44	4.94	5.95	6.47	6.5	5.81
15	7	6.95	6.37	5.93	5.51	4.87	4.46	4.34	4.89	6	6.64	6.73	5.81
20	7.19	7.04	6.32	5.78	5.28	4.65	4.29	4.22	4.82	6.02	6.77	6.92	5.78
25	7.33	7.08	6.24	5.6	5.02	4.41	4.1	4.09	4.73	6	6.87	7.07	5.71
30	7.42	7.07	6.12	5.38	4.75	4.16	3.9	3.94	4.62	5.96	6.92	7.18	5.62
35	7.47	7.03	5.97	5.14	4.47	3.9	3.7	3.78	4.49	5.87	6.93	7.24	5.5
40	7.47	6.94	5.79	4.88	4.16	3.63	3.48	3.61	4.33	5.76	6.89	7.25	5.35
45	7.43	6.81	5.57	4.6	3.84	3.34	3.26	3.43	4.16	5.62	6.82	7.22	5.18
50	7.33	6.64	5.33	4.3	3.5	3.04	3.02	3.25	3.97	5.44	6.7	7.14	4.97
55	7.2	6.43	5.06	3.98	3.16	2.76	2.79	3.05	3.77	5.24	6.54	7.02	4.75
60	7.01	6.18	4.76	3.64	2.81	2.48	2.56	2.85	3.55	5.01	6.35	6.86	4.5
65	6.78	5.89	4.44	3.29	2.47	2.2	2.33	2.64	3.32	4.75	6.11	6.65	4.24
70	6.51	5.57	4.09	2.93	2.15	1.96	2.13	2.43	3.07	4.46	5.84	6.4	3.96
75	6.19	5.22	3.73	2.57	1.86	1.8	1.97	2.23	2.82	4.16	5.53	6.11	3.68
80	5.84	4.83	3.35	2.22	1.69	1.77	1.9	2.05	2.55	3.83	5.19	5.78	3.42
85	5.45	4.42	2.95	1.9	1.65	1.74	1.85	1.91	2.29	3.48	4.82	5.41	3.16
90	5.03	3.98	2.54	1.71	1.64	1.71	1.81	1.84	2.02	3.11	4.42	5.01	2.9

Table 7.6: Irradiance as a function of inclination at Lat 9.5

Tilts	Jan	Feb	Mar	Apr	May	Jun	Jul	Aug	Sep	Oct	Nov	Dec	Yearly Average
0	6.19	6.54	6.46	6.32	6.08	5.53	5.01	4.64	5.14	5.91	6.05	5.99	5.82
5	6.52	6.77	6.53	6.27	5.95	5.38	4.9	4.59	5.15	6.04	6.32	6.33	5.9
10	6.81	6.96	6.57	6.19	5.79	5.21	4.77	4.51	5.14	6.14	6.55	6.62	5.94
15	7.05	7.1	6.57	6.07	5.6	5.01	4.61	4.42	5.1	6.2	6.74	6.88	5.95
20	7.25	7.2	6.53	5.92	5.37	4.79	4.44	4.3	5.03	6.23	6.9	7.09	5.92
25	7.4	7.25	6.45	5.74	5.12	4.54	4.24	4.17	4.94	6.22	7	7.26	5.86
30	7.5	7.26	6.33	5.53	4.85	4.28	4.03	4.02	4.82	6.18	7.07	7.38	5.77
35	7.56	7.22	6.18	5.28	4.56	4.02	3.81	3.85	4.69	6.1	7.09	7.46	5.65
40	7.57	7.14	6	5.02	4.26	3.73	3.59	3.67	4.53	5.99	7.07	7.49	5.5
45	7.53	7.02	5.78	4.73	3.93	3.43	3.35	3.49	4.35	5.84	7	7.46	5.33
50	7.44	6.85	5.53	4.42	3.59	3.12	3.1	3.29	4.15	5.67	6.9	7.4	5.12
55	7.3	6.64	5.25	4.09	3.24	2.82	2.85	3.09	3.93	5.46	6.75	7.28	4.89
60	7.12	6.39	4.94	3.74	2.89	2.53	2.6	2.88	3.7	5.22	6.55	7.12	4.64
65	6.89	6.1	4.61	3.38	2.54	2.23	2.36	2.66	3.45	4.95	6.32	6.91	4.37
70	6.62	5.78	4.25	3.01	2.2	1.97	2.13	2.44	3.19	4.65	6.05	6.65	4.08
75	6.3	5.42	3.87	2.64	1.89	1.77	1.94	2.23	2.92	4.33	5.74	6.36	3.78
80	5.95	5.02	3.47	2.27	1.69	1.73	1.85	2.03	2.64	3.99	5.4	6.02	3.5
85	5.56	4.6	3.05	1.93	1.63	1.71	1.81	1.88	2.35	3.62	5.02	5.64	3.23
90	5.13	4.15	2.63	1.7	1.62	1.68	1.77	1.79	2.07	3.24	4.61	5.23	2.97

Table 7.7: Irradiance as a function of inclination at Lat 10.5

Tilts	Jan	Feb	Mar	Apr	May	Jun	Jul	Aug	Sep	Oct	Nov	Dec	Yearly Average
0	6.47	6.81	6.69	6.34	6.1	5.69	5.28	4.88	5.46	6.22	6.42	6.34	6.06
5	6.47	6.81	6.69	6.34	6.1	5.69	5.28	4.88	5.46	6.22	6.42	6.34	6.06
10	6.76	7.01	6.73	6.26	5.94	5.5	5.14	4.8	5.46	6.34	6.68	6.66	6.11
15	7.01	7.16	6.74	6.15	5.74	5.29	4.97	4.7	5.42	6.41	6.89	6.93	6.12
20	7.21	7.28	6.71	6.01	5.51	5.05	4.77	4.58	5.35	6.45	7.06	7.16	6.09
25	7.37	7.34	6.63	5.83	5.26	4.78	4.56	4.43	5.26	6.45	7.19	7.34	6.04
30	7.48	7.36	6.52	5.62	4.98	4.5	4.32	4.27	5.13	6.41	7.27	7.48	5.95
35	7.55	7.33	6.37	5.38	4.68	4.21	4.07	4.09	4.99	6.33	7.3	7.57	5.82
40	7.56	7.26	6.19	5.11	4.37	3.9	3.81	3.9	4.82	6.22	7.29	7.6	5.67
45	7.53	7.14	5.97	4.82	4.04	3.58	3.54	3.69	4.63	6.08	7.24	7.59	5.49
50	7.45	6.98	5.71	4.51	3.69	3.24	3.26	3.48	4.41	5.89	7.13	7.53	5.27
55	7.32	6.78	5.43	4.18	3.32	2.91	2.96	3.25	4.18	5.68	6.99	7.42	5.03
60	7.14	6.53	5.11	3.83	2.96	2.59	2.68	3.02	3.92	5.43	6.8	7.27	4.77
65	6.92	6.24	4.77	3.47	2.6	2.26	2.4	2.77	3.66	5.15	6.56	7.06	4.49
70	6.65	5.92	4.4	3.09	2.24	1.97	2.13	2.53	3.37	4.85	6.29	6.81	4.19
75	6.34	5.55	4	2.71	1.91	1.73	1.91	2.29	3.08	4.51	5.97	6.52	3.88
80	5.98	5.16	3.59	2.33	1.67	1.66	1.78	2.06	2.77	4.15	5.62	6.18	3.58
85	5.59	4.73	3.16	1.97	1.6	1.65	1.75	1.88	2.45	3.77	5.23	5.8	3.3
90	5.17	4.27	2.72	1.71	1.59	1.64	1.72	1.78	2.13	3.37	4.81	5.39	3.03

7.3 Appendix B2

Additional figures

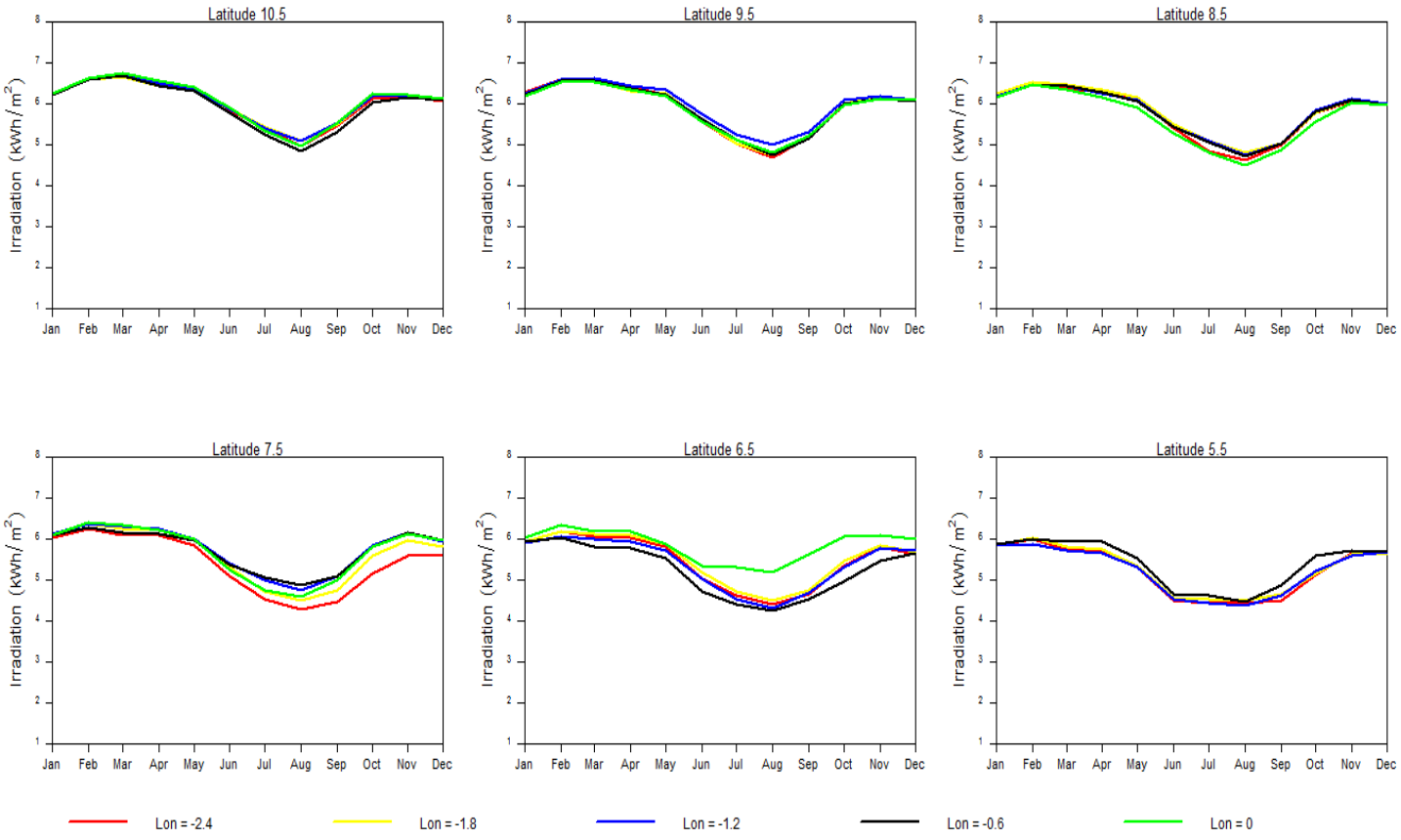

Fig 7.1: Dependence of solar radiation on longitude

Fig presents the average sub-daily cycle of irradiance in each month (deep solid red curve). The irradiation is maximum at mid-day but rises steadily from zero at sunrise and falls back to zero during sunset. It remains zero throughout the night. Maximum electricity production is thus expected at mid-day when the incoming radiation is highest. Fig also presents the average intra-daily cycle of CS irradiance. During some months, CS irradiance was slightly lower than the measured GHI of SARAH2 which is theoretically not possible. However, it must be noted that, both irradiance time series are model outputs (SARAH2 models radiation from satellite measurements) and therefore have a number of uncertainties. Also, both time series were averaged over the whole study area and possibly could lead to some misrepresentations.

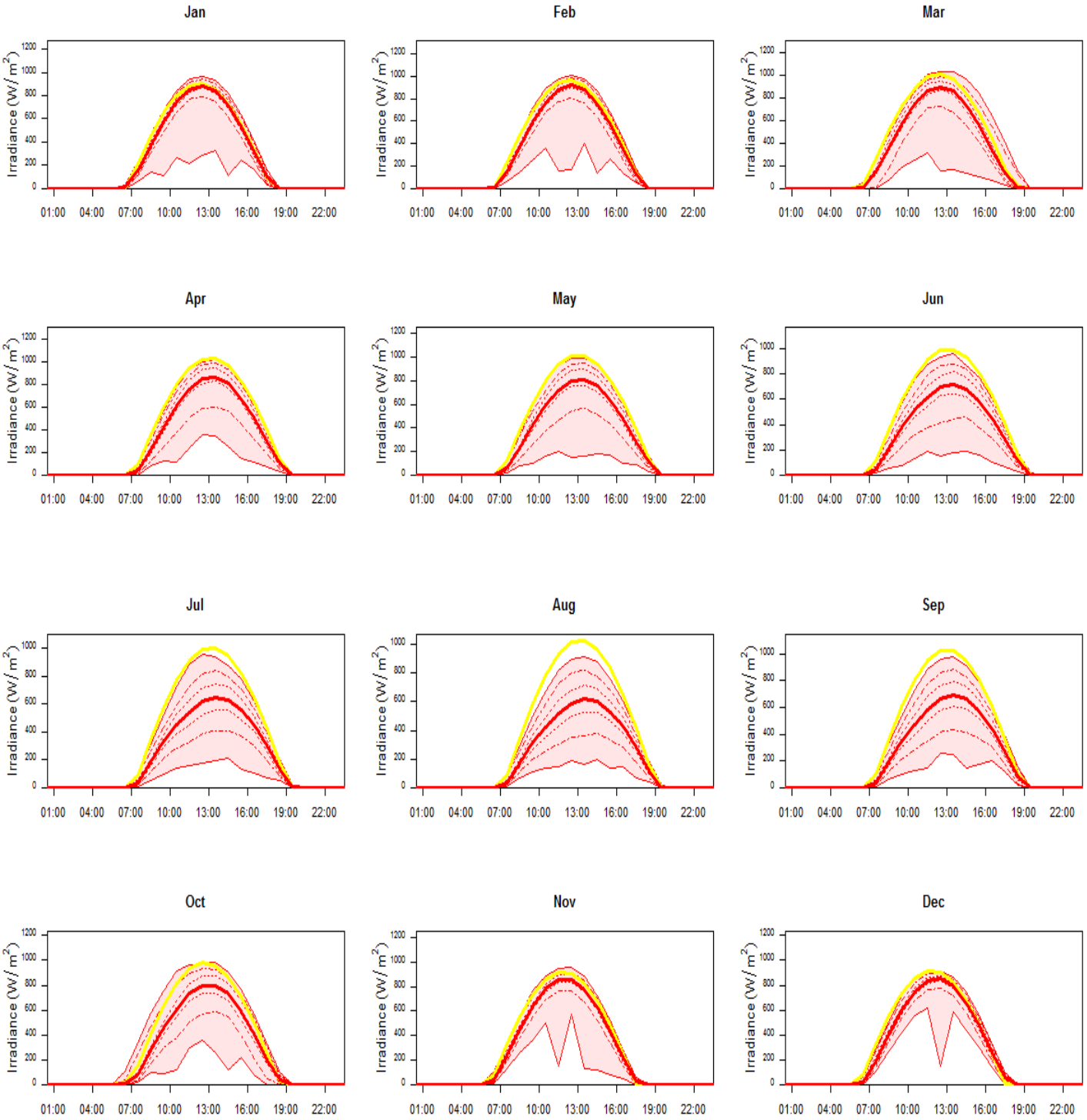

Fig 7.2: Average sub-daily variation (1992-2011) of solar irradiation for all months. [SARAH2 GHI – red curves: Mean (deep red curve) with 5th, 25th 75th and 95th percentiles (dashed red curves) and max and min curves (light red curves). Haurwitz CS GHI – yellow curve]

The cumulative distributive function for solar radiation in Ghana is shown below

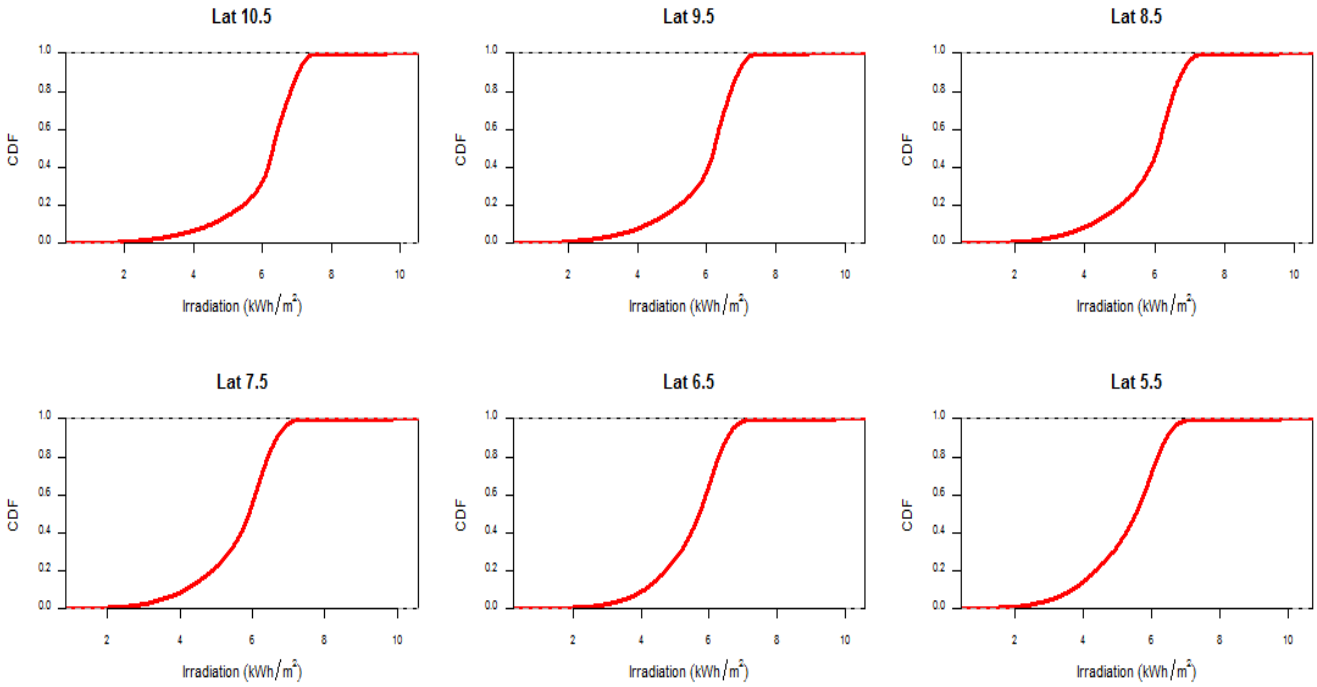

Fig 7.3: CDF of solar radiation for all latitudes

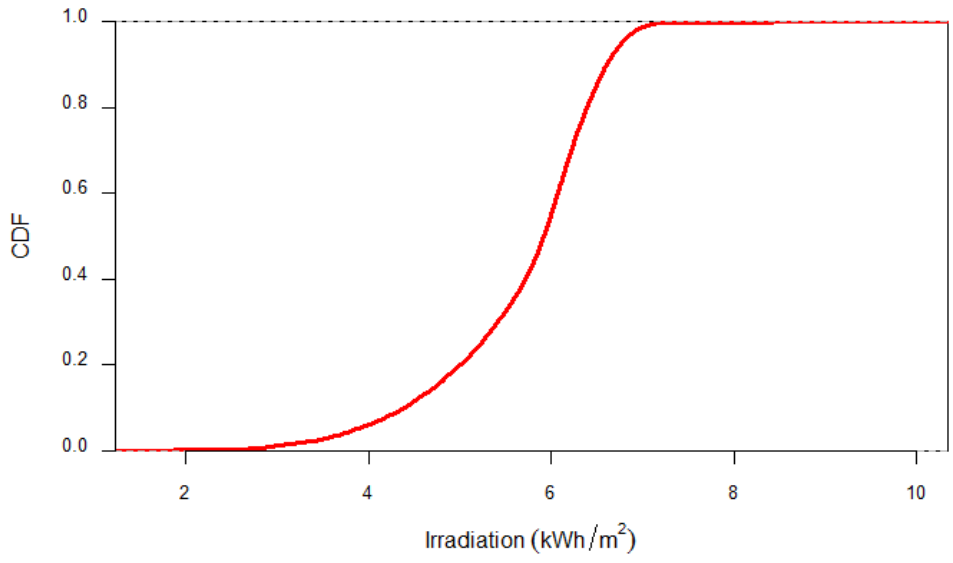

Fig 7.4: CDF of average solar radiation in Ghana

7.4 Appendix C

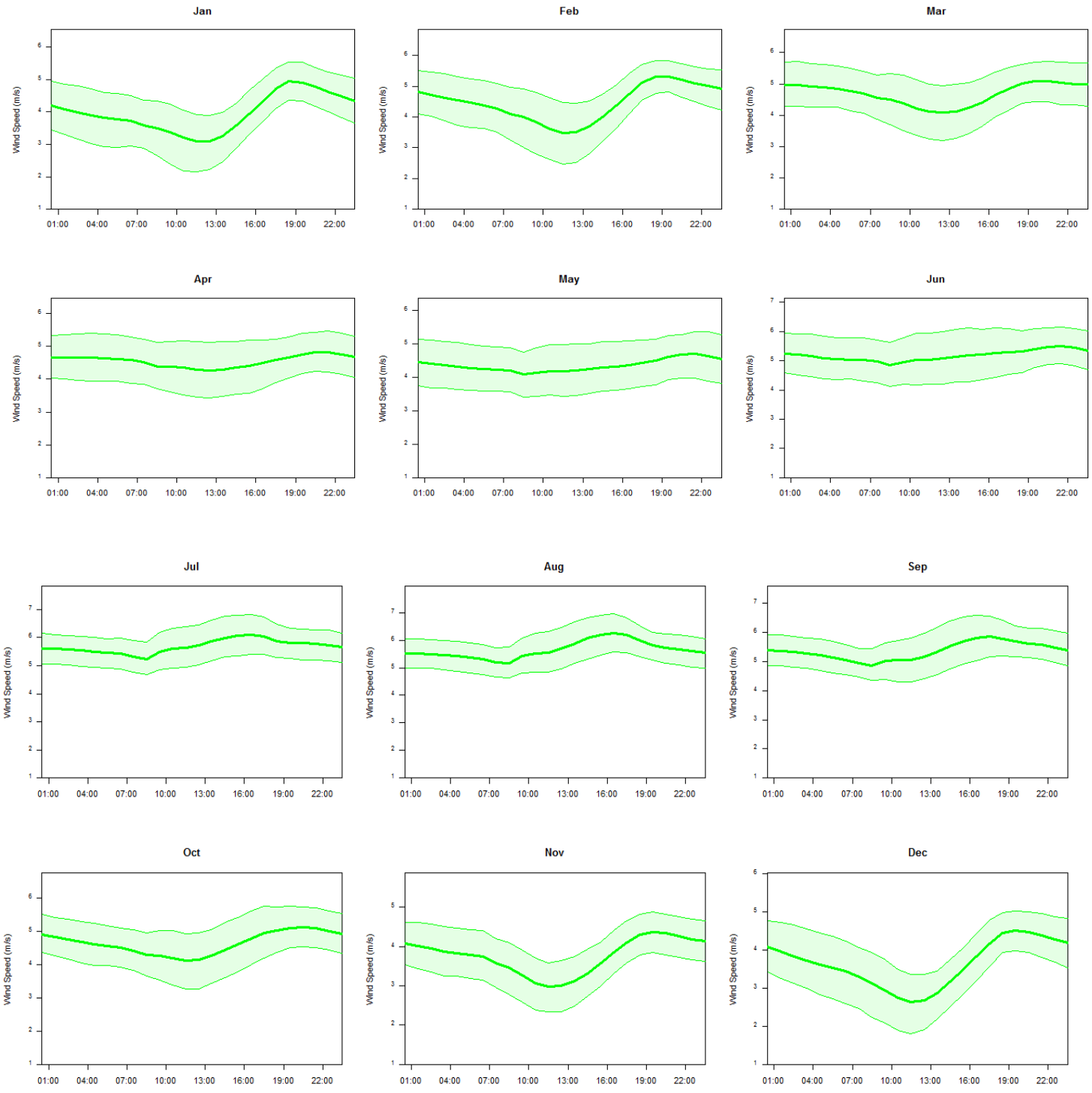

Fig 7.5: : Average sub-daily variation (1992-2011) of wind speed for all months with 25th and 75th percentiles

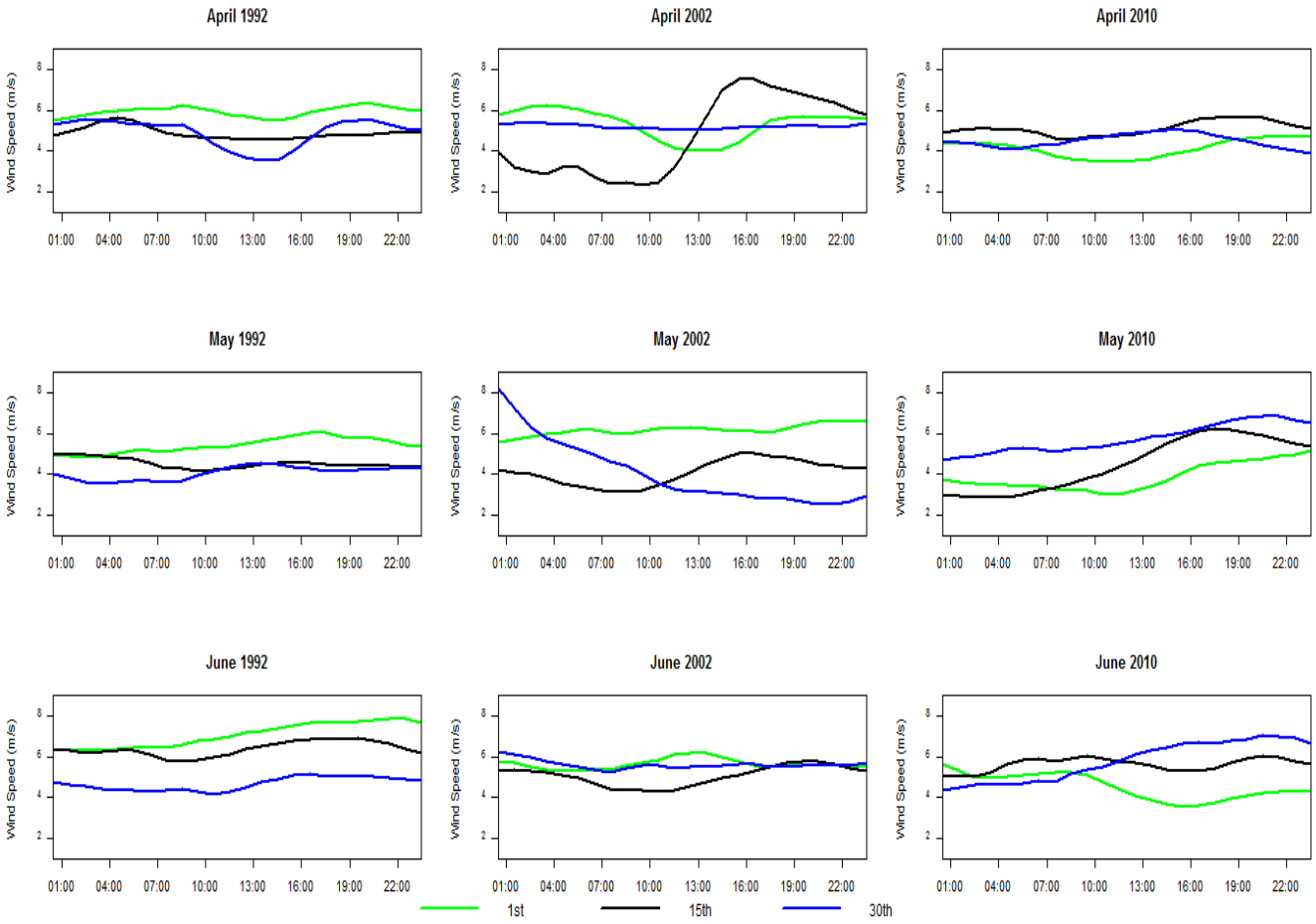

Fig 7.6: Varying patterns intra-daily wind speed of selected days in April, May and June

The hourly wind speed distribution at 80m in each of the selected grid cells are presented in Fig 7.7. Generally, the wind speeds are not so high which is unfavorable for a massive implementation of wind farm projects. Average wind speeds range between 4 to 6 m/s across all selected locations. In terms of power production from the selected turbine, this means that, the 1 MW rated power of the turbine, cannot be attained during most of the time. However, according to Ministry of Energy, actual measurement of wind speed carried out at some specific areas indicate higher daily mean wind speeds of between 6.4 to 8.8 m/s (IRENA, 2015).

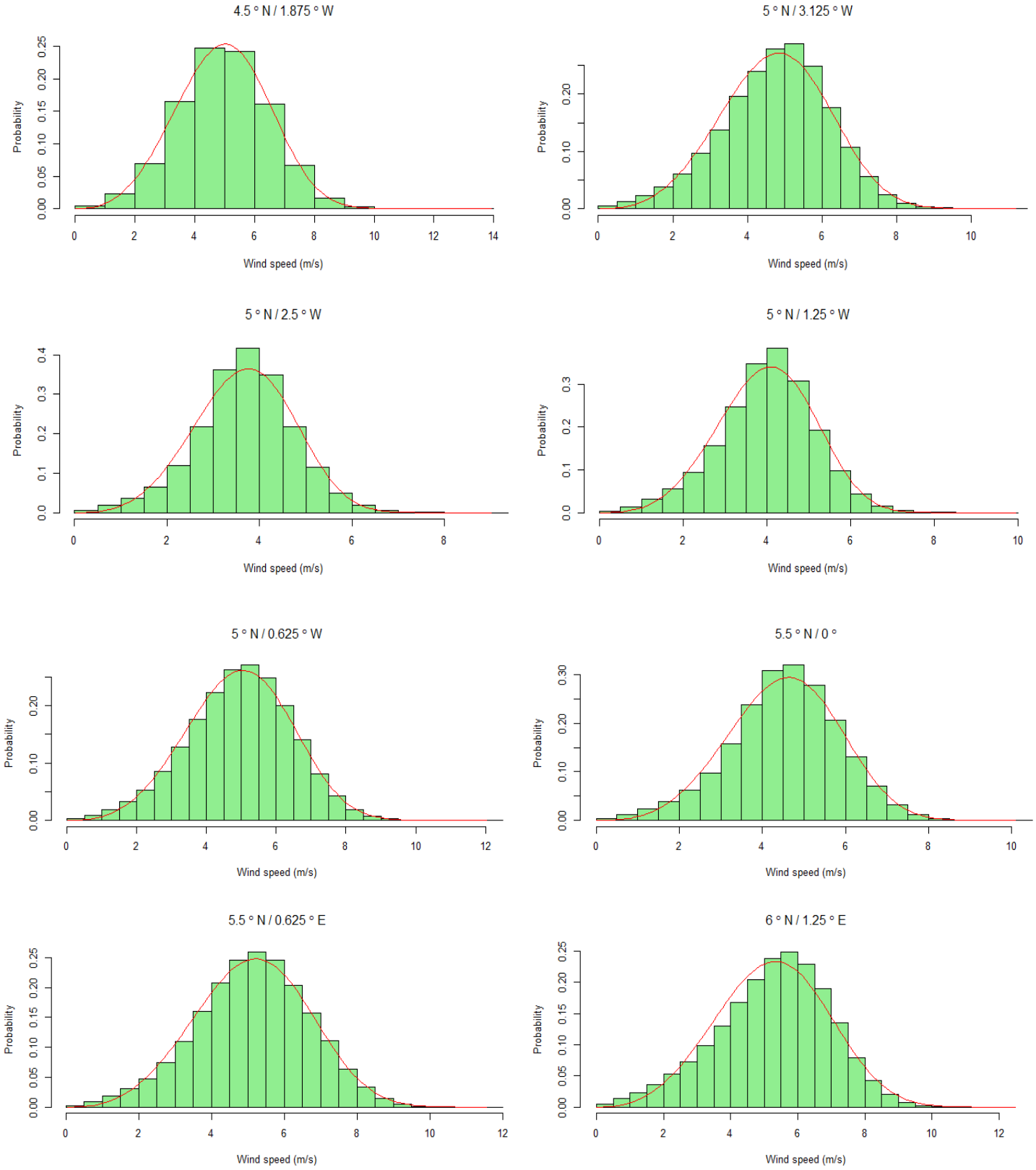

Fig 7.7: Hourly 80m wind speed distribution at selected lat/lon locations (1992–2011

7.5 Appendix D

Additional figures for future VRE configurations

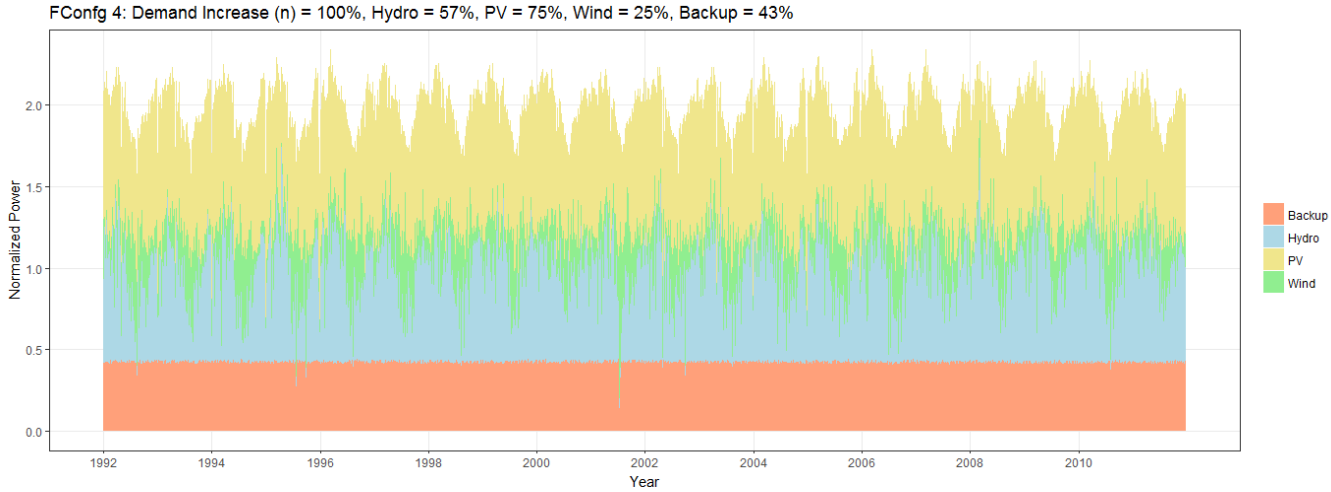

Production Source	Coefficient of Variation (%)
Backup	3.404
Hydro	34.890
PV	16.175
Wind	64.121

Fig 7.8: Intermediate-Future VRE Scenario- Configuration 4

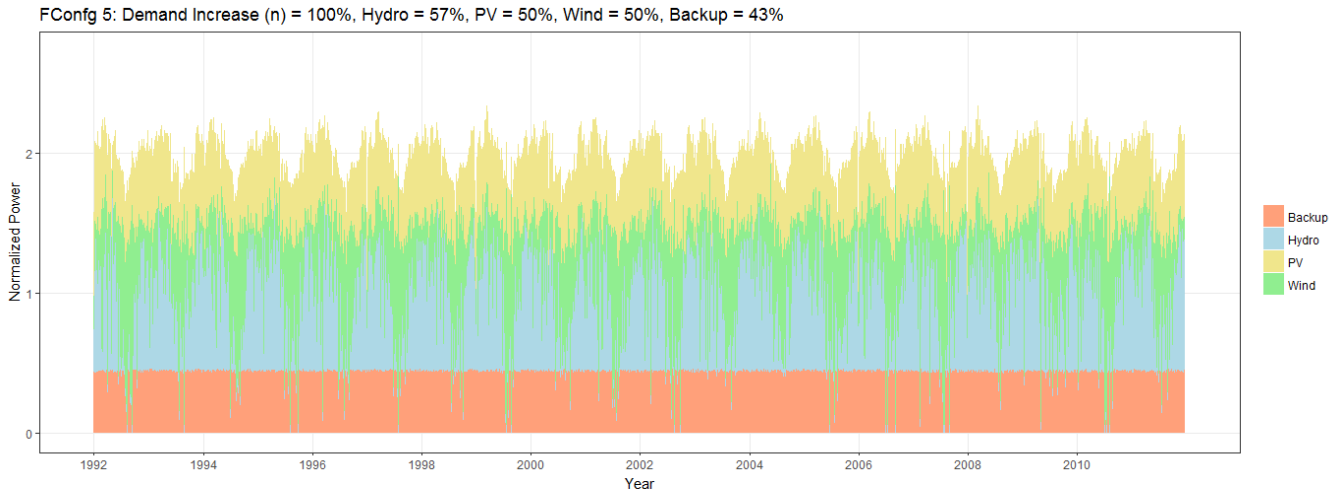

Production Source	Coefficient of Variation (%)
Backup	18.281
Hydro	53.595
PV	16.175
Wind	64.121

Fig 7.9: Intermediate-Future VRE Scenario- Configuration 5

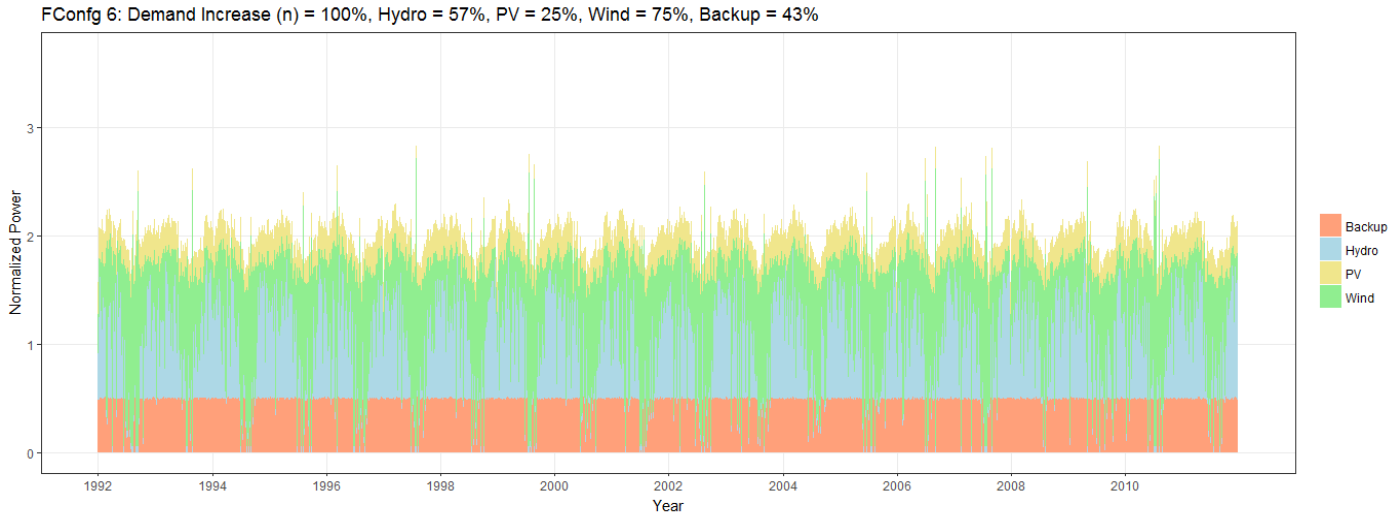

Production Source	Coefficient of Variation (%)
Backup	33.015
Hydro	67.018
PV	16.175
Wind	64.121

Fig 7.10: Intermediate-Future VRE Scenario- Configuration 6

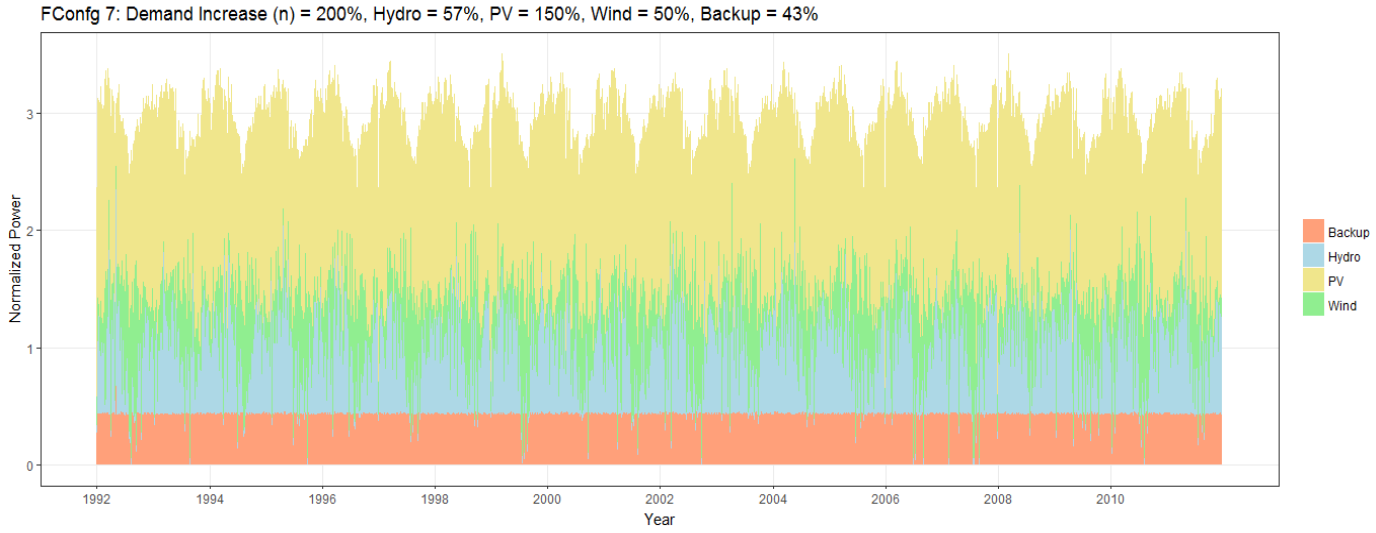

Production Source	Coefficient of Variation (%)
Backup	15.608
Hydro	55.196
PV	16.175
Wind	64.121

Fig 7.11: Far-Future VRE Scenario- Configuration 7

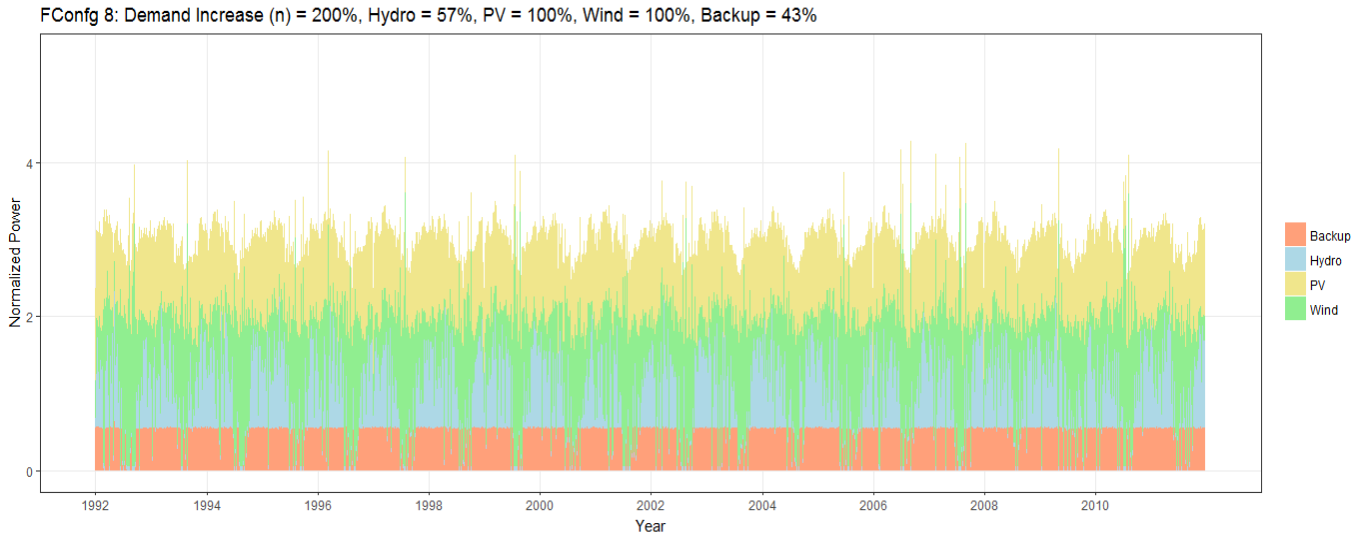

Production Source	Coefficient of Variation (%)
Backup	41.066
Hydro	76.133
PV	16.175
Wind	64.121

Fig 7.12: Far-Future VRE Scenario- Configuration 8

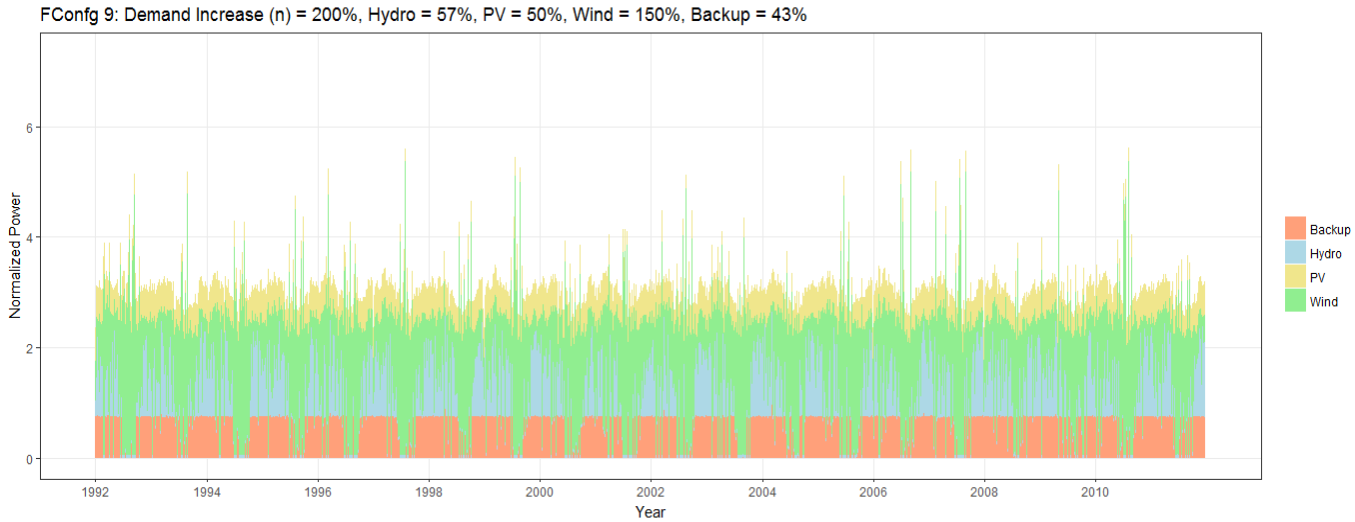

Production Source	Coefficient of Variation (%)
Backup	55.670
Hydro	90.624
PV	16.175
Wind	64.121

Fig 7.13: Far-Future VRE Scenario- Configuration 9